Advanced seismic modeling and analysis of flat-bottom cylindrical steel silos interacting with stored granular-like materials

(Article begins on next page)

04 May 2024

Abstract

The increasing size and complexity of the industrial sites in developing and developed countries would translate to high exposure of these sites to the different natural hazards. Seismic events have proven to be among the most destructive natural hazards making detrimental impacts on the plants' components. Within industrial plants, silos and storage tanks are indispensable assets for several industrial activities, such as agriculture, petrochemicals, food processing and pharmaceuticals, where proper management of raw materials and finished products is essential. As steel shell structure (in the most cases) with massive loading and masses, silos are vulnerable structures whose collapse can trigger Natech accidents, which involve the release of hazardous substances, fires, or explosions. In turn, malfunctioning of these structures can lead to production delays, equipment downtime, increased repair costs, and possibly, human life loss. Latest seismic events have demonstrated an adverse impact on silos structural integrity, imposing dynamic severe conditions and provoking various damage pattern. The work presented in this thesis aims to investigate the seismic behavior of a specific typology of steel silo, that is, flat-bottom cylindrical, particularly focusing on the interaction with the stored granular-like material if subjected to earthquake events.

DICATECh

2023

Mohammad KHALIL

Advanced seismic modeling and analysis of flat-bottom cylindrical steel silos interacting with stored granular-like materials

07

D.R.S.A.T.E.

Doctor in Risk And Environmental, Territorial And Building Development

Coordinator: Prof. Vito Iacobellis

XXXVI CYCLE
Curriculum: ICAR/09 – Structural Engineering

DICATECh
Department of Civil, Environmental, Building Engineering and Chemistry

POLITECNICO DI BARI

07

2024

Mohammad KHALIL

**Advanced seismic modeling and analysis of flat-bottom cylindrical steel silos interacting with stored granular-like materials**

**Prof. Giuseppina Uva**
**Dr. Sergio Ruggieri**
DICATECh - Polytechnic University of Bari

**Prof. Roberto Nascimbene**
IUSS Pavia – EUCENTRE

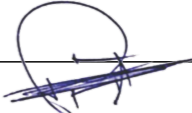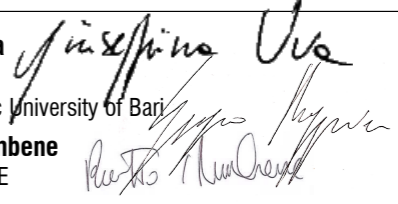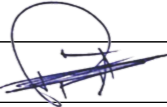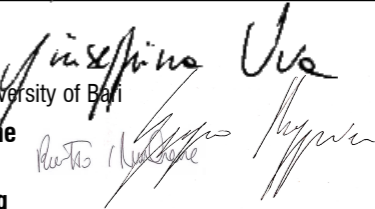**Prof. Christoph Butenweg**
RWTH Aachen University - CWE

Abstract

The increasing size and complexity of the industrial sites in developing and developed countries would translate to high exposure of these sites to the different natural hazards. Seismic events have proven to be among the most destructive natural hazards making detrimental impacts on the plants' components. Within industrial plants, silos and storage tanks are indispensable assets for several industrial activities, such as agriculture, petrochemicals, food processing and pharmaceuticals, where proper management of raw materials and finished products is essential. As steel shell structure (in the most cases) with massive loading and masses, silos are vulnerable structures whose collapse can trigger Natech accidents, which involve the release of hazardous substances, fires, or explosions. In turn, malfunctioning of these structures can lead to production delays, equipment downtime, increased repair costs, and possibly, human life loss. Latest seismic events have demonstrated an adverse impact on silos structural integrity, imposing dynamic severe conditions and provoking various damage pattern. The work presented in this thesis aims to investigate the seismic behavior of a specific typology of steel silo, that is, flat-bottom cylindrical, particularly focusing on the interaction with the stored granular-like material if subjected to earthquake events.

DICATECh

2023

Mohammad KHALIL

Advanced seismic modeling and analysis of flat-bottom cylindrical steel silos interacting with stored granular-like materials

07

# D.R.S.A.T.E.

**POLITECNICO DI BARI**

**07**

2024

Doctor in Risk And Environmental, Territorial And Building Development

Coordinator: Prof. Vito Iacobellis

XXXVI CYCLE
Curriculum: ICAR/09 – Structural Engineering

DICATECh
Department of Civil, Environmental, Building Engineering and Chemistry

Mohammad KHALIL

**Advanced seismic modeling and analysis of flat-bottom cylindrical steel silos interacting with stored granular-like materials**

**Prof. Giuseppina Uva**
**Dr. Sergio Ruggieri**
DICATECh - Polytechnic University of Bari

**Prof. Roberto Nascimbene**
IUSS Pavia – EUCENTRE

**Prof. Christoph Butenweg**
RWTH Aachen University - CWE

# D.R.S.A.T.E.

Doctor in Risk And Environmental, Territorial And Building Development

Coordinator: Prof. Vito Iacobellis

XXXVI CYCLE
Curriculum: ICAR/09 – Structural Engineering

DICATECh
Department of Civil, Environmental, Building Engineering and Chemistry

**POLITECNICO DI BARI**

**07**

**2024**

Mohammad KHALIL

## Advanced seismic modeling and analysis of flat-bottom cylindrical steel silos interacting with stored granular-like materials

**Prof. Giuseppina Uva**
**Dr. Sergio Ruggieri**
DICATECh - Polytechnic University of Bari

**Prof. Roberto Nascimbene**
IUSS Pavia – EUCENTRE

**Prof. Christoph Butenweg**
RWTH Aachen University - CWE

# Politecnico di Bari

## LIBERATORIA PER L'ARCHIVIAZIONE DELLA TESI DI DOTTORATO

Al Magnifico Rettore
del Politecnico di Bari

Il/la sottoscritto MOHAMMAD KHALIL nato a HAMA(SIRIA) il 01/01/1993

residente a Valenzano (BA) in via Capurso, 26 e-mail mo.khalil.it@gmail.com
iscritto al 3° anno di Corso di Dottorato di Ricerca in Rischio e Sviluppo Ambientale, Territoriale ed Edilizio, ciclo 36
ed essendo stato ammesso a sostenere l'esame finale con la prevista discussione della tesi dal titolo:

**Advanced seismic modeling and analysis of flat-bottom cylindrical steel silos interacting with stored granular-like materials**

### DICHIARA

1) di essere consapevole che, ai sensi del D.P.R. n. 445 del 28.12.2000, le dichiarazioni mendaci, la falsità negli atti e l'uso di atti falsi sono puniti ai sensi del codice penale e delle Leggi speciali in materia, e che nel caso ricorressero dette ipotesi, decade fin dall'inizio e senza necessità di nessuna formalità dai benefici conseguenti al provvedimento emanato sulla base di tali dichiarazioni;
2) di essere iscritto al Corso di Dottorato di ricerca _____ciclo_____, corso attivato ai sensi del "*Regolamento dei Corsi di Dottorato di ricerca del Politecnico di Bari*", emanato con D.R. n.286 del 01.07.2013;
3) di essere pienamente a conoscenza delle disposizioni contenute nel predetto Regolamento in merito alla procedura di deposito, pubblicazione e autoarchiviazione della tesi di dottorato nell'Archivio Istituzionale ad accesso aperto alla letteratura scientifica;
4) di essere consapevole che attraverso l'autoarchiviazione delle tesi nell'Archivio Istituzionale ad accesso aperto alla letteratura scientifica del Politecnico di Bari (IRIS-POLIBA), l'Ateneo archivierà e renderà consultabile in rete (nel rispetto della Policy di Ateneo di cui al D.R. 642 del 13.11.2015) il testo completo della tesi di dottorato, fatta salva la possibilità di sottoscrizione di apposite licenze per le relative condizioni di utilizzo (di cui al sito http://www.creativecommons.it/Licenze), e fatte salve, altresì, le eventuali esigenze di "embargo", legate a strette considerazioni sulla tutelabilità e sfruttamento industriale/commerciale dei contenuti della tesi, da rappresentarsi mediante compilazione e sottoscrizione del modulo in calce (Richiesta di embargo);
5) che la tesi da depositare in IRIS-POLIBA, in formato digitale (PDF/A) sarà del tutto identica a quelle **consegnate**/inviate/da inviarsi ai componenti della commissione per l'esame finale e a qualsiasi altra copia depositata presso gli Uffici del Politecnico di Bari in forma cartacea o digitale, ovvero a quella da discutere in sede di esame finale, a quella da depositare, a cura dell'Ateneo, presso le Biblioteche Nazionali Centrali di Roma e Firenze e presso tutti gli Uffici competenti per legge al momento del deposito stesso, e che di conseguenza va esclusa qualsiasi responsabilità del Politecnico di Bari per quanto riguarda eventuali errori, imprecisioni o omissioni nei contenuti della tesi;
6) che il contenuto e l'organizzazione della tesi è opera originale realizzata dal sottoscritto e non compromette in alcun modo i diritti di terzi, ivi compresi quelli relativi alla sicurezza dei dati personali; che pertanto il Politecnico di Bari ed i suoi funzionari sono in ogni caso esenti da responsabilità di qualsivoglia natura: civile, amministrativa e penale e saranno dal sottoscritto tenuti indenni da qualsiasi richiesta o rivendicazione da parte di terzi;
7) che il contenuto della tesi non infrange in alcun modo il diritto d'Autore né gli obblighi connessi alla salvaguardia di diritti morali od economici di altri autori o di altri aventi diritto, sia per testi, immagini, foto, tabelle, o altre parti di cui la tesi è composta.

Luogo e data  Bari 16/04/2024          Firma _____

Il/La sottoscritto, con l'autoarchiviazione della propria tesi di dottorato nell'Archivio Istituzionale ad accesso aperto del Politecnico di Bari (POLIBA-IRIS), pur mantenendo su di essa tutti i diritti d'autore, morali ed economici, ai sensi della normativa vigente (Legge 633/1941 e ss.mm.ii.),

### CONCEDE

- al Politecnico di Bari il permesso di trasferire l'opera su qualsiasi supporto e di convertirla in qualsiasi formato al fine di una corretta conservazione nel tempo. Il Politecnico di Bari garantisce che non verrà effettuata alcuna modifica al contenuto e alla struttura dell'opera.
- al Politecnico di Bari la possibilità di riprodurre l'opera in più di una copia per fini di sicurezza, back-up e conservazione.

Luogo e data  Bari 16/04/2024          Firma _____

# EXTENDED ABSTRACT *(eng)*

The increasing size and complexity of the industrial sites in developing and developed countries would translate to high exposure of these sites to the different natural hazards. Seismic events have proven to be among the most destructive natural hazards making detrimental impacts on the plants' components. Within industrial plants, silos and storage tanks are indispensable assets for several industrial activities, such as agriculture, petrochemicals, food processing and pharmaceuticals, where proper management of raw materials and finished products is essential. As steel shell structure (in the most cases) with massive loading and masses, silos are vulnerable structures whose collapse can trigger Natech accidents, which involve the release of hazardous substances, fires, or explosions. In turn, malfunctioning of these structures can lead to production delays, equipment downtime, increased repair costs, and possibly, human life loss. Latest seismic events have demonstrated an adverse impact on silos structural integrity, imposing dynamic severe conditions and provoking various damage pattern. The work presented in this thesis aims to investigate the seismic behavior of a specific typology of steel silo, that is, flat-bottom cylindrical, particularly focusing on the interaction with the stored granular-like material if subjected to earthquake events.

The first part of the thesis presents a literature compendium about silos, their structural configurations, behavior, failure, and different hazard sources., The second part of the dissertation provides an evaluation of seismic fragility of cylindrical ground-supported steel silos (the silos under consideration are of circular plan, flat smooth walls, unstiffened and constant wall thickness.). The main goal of the first part of dissertation is to propose a numerical procedure aimed to assess the seismic fragility of different cylindrical steel silos, accounting for varying geometries and service conditions (i.e., filling level of granular-like material), and observing different failure modes. Consequently, a set of smooth steel silos was selected for this part of work, considering different geometrical configurations (i.e., varying from squattest to slenderest structures). In addition, different service conditions were simulated, with the aim to

observe the behavior of empty and filled silos (30%, 60%, and 90% of filling degree with respect to the maximum capacity). Thus, for each configuration, a detailed numerical model was developed under proper boundary conditions, adequately simulating the shell structure, the solid material inside, and the interactions between them. After validating the numerical models against existing literature data, three different failure modes were identified and assessed, accounting for the most recurrent post-elastic buckling type (i.e., elephant foot) and considering the possible occurrence of the elastic ones (i.e., diamond or similar shape failures at the middle and top of the structures). In the framework of the proposed procedure, static and dynamic analyses were performed to identify the most probable failure modes and evaluate the probability of exceeding each one. As the output of this proposed approach, the seismic performance of each silo under a specific limit state was provided in the form of fragility curves. The results highlight some novel aspects, starting from the role that service conditions assume in the silos seismic performance up to the possible differences in terms of failure modes for different silos geometrical structural configurations.

In the third part of the thesis, an evaluation of the dynamic overpressure induced by earthquakes in flat bottom steel silos is presented. Aiming to properly understand and predict the dynamic conditions to which silos are subjected, especially under seismic excitations, this part of the dissertation presents detailed numerical analyses to estimate the dynamic overpressure experienced by silos wall under seismic excitation. Consequently, nonlinear finite element, FE, models were created for two geometries of silos, i.e., slender and squat and nonlinear time history analyses were carried out. The detailed models accounted for geometrical and material nonlinearity of steel silos and of stored granular-like solid material. This latter was simulated by employing hypoplasticity as constitutive model. The output of the analyses allowed to quantify the additional dynamic pressure, which was compared to the one provided by the European standards (i.e., equivalent static approach).

Additional improvements might help in fine-tuning the outcomes of the proposed procedure. Nevertheless, this work contributes a reliable technique that allows profes-

sionals and assessors to comprehensively understand the seismic behavior of the ground-supported steel silos and predict their probability of failure.

# EXTENDED ABSTRACT *(ita)*

L'aumento delle dimensioni e della complessità dei siti industriali, nei paesi in via di sviluppo e in quelli sviluppati, si tradurrebbe in un'elevata esposizione di questi siti ai diversi rischi naturali. Gli eventi sismici hanno dimostrato di essere tra i rischi naturali più distruttivi, con impatti dannosi sui componenti degli impianti. Silos e serbatoi di stoccaggio sono risorse indispensabili in settori quali l'agricoltura, il petrolchimico, l'industria alimentare e farmaceutica, dove la corretta gestione delle materie prime e dei prodotti finiti è essenziale. Essendo strutture a guscio in acciaio con carichi e masse enormi, i silos sono strutture intrinsecamente vulnerabili il cui crollo può innescare incidenti Natech, che comportano il rilascio di sostanze pericolose, incendi o esplosioni. Ciò, a sua volta, può portare a ritardi nella produzione, tempi di inattività delle apparecchiature, aumento dei costi di riparazione e, possibilmente, alla perdita di vite umane. Gli ultimi eventi sismici hanno dimostrato un impatto negativo sull'integrità strutturale dei silos, imponendo condizioni dinamiche severe e provocando vari modelli di danno. Questo lavoro indaga il comportamento sismico di silos cilindrici in acciaio a fondo piatto che interagiscono con il materiale granulare immagazzinato. I silos in esame sono a pianta circolare, pareti piane e lisce, non irrigidite e con spessore costante.

La prima parte della tesi fornisce un compendio della letteratura sui silos, le loro configurazioni strutturali, il loro comportamento, i guasti e le diverse fonti di pericolo. La seconda parte della tesi fornisce una valutazione della fragilità sismica di silos cilindrici in acciaio sostenuti da terreno. L'obiettivo principale di questa parte della tesi è proporre una procedura numerica volta a valutare la fragilità sismica di diversi silos cilindrici in acciaio, tenendo conto delle diverse geometrie e condizioni di servizio (ad esempio, il livello di riempimento di materiale granulare) e osservando diverse

modalità di guasto. Di conseguenza, per questa parte del lavoro una serie di silos in acciaio liscio è stata selezionato, considerando diverse configurazioni geometriche (vale a dire, variando dalle strutture più tozze a quelle più snelle). Inoltre, sono state simulate diverse condizioni di servizio, con l'obiettivo di osservare il comportamento dei silos vuoti e pieni (30%, 60% e 90% del grado di riempimento rispetto alla capacità massima). Pertanto, per ciascuna configurazione, è stato sviluppato un modello numerico dettagliato in condizioni al contorno adeguate, simulando adeguatamente la struttura del guscio, il materiale solido all'interno e le interazioni tra loro. Dopo aver validato i modelli numerici rispetto ai dati esistenti in letteratura, sono state identificate e valutate tre diverse modalità di collasso, tenendo conto della tipologia di instabilità post-elastica più ricorrente (ad esempio, piede di elefante) e considerando la possibile comparsa di quelle elastiche (ad esempio, a diamante o simili, cedimenti di forma nella parte centrale e superiore delle strutture). Nell'ambito della procedura proposta, sono state eseguite analisi statiche e dinamiche per identificare le modalità di guasto più probabili e valutare la probabilità di superamento di ciascuna di esse. Come risultato di questo approccio proposto, la prestazione sismica di ciascun silo sotto uno specifico stato limite è stata fornita sotto forma di curve di fragilità. I risultati evidenziano alcuni aspetti innovativi, a partire dal ruolo che le condizioni di servizio assumono nella prestazione sismica dei silos fino alle possibili differenze in termini di modalità di guasto per diverse configurazioni strutturali geometriche dei silos.

Nella terza parte della tesi, viene presentata una valutazione della sovrapressione dinamica indotta dai terremoti nei silos di acciaio a fondo piatto. Con l'obiettivo di comprendere e prevedere adeguatamente le condizioni dinamiche a cui sono soggetti i silos, in particolare sotto eccitazioni sismiche, questa parte della tesi presenta analisi numeriche dettagliate per stimare la sovrapressione dinamica subita dalla parete del silos sotto eccitazione sismica. Di conseguenza, sono stati creati modelli non lineari agli elementi finiti, FE, per due geometrie di silos, ovvero sono state effettuate analisi della storia temporale snella e tozza e non lineari. I modelli dettagliati hanno tenuto conto della non linearità geometrica e dei materiali dei silos di acciaio e del materiale

solido di tipo granulare immagazzinato. Quest'ultimo è stato simulato utilizzando l'ipoplasticità come modello costitutivo. Il risultato delle analisi ha permesso di quantificare la pressione dinamica aggiuntiva, che è stata confrontata con quella prevista dagli standard europei (ovvero, approccio statico equivalente).

# ACKNOWLEDGEMENTS

# LIST OF FIGURES

# LIST OF TABLES

# INDEX

# INTRODUCTION

Industrial plants represent a cornerstone of modern societies and their economic development, serving as the hubs of manufacturing and production across various sectors, and playing a key role in the economic growth and the well-being of societies(Krausmann et al., 2019). These plants consist of sprawling facilities comprising of an intricate network of mechanical and structural components, all working in tandem to ensure efficient, reliable, and continuous operation of the factory(Paolacci et al., 2012). The safety, sustainability, and functionality of plants' relevant structural components are paramount. However, as a multi-component system, the structural integrity of the plants implies the integrity of different components(Brunesi et al., 2015). From a scientific and professional standpoint, civil engineers are tasked with meticulously analyzing the materials, design, and construction techniques to guarantee that these components not only meet safety regulations but also exhibit the durability required to sustain continuous operations(Alessandri et al., 2018). In this regard, the repercussions of structural collapse can be catastrophic, leading to environmental hazards, production interruptions, and most critically, threats to human safety(J. W. Carson & Holmes, 2003). As such, the role of civil engineers in conducting comprehensive assessments, executing preventive measures, and implementing proactive maintenance programs is indispensable. These measures ensure the long-term reliability and safety of industrial plants, thereby safeguarding the investments made in these complex infrastructures. Thus, the ability of relevant plants' components to withstand various loads, environmental conditions, and operational stresses over time is undeniable necessity. These components may include the main building structures, foundations, support systems, piping networks, and very importantly, the storage systems (Figure **0-1**).

Storage systems play a central role in different industrial sectors, serving as crucial components for the safe and efficient containment of a wide variety and substances and materials. These structures are designed to store a variety of materials, from grains and chemicals to liquids and gases, ensuring preservation and controlled re-

lease when needed. A main classification of storage systems can be made by distinguishing tanks (Gian Michele Calvi & Roberto Nascimbene, 2023) storing liquid and silos storing solid materials (Butenweg et al., 2017; Sadowski & Rotter, 2012). However, that difference in functionality makes a big impact on the structural behavior of the system under static and dynamic condition, consequently differences in the design are distinctive.



Figure 0-1 Example of plastic manufacturing plants (The photo is retrieved from the website of Coperion company)

Natural hazards can have wide-ranging impacts on industrial plants. Tornadoes, wildfires, hurricanes, floods, and earthquakes, pose a variety of risks to industrial facilities. Subsequently, operational disruptions, economic losses, and severe safety concerns could increase. Earthquakes, in particular, can be especially destructive due to their sudden and unpredictable nature.

In this context, earthquakes can cause significant damage to buildings, equipment, and other infrastructures. Giving the inherent vulnerable structural system of storage

facilities, as steel shell structures, and their massive loads, latest seismic events (e.g., 2023 Turkey-Syria Earthquake (Hu et al., 2023); 2012 Emilia Earthquake (Brunesi et al., 2015)) have demonstrated that the seismic action had a higher destructive effect on silos compared to the other components in the same site. Thus, attention has been raised on the high seismic vulnerability of silos and its dependence on different geometrical, mechanical, and functional aspects.

## Research problem,

Subsequent to the occurrence of several earthquakes in the mediterranean zone, silos storing solid material represent the most vulnerable industrial units. Hence, as pivotal component of critical infrastructures a proper estimation of their vulnerability under extreme events, and robust design regulations of these structures under transient loads are imperative. While the seismic behavior of tanks has been deeply investigated in the scientific literature, fewer contributions are available for silos storing solids, despite their significance in major strategic sectors such as food and chemical industrial sectors. In this regard, seismic behavior and vulnerability assessment of silos is still conducted with anachronistic approaches featuring poor structuring and several limitations. Thus, it is necessary to develop new dynamic behavior-based approaches which can be comprehensive and, at the same time, can be able of estimating the seismic fragility of silos taking into consideration the interaction with the stored granular material, different conditions of functionality (serviceability condition), different geometrical features, and different possible failure modes.

On the flip side, the seismic design approach proposed by the European standards, Eurocode 8-4 (EN 1998-2, 2005), is based on estimating additional inertial forces due to the acceleration of the material. Where the additional dynamic pressure is substituted by equivalent static pressure. In this regard, the distribution of the equivalent static pressure is controversial (Butenweg et al., 2017) and can exhibit various patterns. In this regard, robust and reliable design regulations necessitate a proper estimation of the dynamic overpressure induced by earthquakes in flat bottom steel silos.

4

In the light of the above-mentioned concerns, an in-depth comprehension of the behavior of silos under static and dynamic operation conditions is essential. For this purpose, advanced numerical techniques based on finite element analysis are employed. The numerical approach incorporates the behavior of the granular stored material in addition to its interaction with the silo structure.

## Research objectives

This research aims at presenting solutions to fill the gaps outlined in the previous section. Consequently, it seeks to introduce an innovative strategy to estimate and improve the understanding of the seismic fragility of ground-supported (flat-bottomed) uncorrugated steel silos storing granular solid material, accounting for the interaction with the solids. Practically, it proposes to integrate different techniques, e.g., nonlinear static analysis, nonlinear dynamic time history analysis, reliability analysis, and probabilistic methods, into one framework to quantify the seismic vulnerability of the silo structures. In addition, an assessment of the dynamic overpressure induced by earthquakes in flat bottom steel silos is presented based on overdetailed FEM simulation outputs.

The target of this work is further elaborated in subsequent specific objectives:

1.  Investigation on the most effective factors that significantly influence the behavior of silos under static and dynamic conditions. That includes a state-of-the-art study on the recent research dealing with silos.

2.  Shaping and introducing a probabilistic assessment-based procedure aimed to numerically evaluate the seismic fragility of different cylindrical steel silos, accounting for the interaction with the stored solids, varying geometries and service conditions (i.e., filling level of granular-like material), and considering the most critical failure modes.

3.  Presenting an evaluation on the dynamic overpressure applied to silo walls under earthquakes and the Eurocode 8-4 (EN 1998-4, 2006) equivalent static approach based on FEM numerical simulation.

## Thesis outlines

This work investigates the seismic behavior of ground-supported steel silos containing granular material. This research mainly proposes an advanced strategy for the seismic fragility assessment of the silo structure by employing nonlinear static analysis and nonlinear dynamic analysis in a probabilistic framework. In addition, an investigation on dynamic overpressure and the equivalent static design approach is presented.

However, the dissertation is outlined as follows.

**Chapter 1** gives an extensive background and exploration on critical aspects and factors that could have a significant influence on the structural performance of silos under static and dynamic conditions. A state-of-art is presented in this chapter covering the silos structural system variation, ensiled material critical properties, international standards load specifications, and possible failure modes.

**Chapter 2** primarily presents a numerical procedure (in the framework of the performance-based earthquake engineering PBEE) to derive fragility curves of steel silos taking into account different possible failure modes. Subsequently, the application of the proposed procedure is demonstrated by performing an investigation on a set of smooth and unstiffened steel ground-supported silos under the seismic effect, varying two main geometrical aspects, that is, radius-to-thickness and height-to-diameter ratios, and presenting different filling levels. This investigation accounts for different geometrical configurations, different service conditions, and different failure modes.

In this chapter, a detailed background on the seismic behavior of silos is provided including analytical, experimental, and numerical investigations conducted in the scientific literature. Then, the structure and the formation of the proposed procedure is elaborated comprising of four steps incorporating silo geometrical characterization, FE model set up and validation, conducting the analysis: i) frequency analysis; ii) nonlinear static analysis; iii) time history analysis, and finally probabilistic fragility calculation.

6

**Chapter 3** conducts an evaluation of dynamic overpressure and the equivalent static approach advocated by the European Standards (EN 1991-4, 2006) based on FE numerical modelling investigation. In the framework of this chapter, silo seismic behavior is elaborated drawing from previous research investigations. In addition, an overview of hypoplasticity, as a constitutive law, is offered. Following this, an illustration of Eurocode's equivalent static approach is presented. subsequent to these discussions, the adopted numerical modelling methodology was detailed, and the observed FEM-based dynamic overpressure was reported alongside the alternatives of the calculated equivalent static approach.

The **Conclusions** drawn from this dissertation are finally listed, also recommending future developments.

# 1. Assessment of Structural Behavior, Vulnerability and Risk of Industrial Silos: State-of-the-Art and Recent Research Trends

**Abstract**: This chapter provides a literature compendium about the main studies on the structural behavior, vulnerability and risk of industrial silos, as one of the most important players of different industrial processes. The study focuses on the main scientific works developed in the last decades, highlighting the more notable issues on circular steel silos as the most widespread typology in practice, such as the con-tent-container complicated interaction, the structural and seismic response, and the several uncertainties in the design and assessment processes. Specifically, this chapter proposes a near-full state-of-the-art on (i) the behavior of silos under different kinds of loads, ordinary and extreme, (ii) the effects of imperfections and the interacting structures (e.g., ring beams, supporting structures), (iii) the stored material properties, the relevant uncertainties and the impact on the silo be-haviour, (iv) the possible failure modes given by the focused structural configuration and the stored materials, (v) assessment and risk mitigation strategies. Throughout the text, some considerations are provided, in order to summarize the more recent research trends about steel silos and to highlight the still open issues on the risk and vulnerability reduction of these kinds of structures.

**keywords**: industrial silos; shell structures; failure modes; silos vulnerability; risk assessment

## 1.1. Introduction

Storage silos are widely used in several engineering services and applications, whether in construction work, industry, agriculture or even aerospace sector. The main task of these kinds of structures is the possibility to store a huge range of differ-

ent materials such as liquid and solid, that are useful for the industrial processes, treatments and productions. It has to be noted that silos are essential parts of different industries that consist of structures usually subjected to numerous accidents, which cause severe losses and injuries to occupants and damage on the surrounding environment. In general, past hazardous events as earthquakes have shown critical facilities subjected to large damage and catastrophic consequences. On top of that, it shows the design methods for new industrial structures have non negligible uncertainties, especially for extreme events. This document will also highlight some aspects on the entire structural stock constituting plants where silos are present. As a matter of fact, silos could be defined as huge vessels used as storage for massive quantities of granular bulk solids with capacities that vary from tons up to thousands of tons (Rotter, 2001). Nowadays silos can be constructed using typical construction materials (e.g., rein-forced concrete, RC, and steel) and they could be indicated as silos, bins, bunkers or hoppers. Historically, the first examples of silos date back to a hundred years ago where they were built using field stones. Their shape was standardized as a cylindrical structure covered with a trullo or domed roof and provided with an opening as a front door used for unloading purposes. Over the last decades, with the advancement of technology and the spread of the most recent structural materials, many examples of silos can be found that are constructed using different kinds of materials, such as steel, stainless steel, concrete, plastic, and aluminum. Likewise, different structural configurations and arrangements can be observed in the practice, such as flat-bottom ground-supported silos or elevated ones resting on a special supporting system. Firstly, given the stored material, a first classification can be outlined: silo is the term used to refer to the container used to store solid materials, while tank is the term applies to the container that stores liquid. Owing to the fact that the shape and the de-sign are different, therefore, they shall deserve different treatments. Herein, the silos storing solid could be classified basing on the supporting system (flat-bottom ground-supported silos and elevated silos), on the aspect ratio (squat or slender), or on the construction method (welded/bolted for steel silos, and slip/step form for the RC silos). Specifically, steel silos could be distinguished as

10

stiffened or unstiffened, whether corrugated or flat-wall silos, with either single sheets or double sheets. One of the main uses of silos in manufacturing processes is the intermediate storage between successive operations, or among different stages from production to transportation. Figure 1-1 shows an example of silos battery, serving as a grain-storage with a capacity of thousands of tons in an industrial site located in Italy.



Figure 1-1 View of silos battery used for grain storage with capacity of 3955 tons (Campo San Martino, Italy).

The aim of this chapter is to provide a near-full state-of-the art about silos as above defined, accounting for the wide range of these typological structures. The study is directed to circular silos with main focus on steel ones (elevated and flat bottomed), as they are the most widespread silos in the practice. The first aspect to highlight is the structural nature of circular silos, which are shell structures, and, for this reason, the terms silos and shells (refereeing to the silo walls) will be often used alternately. Following, a general summary of the main research topics connected to circular silos is mentioned, which will be detailed and discussed in the following sections of the chapter and that aim to outline the main structural behavior aspects and the main risk and vulnerability sources associated to these structures:

a. Structural integrity and the response of the silo to gravity loads (dead loads, grain loads) (Rotter, 1998a; Sadowski & Rotter, 2011b), seismic loads(Rotter & Hull, 1989; Veletsos & Younan, 1998); the impact of the different aspects on structural be-

havior of silos, such as supporting system arrangements, silo-columns attachment (Jansseune et al., 2016; Zdravkov, 2018), ring beam (Topkaya & Rotter, 2011), imperfection measurement (Ding et al., 1996b), imperfection-sensitivity of the shell (Fajuyitan & Sadowski, 2018; Jansseune et al., 2016), imperfection methods representation (Knoedel et al., 2017)and buckling behavior (Rotter et al., 1989; Sadowski & Rotter, 2011a). Furthermore, some aspects regarding the structural integrity improving (Jäger-Cañás & Pasternak, 2017; Ning & Pellegrino, 2015) and strengthening (Batikha et al., 2018) are provided.

b.      Identification of the dynamic properties and the dynamic response of silos under extreme load conditions, as earthquakes(Butenweg et al., 2017; Veletsos & Younan, 1998) and blast loads (Temsah et al., 2021).

c.      Properties of the bulk solids and influence on the silos vulnerability on the base of material properties variation, behavior of the stored material during discharging and its influence on design loads variation(Kobyłka et al., 2020; Volpato et al., 2014), particle-silo interaction under different load conditions, such as static and dynamic actions (Chen et al., 2020).

d.      Design standards of silos, looking at the main limitations, deficiencies and possible improvements (J. Carson & Craig, 2015).

e.      Failure modes of silos, such as the yielding and buckling of cylindrical shells (Jansseune et al., 2016), the main causes and several phenomena leading to collapse(Zaccari & Cudemo, 2016).

f.      Assessment of existing silos, by means of destructive and non-destructive test , and in-situ measurements(Ding et al., 1996a).

## 1.2. Structural typology and arrangement of circular silos

### 1.2.1. Construction material and geometry

Regarding the construction material, as any other structures and infrastructure, silos are usually built by means RC, steel, stainless-steel, aluminum. In some

cases, composite material can be used for some shell structures, as for special industrial applications or for the aerospace field(Castro et al., 2014), Historically, silos were constructed using wood, brick or stone as farm silos. However, steel and RC are the most spread as nowadays construction materials for silos in the different sectors. Whereas metal silos are characterized as thin-walled structures, RC ones have relatively thicker walls. Therefore, the first ones are more sensitive to compressive stresses and buckling, while the second ones are more sensitive to horizontal pressure. For that reason, RC silos are always preferable for tall and slender silos, where the axial compression forces are the governing stresses but not the circumferential ones (Janssen, 1895). However, this is not applicable to squat silos, where the horizontal pressure and the circumferential stresses are dominant, but not the vertical compression, thus steel is preferable.

Silos shapes are object of classification, according to the purpose and the usage of the container. The circular plane shape is the most common feature among the majority of silos in industry(Rotter, 1998a), however, the in-plan shape variation could occur in the supporting system un-der the silo. Thus, two main configurations are recognized: (i) ground supported silos(Vidal et al., 2005), where the shell body rests directly on the foundation as anchored or unanchored to the ground; (ii) elevated silos (Kanyilmaz & Castiglioni, 2017), where the supporting system could be a structural frame or made by isolated columns (e.g., district supported silos)(Jansseune et al., 2016). In both configurations, an adequate clearance under the discharge gate of a silo is required to allow for easy placement of a discharge conveyor, or other device. Considering that, for the second configuration, a large space is required to allow for a possible transportation means beneath the elevated silo. However, for any of these typologies, the structural behavior of the shell body varies under different circumstances and different applied loads(Rotter, 2001).

## 1.2.2. Supporting arrangement

Silos vary in the supporting system depending on the capacity, usage, and operation. Hence, a significant variation in the structural behavior and the response to

different excitations (e.g., seismic loads) occurs as a function of the supporting arrangement. Assuming that ground supported silos rest directly on the foundations, different support arrangements could be recognized for elevated silos (for instance, see Figure 1-2) depending on the silo size and on the magnitude of the force introduced into the shell body by the local support. Light silos could be discretely supported by columns, where a limited number of equidistant isolated columns are used with (Zeybek & Seçer, 2020)or without (Gillie & Holst, 2003; Jansseune et al., 2013)transition ring girder around the circumference. In addition, different means are developed to arrange the column-shell attachment, so that the resistance of the shell body to the local buckling and local failure is increased.
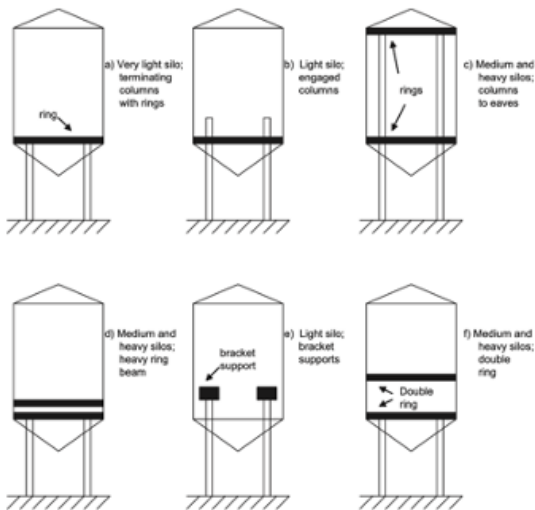


Figure 1-2 Alternative arrangement for silos with different supporting structures (Rotter, 2001).

Talking about the discretely supported silos, the main deficiency is that the structure suffers high local axis compressive stresses concentration, thus possible local failures can occur such as plastic yielding or elastic buckling. Concerning to this topic, Jansseune et al. (Jansseune et al., 2013) introduced a study in which a possible solution is suggested to increase the failure load of silos for this configuration. It consisted in adding longitudinal stiffeners as localized above each support resulting in a positive significant influence on the buckling behavior/loads. Nevertheless, it proves

to be disadvantageous from a certain critical height over which the column is attached to the silo. The dependency of the buckling be-haviour and the failure load on the thickness and radial width of the stiffeners was investigated in (Jansseune et al., 2015). Small silos with discrete supports could also be supported on local brackets attached to the side of the shell (for instance, see Figure 1-2). Later, Doerich and Rotter (Doerich & Rotter, 2008) presented a study outlining the behavior of discretely supported silos on several brackets rigidly connected to stiff columns. This study observed the local pre-buckling deformations and bifurcation mode and the local plastic collapse.

Another aspect which gains more interest among researchers is the ring girder, since it has a major role in reducing the potential buck-ling. The ring girder beneath the silo is responsible for redistributing reactions forces from supports into a more uniform stress state in the cylindrical shell body (Zeybek & Seçer, 2020). This aspect is dependent on the relative stiffness between columns and shell. In addition to that, the silo ring girder has a main role in carrying the circumferential force and to re-sist the radial component of the inclined tension in the hopper (Khalili & Showkati, 2012).

In discretely supported structures, a nonuniform axial compressive stress is developed in the shell wall. The uniformity degree of the stresses could be assessed by the criterion developed by Topkaya and Rotter (Topkaya & Rotter, 2011)basing on the relative stiffness of the ring beam and the cylindrical shell. Topkaya and Zeybek (Topkaya & Zeybek, 2018) presented a study aimed to assess the applicability of this criterion to cylindrical shells, accounting for global shear and bending. Combinations of different ring beam and cylindrical shell under global shear and bending actions were numerically analyzed, where the non-uniformity in the axial stresses was quantified. In conclusion, the result confirmed the applicability of using this criterion for the mentioned load conditions. The ratio between shell and beam stiffness was also addressed by Zeybek et al. (Zeybek et al., 2019), where a closed section ring beam with less stiffness than the ideal one was investigated. Still, the effect of the stiffness ratio on the ring beam stresses and on the buckling capacity of the shell was observed. The resultants stresses were recorded using a finite element (FE) parametric study

and the analytic solution of Vlasov's curved beam theory (Vlasov, 1961). The paper concluded that the design of a ring beam based on Vlasov's theory equation is conservative, since it ignores the contributions made by the attached shell and hopper. Moreover, the resulted stress reduction, compared to the values of the Vlasov's theory, could be attributed to the stress redistribution being partly achieved by the shell while this redistribution is determined by the shell-ring stiffness ratio. The shell buckling capacity suffers from significant reduction when the shell-ring stiffness ratio, $\psi$, exceeds the value of 0.1, and this becomes dramatic when $\psi$ exceeds 1.0 (Zeybek et al., 2019). With this regard, Zeybek and Seçer (Zeybek & Seçer, 2020)provided design expressions for a ring beam of elevated steel silos and the effect of its relative stiffness (shell/ring stiffness ratio) on the ring behavior considering different supporting systems. These parameters were varied by in turn considering four columns, four columns with secondary beams, and eight columns beneath the silo, with the aim to develop design guidelines for the support conditions (Zeybek & Seçer, 2020).

### 1.2.3. Imperfection effects and modelling

Silos in typical cases, steel silos design concerns about avoiding stability failures, as occurs in many different shell structures, whether in the form of local or global buckling failure. However, the buckling capacity is very sensitive to the geometric imperfections as a function of amplitude and form. Geometric imperfections can be defined as the shape deviations from the perfect structure due to the manufacturing process. Hence, in the design of silos, a local high pressure must be im-posed on the wall, for accounting the existence of geometrical imperfections.

In spite of the extensive experimental and theoretical works in the literature addressing the behavior of the axially compressed cylinders (Knoedel et al., 2017; Rotter, 1998b; Rotter & Teng, 1989), there is still a gap between the predictions obtained by the numerical models and the realistic results provided by the experiments. However, the usual scatter among numerical and experimental predictions, in terms of buckling capacity, could be chiefly traced back to the structural imperfections that are unavoidable in the practical construction(Teng et al., 2005). In addition, it is worth considering

that this discrepancy is much severe when combining other imperfection types, such as loading imperfections (Ning & Pellegrino, 2015; Wagner et al., 2020). This issue is considered as one of the main classical problems about homogeneous isotropic structural mechanics, which has not been fully understood (Rotter, 2006a). The classical formulation for estimating the buckling load of cylindrical shell was derived more than hundred years ago, without considering any kind of imperfection(Vynne Southwell, 1914):

$$N_{pre} = \frac{2 \cdot \pi \cdot E \cdot t^2}{\sqrt{3(1 - \vartheta^2)}}$$

1-1

where $N_{pre}$ is the buckling load of actual perfect cylindrical shells, E is the elastic modulus of the construction material, t is the wall thickness, and $\vartheta$ is Poisson's ratio of the construction material. How-ever, it has been long stated that the reduction of the geometrical im-perfections decreases the discrepancies between the experimental results and the analytical (Simitses, 1986; VON KARMAN & TSIEN, 1941) or numerical (Bisagni, 2000) estimates. Still, these differences are greater and greater in the case in which the axial com-pression is more significant than either pressure or torsion(Simitses, 1986). Nevertheless, there are no closed-form solutions to account for imperfection during the design phases (Castro et al., 2014).

Typically, in the design practice of thin-walled shell structures, the influence of the geometric imperfections could be considered by employing techniques known as artificial substitute imperfections (ASI)(Winterstetter & Schmidt, 2002). For example, eigen-mode imperfection technique could be adopted where the imperfection is assumed in the form of the bifurcation buckling mode taking into account varying imperfection amplitudes. Thus, the buckling strength could vary depending on the considered buckling mode and amplitude(Bisagni, 2000; Teng & Song, 2001). Eigen-mode imperfection is adopted in preliminary design of cylindrical shell structures; however, it could lead to a very conservative design and it is not easy to define the order and the magnitude of the rationally eigen-mode shape imperfections (Ismail et al., 2015). Techniques of ASI are developed in the literature based on probabilistic methods to represent the geometric im-perfection in cylinders. For instance, Monte Carlo simula-

tion and first-order second-moments method were developed by Elishakoff et al. (Elishakoff et al., 1987) aiming to determine the stochastic distribution of the buckling load. However, imperfection representation based on probabilistic methods are rather complex(Wagner et al., 2017). In the same context, Kriegesmann et al. (KRIEGESMANN et al., 2010) developed a probabilistic design procedure for cylindrical shells with a reduced computational cost comparing to the conventional ones. Away from probabilistic methods, different perturbation methods were introduced as deterministic approaches, such as the Single Perturbation Load Approach (SPLA) firstly proposed by Hühne et al. (Hühne et al., 2008) and dealing with thin-walled cylindrical composite shells. Inspired by SPLA, single perturbation displacement approach and sin-gle boundary perturbation approach were later developed (Wagner et al., 2017). Particularly, according to SPLA, the geometrical imperfection effect in a cylindrical shell could be included by introducing a radial perturbation load into the middle part of the cylinder. However, it was proved that using SPLA in the analyses of cylindrical shells provides realistic buck-ling characteristics(Castro et al., 2014). SPLA has been used in many studies for different kinds of cylindrical shells as isotropic metallic (Jiao et al., 2018)or composite (Castro et al., 2014; Khakimova et al., 2017). Unlike probabilistic approaches, SPLA is independent from the need of measured imperfections, however some limitations are noticed, as it does not cover all types of imperfections, as the boundary condition imperfection. Therefore, comparing the numerical results with the test buckling loads, the SPLA method can be not enough conservative, as shown in (Khakimova et al., 2017). Using this geometrical imperfection approach for isotropic metallic shells, the obtained results provide superior design loads if compared with the standard of NASA SP-8007 (Peterson et al., 1968), especially for those shells showing an axisymmetric buckling pattern in the pre-buckling range under axial loads (Wagner et al., 2017).

After, Multiple Perturbation Load Approach (MPLA) was introduced by Arbelo et al.(Arbelo, Degenhardt, et al., 2014) as an extension of the SPLA for composite cylindrical shell. According to this approach, multiple perturbation loads are considered instead of the single perturbation load. Thus, three parameters were accounted for: the

location, the number and the magnitude of the considered loads. Based on numerical and experimental approaches, Jiao et al. (Jiao et al., 2018) stated that MPLA is a more rational design method, especially for metallic cylindrical shell structures, comparing to SPLA. As a matter of fact, the lower-bound of cylindrical shell is sensitive to the number of perturbation loads, especially when these loads are evenly distributed along the circumferential direction. Still, the smaller inhomogeneous degree of the perturbation loads magnitude, the more possibility to acquire a robust lower-bound buckling load.

Steel silos are constructed conventionally by rolling separated steel panels and by welding them to form the silo walls, thus, unique imperfection types develop in the silo walls as consequences of the construction process. Another study proposed by Ding et al. (Ding et al., 1996b) indicated that the geometric imperfections in silos are closely associated with the joints of steel panels forming the wall. Using a numerical approach, Jansseune et al.(Jansseune et al., 2016) presented a study investigating the impact of different imperfection forms on the failure behavior of locally supported steel silos, considering different arrangements of stiffening/supporting and different equivalent imperfections shapes, e.g., nonlinear buckling mode, linear bifurcation mode, several post-buckling deformed shapes of the perfect shell, a weld-induced imperfection accounting for varying amplitudes and orientations. The study ranked the relevant imperfection shapes according to their adverse effects on structural behavior and response in terms of nonlinear buckling modes and post-buckling deformed shapes. It is worth noting that the circumferential weld depression (also named type A) is a realistic imperfection as it is closely related to the fabrication process of silo. However, it is relatively considered the most deleterious comparing to other imperfection forms according to this study. The study concluded that the inward imperfections are more unfavorable than the outward ones(Jansseune et al., 2016).

Nevertheless, optimization techniques, such as the one proposed by Ning and Pellegrino(Ning & Pellegrino, 2015), could be applied to the structural form of cylindrical shell for minimizing the discrepancy between the geometrically perfect structure and geometrically imperfect structures, i.e., producing imperfection-insensitive axially

loaded cylindrical shells. The technique mainly relays on achieving a reduction of the local radius curvature by changing the cross-section of the shell, to have an optimized wavy or sinusoidally corrugated wall based on numerical and experimental investigation(Jiao et al., 2018; Ning & Pellegrino, 2015). The optimized cross-section provides a shell with a low sensitivity to geometrical imperfections, and high critical buckling stress than those of conventional circular cylindrical shell. Eventually, the shell failed with highly localized buckling modes leading to a superior mass efficiency more than almost all previously reported stiffened shells (Ning & Pellegrino, 2015).

## 1.2.4. Buckling types and analysis

As with most of the conventional steel structures, buckling under vertical compressive stresses is the critical consideration for the thin-walled steel silos as prone to a loss of stability(Rotter et al., 1989; Sadowski & Rotter, 2010). The main sources of the vertical compressive forces in silos are the frictional traction pressure imposed by the stored material and the horizontal pressure. While the horizontal pressure imposed by the initial filling slightly increases with stored material depth, the frictional traction pressure significantly increases as the depth of the stored material increase, as shown in Figure 1-3 and according to the Janssen's theory (Janssen, 1895). For this reason, the tall (or slender) silos are built with RC material, where the vertical traction pressure dominates the horizontal one. Instead, steel shells are susceptible to vertical pressure, thus, the shortest (or squat) silos are usually built with steel, especially where the horizontal pressure is dominant with regard to the vertical traction pressure.
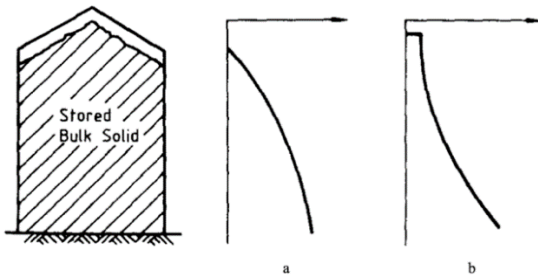


Figure 1-3 Silo and wall loads: (a) normal pressure; (b) vertical compression variation (Rotter et al., 1989).

20

Historically, an extensive knowledge was developed about the buckling behavior of an empty cylindrical shell under uniform com-pression even in combination with internal pressure. Different aspects of buckling and post buckling behavior of shell structures under uniform and well-quantified loads were addresses by several researchers, as defined in (Rotter, 2006b) and references therein. In (Teng, 1996)Teng extensively presented the research work performed on shell buckling through the last century. Nevertheless, the buckling strength of silos is dependent on many factors, such as the magnitude and distribution of both the frictional and horizontal pressures, the im-perfections amplitude and shape, the elastic restraint of the stored material against buckling. For instance, the eccentric filling or discharge causes variation in the applied pressure resulting in a worse stress state in the bin wall than even higher uniform pressure (Dogangun et al., 2009). Therefore, some studies were introduced in the lit-erature addressing the buckling behavior of silos under eccentric discharge. One of the earliest comprehensive studies was conducted by Rotter (Rotter et al., 1989), in which experiments were per-formed to investigate the buckling behavior of a cylindri-cal shell un-der pressure directly induced by the stored solids. This study took into consideration buckling strength increment derived from the stored solid stiffness. The study treated a flat-bottom silos considering con-centric/eccentric filling and dis-charge. For concentrically filled silos, according to the result of experiments, a benign buckle of mostly axisymmetric mode was observed with significant reserves of post-buckling strength comparing to the empty pressurized cylinders. For silos under con-centric discharge, an accentuated buckling mode was observed. However, larger and different buckling modes were observed under eccentric discharging with a cata-strophic collapse. In addition, two main remarks were also recorded as outcomes of this study: the first one is related to the filling depth, where it was found that the criti-cal filling depth under discharges is as low as that one when the silo under filling loads only; the second one is relevant to the channel of flowing, where it was found that it was not critical to the buckling strength(Rotter et al., 1989). Similar issues were studied by Rotter (Rotter, 2006a), which presented buckling features outlining of thin shells under axial loads. The study addressed moderately slender perfect silos.

Within this study, the author tried to come up with practical design recommendations. In this context, the study concluded that the behavior of these shells has many complexities, and to derive design rules out of the observed buckling features is far from being complete.

Moreover, the author stated that the effect of unsymmetrical axial distribution among the cylindrical is the most critical point to under-stand. On the topic, the European standard EN 1991-4 (EN 1991-4, 2006) suggests a unique approach (mentioned in section 1.5.5) to characterize the un-symmetric pressure exerted by eccentricities in silo filling/discharging. Sadowski and Rotter (Sadowski & Rotter, 2010) introduced a study addressing the buckling behavior and imperfection sensitivity of a moderately slender silo, considering the real-life conditions and more realistic situations by taking into consideration the eccentric solids flow and the associated unsymmetrical pressure on the silo wall. The study adopted the approach suggested by the European Standard EN 1991-4 (EN 1991-4, 2006) to characterize the unsymmetric pressure exerted by the eccentric discharge. The study defined the critical regions of the highest compressive axial membrane stresses where the silo may buckle, providing a dissertation on the phenomenon of the mid-height buckling failure that was frequently observed in the practice. In this phenomenon, a very high membrane stress developed in the thin wall coinciding with the lower bulk-induced internal pressures in the flow channel leads to eliminate the elastic restraint provided by the solids. The study mainly stated that a silo designed for symmetrical filling/discharging conditions only (according to EN 1991-4 ) may encounter a disastrous failure if eccentric discharging develops. In addition, this work was resumed by Sadowski and Rotter (Sadowski & Rotter, 2011a) for very slender silos, taking into consideration the imperfection sensitivity of the buckling failure mode. Similar-ly, this study characterized the unsymmetric pressure induced by the eccentric discharge in accordance with the description provided by EN 1991-4. Then, the geometric and material nonlinearities were considered for buckling calculations according to the European standards EN 1993-1-6 (EN 1993-1-6, 2007). Authors concluded that the approach of EN 1991-4 for unsymmetrical pressure modelling (induced by eccentric dis-charge) is highly damaging for a

22

very slender stepped-wall metal silo if it is designed only for symmetric pressure. The nonlinear FE model yielded that the European provisions EN 1993-1-6 should be re-edited as they are formulated considering experiments under axisymmetric conditions only.

However, the vulnerability of cylindrical shells to the different buckling modes could be reduced and the structural efficiency could be enhanced by adopting alternative structural arrangements, such as a closely stiffened shell, a cylindrical shell reinforced by stringers/corrugations(Błażejewski & Marcinowski, 2013), and rings (Jäger-Cañás & Pasternak, 2017), or even fiber (Jäger-Cañás & Pasternak, 2017)reinforced polymers (Batikha et al., 2018). In other words, the basic idea is to use a higher efficient material in silos construction. In practice, the shell body of the silo could be combined with ring or vertical stiffeners, aiming to reduce the thickness of the shell without decreasing the buckling resistance of the silo. Corrugated walls could also be used in combination with different stiffeners, as for example shown in Figure 1-4.

In the last few years, several researchers reactivated the research about stiffened shells used in the field of civil engineering. Some research directions approached the interaction of different strengthening techniques with corrugated shells. For instance, Błażejewski and Marcinowski (2013) introduced a study in which they investigated the buckling behavior of vertical stiffeners attached to the shell body of a corrugated silo. The considered stiffeners have the characteristics of cold formed steel sections. The paper deals with numerical modelling of the elasto-plastic collapse of the columns and it was revealed that the buckling resistances obtained by the proposed numerical approach were greater than their counterparts yielded by the European standard, appearing to be more realistic. In the same context, Rejowski et al, (Rejowski et al., 2023) presented a study devoted to assess the stability of steel cold formed silo stiffeners, through a FE analysis. In this study, different modelling approaches were considered along with the symmetric and axisymmetric loads imposed by the stored material, according to EN 1991-4 (EN 1991-4, 2006). The numerical calculations addressed a real cylindrical silo of corrugated sheets, with a 17.62 m height, 8.02 m di-

ameter and strengthen by 18 vertical stiffeners of open thin-walled load-bearing pro-files. The stability FE studies showed that the methods provided by EN 1993-1-6 (EN 1993-1-6, 2007)could be conservative, especially when considering the stiffener as a beam resting on elastic foundation, while the orthotropic shell theory is more realistic when comparing to the FE outcomes. Thus, authors suggested a modification on the column elastic foundation stiffness resulting in comparable outcomes to the obtained FE solutions. The same authors proposed a method for the buck-ling strength esti-mate for stiffened corrugated silo with different geometry and including a simplified model.



Figure 1-4 Silo corrugated walls in combination with the vertical stiffeners (well-known as silo col-umns) (Uckan et al., 2015).

Another way to increase the mass efficiency of thin-walled shells is represented by ring stiffeners. Jäger-Cañás and Pasternak (Jäger-Cañás & Pasternak, 2017) pro-posed a design procedure to bridge the gap in the standards related to quantifying the beneficial effect of ring stiffeners attached to the shell body under axial compression. The study addressed metal the study investigated the applicability of the available de-sign procedures for structures with significate radius/thickness ratio up to 10000 (this ratio is limited to 5000 in EN 1993-1-6). The study revealed that high slender stiff-ened cylinders showed about 380% strength gains as benefit from the ring-stiffening, if compared to the unstiffened case. Recently, a numerical study calibrated with ex-perimental series presented by Li et al.(Li et al., 2021). The study employed the 3D

scanning technology to measure imperfection, and the FE analysis yielded very close result to the ones of experiments. The research evaluated the influence of different factors (ring-stiffener parameters, imperfection amplitude, ring geometry) on the buckling load of cylindrical shell. Authors concluded mainly that the buckling capacity of ring-stiffened shells decreases significantly until the stiffener spacing is greater than two buckling half-wavelengths.

## 1.3. Earthquake loading and seismic response of silos

Accounting for seismic excitations, as one of the main hazardous actions on structures and infrastructures, the response of silos has long been the subject of intensive research studies(Rotter & Hull, 1989). A considerable research work has been undertaken through the last century addressing fluids-filled tanks to quantify the wall loads induced by seismic excitation where the sloshing action is a governing factor(Malhotra et al., 2018). However, what distinguishes silos from tanks is that the filling material is of solid nature. Consequently, only a specific portion of the seismic inertia load is transmitted to the walls thanks to the shear strength and the stiffens of stored bulk. Thus, the stored material properties have a significant effect on the silo seismic response. For instance, the wall-solids interaction and its effect on seismic response is a critical point to be mentioned (Guo et al., 2016). In general, the imposed loads by seismic excitation on a circular cylindrical silo walls are significant and could cause unsymmetrical pressures distributions on the silo walls. The main parameters governing the seismic response of the system are: (i) the height-to-radius ratio(Mehretehran & Maleki, 2018); (ii) the physical properties of the contained material(Guo et al., 2016); (iii) the characteristics of the ground motions(Younan & Veletsos, 1998); (iv) the effects of the wall flexibility(Younan & Veletsos, 1998). Several studies in scientific literature were introduced to increase the knowledge about the response of cylindrical silos storing granular material to earthquakes(Mansour, Pieraccini, et al., 2022). In this context, shaking-table/vibration tests (Holler & Meskouris, 2006; Silvestri et al., 2016)were carried out in many cases, aiming to characterize the response of the system and observe the relevant parameters, such

as the dynamic wall pressure, base shear, base moment in the wall, and the stresses exerted on the silo's foundation.

Going into detail, Younan and Veletsos (Veletsos & Younan, 1998) analytically examined a vertical, rigid and circular cylindrical tank storing homogeneous and linear viscoelastic solid under a harmonic earthquake-induced ground motion. The purpose of the study is to introduce a simple and reliable method of analysis for this kind of system. An analytical formulation was developed to describe the seismic response of the filled silo, which was adopted by the European standards EN 1998-4 (EN 1998-4, 2006). In particular, the seismic response of the system can be analyzed by quantifying the contributing mass to the base shear, which was demonstrated to be governed by the slenderness ratio and by the wall flexibility (relative to that of the stored material). Based on a FE model, Rotter and Hull(Rotter & Hull, 1989) derived design criteria for steel squat ground-supported silos, accounting for earthquake response under quasi-static horizontal body force (uniform horizontal acceleration). In this study, the stored mate-rial was characterized by its elastic modulus as an isotropic and homogeneous material. The results obtained in this study were implemented in EN 1998-4(EN 1998-4, 2006). With this regard, aiming to verify load assumptions recommended by EN 1998-4, Holler and Meskouris (Holler & Meskouris, 2006) characterized the behavior of seismically excited granular material steel silos. The study considered the variation of some key parameters, such as aspect ratios, the influence of the nonlinearity of the granular material, the wall-solids interaction effect and the soil-structure-interaction influence. The results of this study suggested to reduce the effective mass considered in the analysis to achieve more economic and realistic design than the ones provided by EN 1998-4. Specifically, the proposed loads are conservative in the case of squat silos, while they are adequate for slender silos. Similarly Yakhchalian and (Nateghi & Yakhchalian, 2012) presented further numerical investigation addressing the seismic behavior of flat bottom ground supported steel silos. The study emphasized the influence of the aspect ratio on the seismic response and concluded that assuming a constant value of acceleration distribution along the height of squat silos (based on EN 1998-4) leads to conservative design pressures for a

squat silo, while this assumption is not conservative for a slender silo. Nateghi and Yakhchalian (Nateghi & Yakhchalian, 2011) further investigated the effect of granular material-structure interaction under earthquakes for RC silos. This study takes into consideration different sources of nonlinearity in silo walls and in granular material. As main result, it was observed that shear cracks have developed when the interaction is neglected in the model. Silvestri et al. (Silvestri et al., 2012) evaluated, with an analytical approach, the exerted actions provided by grains on walls in circular flat-bottom silos during earthquake, leading to a new physically-based evaluation of the effective mass of grain. The study excluded the wavy wall silos. In particular, this study was devoted to the evaluation effective mass that acts on the silo walls during the earthquake. It turns out that this mass could be far less than the value proposed by EN 1998-4 (80% of the total mass). Consequently, lower horizontal actions than the one pro-vided by EN 1998-4 can be adopted (especially for squat silos) ¬and this result is also in accordance with the outcomes of the study presented by Holler and Meskouris (Holler & Meskouris, 2006). For example, for a low height/diameter ratio (less than 1), the effective mass can be assumed in a range from 30% to 70% of the total mass of the silo, with a variation depending on the friction coefficient developed between silo wall and filling material. Nevertheless, some theoretical limits were founded (Pieraccini et al., 2015). Refinements of the theoretical framework of Silvestri's approach (Silvestri et al., 2012) were introduced by Pieraccini et at.(Pieraccini et al., 2015), which provided a new set of analytical formulas for estimating wall pressures, wall shear and bending moment. A series of shaking table tests on scaled silos was performed by Silvestri et al. (Silvestri et al., 2016) offering an experimental verification of EN 1998-4 provisions and the analytical approach introduced in(Silvestri et al., 2012). The experimental campaign (on a silo-sample made of polycarbonate sheets) revealed the strong effect of the wall-grain friction coefficient on the base over-turning moment. This fact is in consistent with the analytical approach in(Silvestri et al., 2012), whereas this effect is disregarded by EN 1998-4. Moreover, the results of this study stated that the base overturning moment is conservatively estimated by EN 1998-4. It also suggested that the horizontal acceleration is not linear

in the vertical profile under earthquake input, although it is almost constant under low-frequency sinusoidal input. Later, basing on these findings, Pieraccini et al.(Pieraccini et al., 2017) presented an analytical formulation aiming to predict the natural periods of grain-silos. A study presented by Durmuş and Livaoglu (Durmuş & Livaoglu, 2015) investigated the effect of soil structure interaction (SSI) on the dynamic behavior of silo system containing bulk material under seismic activity. The study concluded that the SSI could be ignored in practice, especially for squat silos since there are no considerable effects. Recently, Butenweg et al. (Butenweg et al., 2017)presented a study comparing applicable analysis approaches for seismic load calculations of grain-filled cylindrical steel silos. The results provided by static equivalent load approach and nonlinear time history analysis were compared. Both grain behavior nonlinearity and grain-wall interaction nonlinearity were considered for nonlinear time history analysis, as well as the SSI. Authors concluded that using a simplified linear acceleration profile along the height provides conservative results. Alternatively, it is suggested to use multimodal analysis on a simplified beam model to determine a more realistic acceleration profile. In addition, the study affirmed that the approach of static equivalent loads does not accurately consider the fact that stresses vanish through the bulk material, especially in squat silos. Mehretehran and Maleki (Mehretehran & Maleki, 2018) investigated the effects of different aspect ratios on the dynamic buckling behavior of steel silos subjected to horizontal base excitations. Incremental dynamic analysis was considered for this study considering 10 different earthquake records. The main findings by this study suggested that, in presence of ground motions, slender silos are more vulnerable to buckling failure while squat silos present a considerably higher resistance under same seismic conditions. Recently, the same authors extended their investigation about aspect ratio influence on the silo dynamic behavior (Mehretehran & Maleki, 2021), by considering stepped walls steel silos under seismic excitation. Considering horizontal and vertical components of ground motion accelerations, different buckling modes were found, depending on the aspect ratio. Particularly, local diagonal shear wrinkles were observed in the elastic range for squat and intermediate slender silos, while elephant's foot buckling modes in the elasto-plastic range were

observed at the base for slender ones. Regarding the vertical component of the seismic excitation, it was stated that for silos this component has a quite marginal effect, and it could be ignored. Silvestri et al. (Silvestri et al., 2022) presented a study reporting a series of shaking table tests on a full-scale flat-bottom steel silo filled with wheat. The experimental study aimed to evaluate some parameters, such as the static pressure, the basic dynamic properties of the considered silo and the dynamic overpressure. To this aim, the fundamental frequency of vibration, the dynamic amplification and the dynamic overpressure were observed. On the level of static pressure, this study stated that, the horizontal static pressure distribution is qualitatively consistent with the theoretical expectations, during the dynamic tests, a redistribution of static pressures occurs due to the compaction of the granular solids. On the other hand, regarding the dynamic response, this study revealed that the damping ratio increases with increasing acceleration, consequently the dynamic amplification factor decreases. However, the dynamic amplification factor generally increases along the silo wall height (up to values around 1.4 at the top surface for earthquake inputs with a close-to-resonance frequency content). The resonance frequency (around 11 Hz for the case at hand) depends to a certain extent on the acceleration and on the granular solid compaction. In addition, the study stated that the measured dynamic overpressures seemed to be different from the EN1998-4 expectations with slightly larger values. Jian et al. (Jing, Chen, et al., 2022) presented a series of shaking table tests on flat-bottom ground-supported steel silos with corrugated walls. The experimental program aimed to evaluate the dynamic response and energy dissipation capacity of the system considering three different aspect ratios and their different seismic records. The results emphasized the fact that the energy dissipation capacity is much larger for the silos with full or half filling conditions (aspect ratio=1, 0.5) comparing to the empty condition (aspect ratio= 0). Furthermore, the study concluded that the acceleration vertical profile is a function of the aspect ratio, and the silo with full filling condition (aspect ratio = 1) had a smaller dynamic response than the one with half filling condition (aspect ratio = 0.5).

Regarding the elevated silos seismic behavior, it is worth mentioning that, in spite of the fact that the stored material behavior and solid-structure interaction have a significant importance for the seismic response of ground-supported silos (i.e., additional stresses develop in shell walls due to the response of ensiled materials(Rotter & Hull, 1989; Younan & Veletsos, 1998)), this is not applicable for elevated silos where the main concern is the supporting system and its attachment to the shell body of the silo. In fact, the stored material behavior and solids-structure interaction can be ignored in the analysis of elevated silos. For instance, a simplified approach is usually adopted for numerical studies, by simulating the silo content through static pressures and lumped-distributed non-structural masses (Kanyilmaz & Castiglioni, 2017).

### *1.4. The contained material properties, behavior and the imposed load*

After talking about the silos and their interactions with the external environment and the internal materials, the effective behavior of the mate-rial inside the silo is considered. As just mentioned in the Introduction, the main difference between silos and tanks is the contained material, which makes the difference in the loading conditions, grain-wall interaction condition and the response to different excitations. While tanks are used to store liquids that exerts only normal and symmetric pressure on the wall in the circumferential direction, silos are used for solid bulk materials exerting a normal pressure and interaction traction (symmetric or asymmetric) on the wall (Rotter, 2001). Different problems make the silos usage and design more problematic than tanks, which can be identified in the stored material anisotropy, material behavior asymmetry, and filling/flowing eccentricity. The stored material covers a large scope of free-flowing granular bulk with particle size ranging from micron size powders to lumps of 150 mm or larger. However, the contained material could be classified in multiple ways according to the relevant properties, as for example largely treated in (Maj & Ubysz, 2020a). Thus, each silo is designed for a limited range of solids, where using the silo to store bulks out of the anticipated range could imply damages. On the level of practical design, the different international standards ad-vise to determine the relevant material properties using either the pro-vided tables or the experi-

mental tests, as provided by the Australian standards (AS 3774-1996). Differently, the European (EN 1991-4) and the American standards (ACI 313-16) opt for the determination by test results. Still, the commentary part of ACI 313-16 suggests using tables as guide for the only initial estimation.

### 1.4.1. Filling material properties

The typical filling solids in silos could be basically characterized by: (i) the bulk unit weight; (ii) internal friction angle; (iii) and grain-wall friction coefficient. Several factors, such as temperature, moisture content, composition, grading, have a strong influence on the properties of the stored material and shall be accounted for in the design and assessment of silo structures. For example, the moisture content of the stored material has a strong effect on the coefficient of wall friction and on the angle of internal friction, which is also distinctly affected by the bedding material that varies according to the filling method (Schulze, 2021). Thus, a wide variability on the pressure ratio exists due to the effect of the abovementioned parameters change. Eventually, this variability of material properties casts a shadow over the silo operations, and it could cause asymmetry of loads, flow disturbance and frictional vibration (Horabik & Molenda, 2002). About this latter topic, intensive information can be found in (Maj & Ubysz, 2020a).

### 1.4.2. Discharging Patterns

Idea silos must ensure a regular solid flowing compatible with the intended patterns specified by the design that avoid the discharging problematic phenomenon. Consequently, the desired flow rate and the intended operation of the silos are guaranteed. Depending on the grain-wall friction characteristics and the flatness of the hopper wall (silo bottom hopper) (EN 1991-4, 2006), two main flow patterns could be distinguished when bulk solids is discharged (gravity flow) from the bottom of the silo. The first main type of flow pattern is mass flow (as shown in Figure 1-5-a), where the whole mass of the material moves downward whenever the outlet is opened (given that arching does not happen). The second main type of flow pattern is represented by the funnel flow (also known as core flow or pipe flow), where the material flows

from the top to the outlet through a funnel built by means of the material itself. In case of funnel flow, it is possible to develop stagnant zones (symmetric or asymmetric dead zones) in the upper silo part making pipe flow (as shown Figure 1-5-b), or in the lower silo part making mixed flow (as shown in Figure 1-5-c). Moreover, depending on the material proper-ties, outlet position and number of mobilized outlets, eccentric pipe flow (as shown in Figure 1-5-d) could develop as a one o funnel flow types, with eccentric channel forming near to the wall and exerting unsymmetrical pressure (Sadowski & Rotter, 2010).
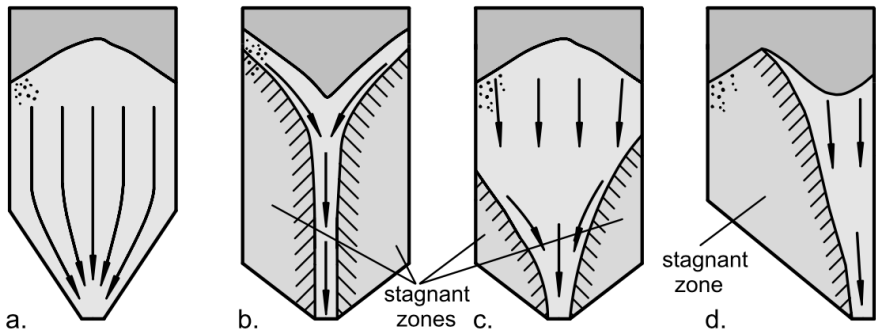


Figure 1-5 Flow profiles: (a) mass flow; (b) funnel flow (pipe flow); (c) funnel flow (mixed flow); (d) funnel flow (eccentric pipe flow) (Horabik & Molenda, 2002)

In the case of mass flow, the material at the center of the silo moves downward with the highest velocity, while the material near to the walls moves with the lowest veloci-ty due to the friction or to the flat-ness of the hopper wall (Schulze, 2021). For overly frictional or extreme flat hopper walls, flow velocity of the material vanishes near to walls and the mass flow pattern converts to be funnel and this gives an interpretation on how the flow pattern could vary during the silo lifetime, de-pending on the material and grain-wall frictional interaction characteristics. When the discharge process is proceeding, there is an increase in pressure imposed on silo walls. This increase is considered by the different international standards, which vary in the complexity and the accuracy. For example, depending on the storage capacity, the geometry, the possible filling/discharging eccentricities, EN 1991-4 suggests different approaches to calculate the additional stresses exerted through discharging.

With this regard, Vidal et al. (Vidal et al., 2005)presented a new dynamic model (employing Drucker-Prager plasticity model) for silo discharge simulation, considering mixed flow and mass flow silos. The study also investigated the variation impact of the wall friction and outlet radius. The outcomes of the study reported that the flat-bottom silos with mixed flow present overpressure values lower than the ones obtained in the case of hopper silos with mass flow pattern. Moreover, the overpressures mainly occurred in the lower part of the flat-bottom silo (14 m high and 2 m radius). The study also indicated that the discharge pressure increases as the size of the outlet increase and the grain-wall friction coefficient decreases.

## 1.5. International standards and solid-induced design loads

This section aims to define the general prescriptions provided by the main international codes quantifying the loads imposed by the stored mate-rial on silo walls. Thus, defining the uncertainties, deficiencies, and possible development in this aspect. As imposed loads impact the structure geometry and its structural arrangement, determining the relevant loads is one of the critical points in the design and assessment of the silo structure. Hence, solids-induced loads are of large magnitude, and they represent the dominant action on the silo, which has to be determined in a realistic way for having a reliable and robust de-sign. Historically, three scientists developed three different widespread theories for calculating the lateral pressure imposed by the stored material on the silo walls: Janssen in 1895 (Janssen, 1895), Airy in 1897 (AIRY, 1898) and Reimbert in 1976(Reimbert & Reimbert, 1976). However, till nowadays the recent standards (e.g., EN 1991-4, ACI 313-97, and ANSI/ASAE S433.1 JAN2019) adopt the Janssen's approach. Focusing on the main international codes re-ported in this work, 4 directions can be followed, as below reported. Nevertheless, the first standard accounting for the topic of the loads calculation in silos was the German standard, published in 1964 and reissued in 1987 and 2005 (DIN 1055-6:2005 ( 2014)), which was followed by several attempts to codify solid-induced pressure acting on silo walls. It has to be noted that the abovementioned standards vary in accuracy and complexity when dealing with solids-exerted load calculations.

This variance is especially noted in terms of classification, discharging loads estimation, and eccentric representing. Section 1.5.5 briefly shows the most comprehensive approach among the ones of the abovementioned standards that is suggested by EN 1991-4. However, mutual deficiencies were noted between these standards. For example, loads imposed on internals (defined as inserts used to control the flow pattern and eliminate the discharge disturbance phenomenon (Härtl et al., 2008)) are simply addressed by AS 3774-1996, while they are poorly considered by EN 1991-4, and never mentioned neither in ACI 313-16 nor in ANSI/ASAES433.1 JAN2019. Moreover, none of these standards deals with the imposed effect by these internals on silo walls, as well as sol-ids-exerted loads in case expanded flow developing.

## 1.5.1.    EN1991-4 (2006)

Commonly called "Eurocode", it is widely recognized as the world's most advanced standard of its kind, as well as the most comprehensive silo design code currently in use (J. Carson & Craig, 2015). Based on the reliability of the structural arrangement and the susceptibility to different failure modes, Eurocode's provisions classify silos into 3 different action assessment classes (named action assessment class 1, action assessment class 2 and action assessment class 3), which help to determine the level and the sophistication of analysis. These classes take into account the storage capacity, the geometry, the possible filling/discharging eccentricates. In addition, another classification based on the aspect ratio is considered by this standard. Thus, Eurocode proposes designs with essentially equal risk, in terms of load determination, which helps to provide logical treatment of different loads with varying complexity, e.g., the eccentric loads and discharge pressure. Therefore, this fact gives an advance over other international standards (Khouri, 2005). A noted insufficiency exists in covering some common load cases, such as the loads imposed by the grain swelling, expanded flow (combination of funnel and mass flow (Schulze, 2021)), external equipment and load variations due to inserting internals.

## 1.5.2. ACI 313-16 (2016)

This standard is directed to study the RC silos. Anyway, calculating methods of the loads exerted on silos should be independent from the construction material. This standard adopted Janssen's theory (Janssen, 1895) to calculate the static uniform filling pressure on walls. The dis-charge-induced pressure is computed by using a minimum value of the overpressure factor ($C_d$), assumed equal to 1.6. However, this is a rough estimation, and it is relatively large if compared to the load magnifying factors (horizontal pressure discharge factor, $C_h$, and wall frictional traction discharge factor, $C_w$) recommended by EN 1991-4 and determined based on equations after considering the action assessment classes of the silo. The old edition of this standard (ACI 313-97) ignored the calculation of non-uniform pressure exerted by asymmetric flow and did not endorse any method for evaluation the effect of the asymmetric flow. The current edition (ACI 313-16) mentioned two methods to deal with pressure induced by the asymmetric flow. In other words, it takes into consideration several aspects, such as the industry's experience of the professional design, the characteristic of flow pattern, the nature of the surfaces and the stored material and suggests using either flow channel method or eccentricity method. In this sense, Eurocode suggests different approaches to deal with the non-uniform pressure induced due to asymmetry, by considering patch loads or nonuniformly distributed pressure based on the silo classification, wall thickness, aspect ratio and eccentricity.

## 1.5.3. AS 3774-1996 (1996)

The Australian standard was first published in 1990 and revised in 1996 and it is considered the most compatible code with the European standard, even though it does not adopt the action assessment classification. However, it considers different systems of classification for containers depending on geometry, wall surface characteristics, means of flow promotion, pattern and geometry of the flow. Further classification systems for the bulk solid are considered on the base of the particle size. In addition to that, this standard recognizes 4 different load groups, which are subdivided into load types. The load groups are: group A (dead loads), group B (normal ser-

vice loads), group C (environmental loads) and group D (accidental loads). However, some deficiencies exist in quantifying solids-exerted loads in case of mixed/expanded flow.

### 1.5.4.   ANSI/ASAE S433.1 JAN2019 (2019)

This standard was developed in 1988 by the American Society of Agricultural and Biological Engineers (ASABE) and it was approved for first time as American national standards in 1991. Later, the most recent version was revised and approved by the American National Standard Institute (ANSI) in 2019. The scope of this standard was limited to provide only centric filling/discharging loads (adopting Janssen's theory) and flowing methods to store agriculture whole grains. However, it does not provide any rules to cover the solid-exerted loads in case of mass flow, expanded flow pattern, and some hopper geometries (e.g., asymmetric cone/square pyramid and multiple hoppers joined together).

### 1.5.5.   Loading philosophy according to EN 1991-4:2006

Generally, three main factors must be considered to estimate the loads exerted on silo walls: the silo geometry, the stored material properties, and the discharge flow pattern. Since the pressure applied on the silo wall differs depending on the stored material situation (flowing or stationary) and on its flowing pattern, the assumption of a uniform distribution around the perimeter of the bin is one of the most common design errors causing failures (Dogangun et al., 2009). As a matter of fact, an increment of the uniform pressure may be imposed to cover the discharging and unsymmetrical actions caused by eccentric filling/discharging. Generally, the loads imposed by the stored material on silos could be classified to horizontal wall load, wall frictional pressure, patch loads, hopper loads, and kick loads. This Section addresses solids-exerted loads on the silo walls. These loads could be symmetric or asymmetric, either distributed or patch loads and they are represented according to the different standards. For instance, according to EN 1991-4 and de-pending on the action assessment classes of the silo and its geometry, the loads imposed by the stored material on the vertical silo wall could be calculated. These loads are generally

36

classified into two main categories: (a) filling loads; (b) discharge loads. The design may depend solely on the filling loads, only if the internal pipe flow is guaranteed. However, the filling loads are represented by a uniform symmetric pressure, that is a static pressure subdivided into horizontal and frictional traction induced by the stored material and affected by several factors, as the silo geometry, material properties and the wall-material interaction coefficient. In addition to the symmetric filling pressures, filling patch loads, expressed in terms of localized horizontal loads, should be considered without an associated frictional traction. Patch loads are considered to account for unsymmetrical pressures caused by a possible eccentric pile of filling, especially in case of small eccentricities. On the other side, unsymmetrical distribution of the horizontal pressure should be considered in case of large eccentricities. Similarly, discharge loads are represented by a uniform symmetric distributed pressure in combination with patch loads. The uniform discharge pressure can be considered by increasing the uniform filling pressure using discharge magnifying fac-tors, in order to account for the increasing in both the horizontal and frictional pressure. Discharging patch loads can be considered in a pattern of only normal pressure (no frictional traction) to account for the accidental asymmetry of loading during discharge in case of small eccentricities, while the unsymmetrical horizontal pressure on the wall should be accounted in case of large discharging eccentricities. Patch filling/discharging loads may be ignored for silos in action assessment class 1, while a uniform increasing in the symmetrical pressure may be used when considering special structural arrangements to substitute these loads in the action assessment class 2. When large eccentricities are expected, as large outlet eccentricity or large filling eccentricity with high slenderness, a special procedure must be followed to account for the unsymmetrical wall pressure distribution resulted by the eccentric pipe flow channel. In the end, the loads on the vertical walls could be expressed in terms of symmetrical loads, due to filling and discharge that include horizontal pressure and frictional traction. In addition, the unsymmetrical loads caused by filling/discharging eccentricities should be represented either by considering patch loads for small eccentricities, or by considering unsymmetrical pressure (horizontal pressure, defined as $p_h$, and wall friction-

al traction, defined as $p_w$) for larger eccentricities, depending on the action assessment class of the silo.

## 1.6. Failure in silos: main causes and modes

Depending on the function, location (e.g., industrial site) and usage of silos, un-conventional conditions and loads could be imposed on the silo structure in combination with solids-exerted pressures. Thus, extensive stresses/deformations could develop in the walls. However, as thin-walled structures, steel silos have a susceptible structural configuration, storing massive content of the material that could touch thousands of tonnes. Hence, unusual failure modes are frequently observed in the real life, leading eventually to a catastrophic collapse with considerable consequences, costs, and even loss of life. Moreover, silos could lose their functionalities due to discharge disturbance phenomena, such as arching(Walker, 1966), ratholing (Schulze, 2021), silo quake (Muite et al., 2004), segregation (Y. Liu et al., 2019). However, these phenomena are basically affected by different parameters, such as the solids properties/behavior, wall frictional characteristics, filling method and the discharge flow pattern. However, different failure modes and shapes could occur in silos depending on the capacity, geometry and the construction material, as it is reported in the literature (Maj, 2017; Maraveas, 2020; Rotter, 2009). For instance, elephant's foot buckling (an outward bulge just above the base of the cylinder) is one of the main failure modes that can be noted in the steel cylindrical shells, as a result of combination of axial compressive stresses, circumferential tensile stresses and high shear stresses(Rotter, 2006b). In the following, several causes of silos damage are reported, accounting for several topics developed in the scientific literature, such as design errors, constructional errors, misuse errors, maintenance errors, up to define the collapses provided by soil damages, extreme events such as earthquakes, thermal ratcheting, and dust explosion phenomena. When talking about silos failures, the complete collapse is often achieved when an extensive deformation occurs, and, in most of the cases, the failure could be attributed to lack knowledge in the abovemen-

tioned aspects or in the combination of any of these categories that contribute to the collapse.

One of the most commonly design errors is the lack of the knowledge about the flow pattern in case of the discharging process, where the designer should be aware of the required flow pattern based on the functional requirement. The silo design should guarantee that the discharge process follows the assumed flow pattern (J. W. Carson & Holmes, 2003). Moreover, silo design should account to resist the imposed pressure through the intended discharge process, which varies according to a flow pattern. Furthermore, the actual flow pattern may oscillate between mass flow and funnel flow, as a function of several governing parameters including the moisture, particle size and temperature of the stored material(J. . Carson & Jenkyn, 1993). Therefore, any mis-assessment in any of these aspects could lead to deficiency in the usage and it may lead to failure with devastating results. For example, the discharge pressure could be ignored when pipe flow - but not inclined pipe - is ensured by the geomatical design or by mechanical equipment, while unsymmetrical pressure should be considered when mass or mixed flow occurs with or without partial contact to the silo wall. With this regard, Zaccari and Cudemo (2016), reported the failure event of a steel silo containing thousands of tonnes of limestones used in thermal-power plant. The failure involved a very huge shell deformation of the wall, as shown in Figure 1-6, which is constructed with a stepwise manner of thickness. The study attributed the failure to the miscalculation of the pressure distribution imposed by the eccentric solids flow(Zaccari & Cudemo, 2016). with the same regards, since the flow pattern is extremely influenced by the stored material properties, researchers, e.g.,(J. W. Carson & Holmes, 2003), and some standards, e.g., (EN 1991-4, 2006)(ACI 313-16:2016, 2016), stated that the material properties should be determined by testing representative samples of the material, instead of using some tables to determine the material properties that could be risky at best.

Figure 1-6 Huge shell deformation caused by buckling (Zaccari & Cudemo, 2016).

As just anticipated above, another cause of failure is given by the asymmetric dispo-sition of the filling material (eccentric material withdraw-al). In such case, an eccen-tric flow channel can develop in silos, occur-ring in several situations such as the nonuniformity in outlets opening, or improper design of the feeder. This phenomenon causes a severe non-uniform circumferential pressure(Sadowski & Rotter, 2010), which is either over-looked by the designer or incorrectly accounted, and eventually it causes collapse or buckling at best, as shown in Figure 1-7. Therefore, more failures have occurred under the condition of asymmetric flow patterns than any other(Sadowski & Rotter, 2011a). In this context, Kobyłka et al. (Kobyłka et al., 2019) stated that non-symmetric pressure could be imposed on the silo wall due to inserts or asymmetric flow patterns. Moreover, an experimental study introduced by Ham-madeh et al. (Askif et al., 2020) revealed that the change in the location of the inserts (particularly top cone with trunk cone bottom) has an important impact on the flow pattern and on the flow pressure. Practically, the study stated that, an improved flow shape is developed with a corresponding lesser flow dynamic pressure if inserts are positioned close to the transition section of the silo. However, the generated non-symmetric pressure could combine with the local pressure peak, causing structural deficiencies even for a slightly asymmetric flow pattern that could be ignored by the designer. With this regard, Horabik et al. (Horabik et al., 2002) found that the load

40

asymmetry resulting from off-center discharge could be reduced by the anisotropy of the mass of the grain, which could be achieved by imposing an off-center filling.

Moreover, another of the failure causes that could be avoided in the design stage is the changing in the storage condition. As the majority of the solids stored in silos in practice has a high dependency on different parameters (Horabik et al., 2020), such as compaction, moisture content, and internal/atmosphere temperature fluctuations. For example, some bulk solids tend to expand with higher moisture content, leading to a possible in-creasing in the lateral pressure on the silo wall, thus increasing in the hoop stresses(J. W. Carson & Holmes, 2003), which may be not accounted for in the design stage. However, that could be avoided by designing for wider range of possible moisture content.



Figure 1-7 Extreme damage in grain silo caused by asymmetric flow pattern (Zaccari & Cudemo, 2016).

Silos could suffer from other issues, such as construction errors. Typical examples of constructional errors are the unauthorized design changes and poor-quality workmanship, as it regularly happens in other construction sites. Nevertheless, the effect of these errors could be eliminated by avoiding unauthorized changes in the design during the construction, following the work plan set by the designer and employing qualified contractors by ensuring close inspections of the construction process (J. W. Carson & Holmes, 2003). Still, despite of a proper design and a precise construction work, silos could fail. The reason of this occurrence could be utilizing the silo for ap-

plications differs from the purposes for which it has been designed. In fact, silos are very sensitive to the material filling and the related properties(Horabik & Molenda, 2002). Different logistic issues could be raised when the stored material presents a wide variation from the material considered in the design, such as the variation in the flow pattern, or the different load conditions. In addition, possible flow obstruction could be experienced such as arching. In case of arching phenomenon developing, the full weight of the silo content applies on the formed arch that transfers it, in turn, to the arch ends. Eventually, if high concentrated reaction forces are applied on the silo walls, this provokes potential local plastic failures, as for example shown in Figure 1-8. Furthermore, using the silo to store different materials could also result in self-induced silo vibration and dynamic loads(Muite et al., 2004). However, at some point of the silo life, the changing of the usage purpose of the facility could be required and, to avoid any cata-strophic consequences, a structural assessment should be implemented to check any possible deficiencies that would yield from these changes.
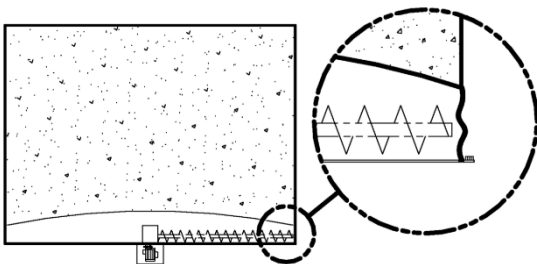


Figure 1-8 potential failure mode due to buckling of unsupported wall in case of arching phenomenon(J. W. Carson & Holmes, 2003).

To ensure long life span and safe operation of silos, it is necessary to provide a regular maintenance. With this regard, it is necessary to observe the visible defects on silos, which are caused by the ordinary or overuse of the silo structure. Typical defects in steel silos could be local deformity, waviness, dents, thickness reduction, and distorted joints/bolt-holes, as mentioned. However, other common defects are typically observed for RC silos (Maraveas, 2020)(e.g., cracks, corrosion, exposed rebar, spalling concrete and deterioration in RC walls). While ignoring the need for maintenance and overlooking the observed distortions could lead to potential collapse and structural deficiencies, improper maintenance can end with counterproductive effects. For ex-

ample, changing the internal wall surface finishes by painting may lead to change in the frictional properties of the wall. Consequently, new frictional characteristics can diverge from the specifications set out in the design, resulting in a significant impact on the flow pattern and thus on the solids-exerted loads (Saleh et al., 2018). Obviously, cladding or internal lining material should be durable, and not react with stored substances inside the silo. With this regards, same effects are ap-plied if the internal wall surface finishes change due to the corrosion (roughening) or abrasive wear (polishing or roughening) over time (EN 1991-4, 2006).

Furthermore, as any other structures, silos could collapse due to failure of the soil. Considering that silos have a small floor area or diameter compared to the height (whether it is steel or concrete), large stresses can develop in the soil under it, mainly due to the massive weight of the bulk material. Generally, the silo's foundation design is more critical if compared to other standard structures. In the typical case, uniform stresses (pressure bulb) develop in the soil under foundation and problems could raise when the pressure blub is distorted due to off-center filling/discharging (Dogangun et al., 2009) or when lateral loads as wind and earthquake occur (Durmuş & Livaoglu, 2015). When pressure blubs overlap under adjacent silos (e.g., cellular structure), the soil is overstressed, and the structure ends up with extreme settlements. A typical example of this effect is the well-known case of the Transcona Grain Elevator accident(Puzrin et al., 2010), Canada, where the plant was made by 65 bins covering several square miles. The silos battery was built hundred years ago and it failed after only one month after the construction completed (Figure 1-9), as it was loaded to 87.5% of its capacity within a month (quick loading)(Puzrin et al., 2010). It was observed that foundation failures in clay occurred when the silo is quickly loaded for the first time(Dogangun et al., 2009). Luckily, the foundation problems were solved, the grain elevator was righted, and it is still in use.
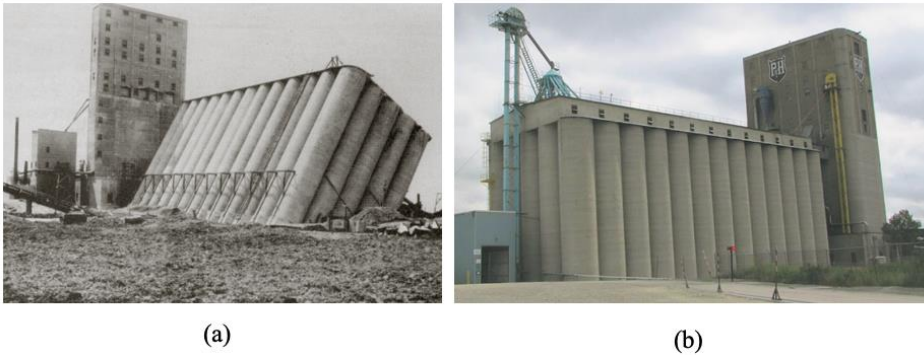
Figure 1-9 Soil failing underneath grain silos battery: (a) after accident; (b) recent photo of the righting bins.

Another highly investigated cause of silos collapse is the exposure to extreme events, such as earthquakes. Seismic action can cause serious accidents as observed for example in Italy after the recent 2012, Emilia–Romagna earthquake event. As occur for buildings(C. Liu & Fang, 2020), extreme events like earthquake can provide progressive collapses that in silos can occur also for static loads(Kenneth, 2003). Focusing on earthquake, in similarity with the buildings, damages on silos structures can be firstly observed and mapped(C. Liu, Fang, & Zhao, 2021), and after in the case of not total collapse, they can be adequate with proper retrofit techniques (C. Liu, Fang, & Yan, 2021). Another topic of interest is the kind of hazardous event, which can cause different responses on the focused structure, on the base of some characterizing parameters (e.g., magnitude, ratio, or see (Sun et al., 2013) for more information). In general, silos under earthquake suffer from additional stresses combined with the ones induced by the stored material, mechanical equipment and different sources. Slender silos are the more vulnerable to horizontal forces, as they could be subjected to over-turning due to high seismic inertial forces, especially when the an-choring or the foundation fails. What makes this effect more problematic, is the massive weight of the stored material, which increases the weight of the entire structure. As shown in Section 1.3, the effective seismic mass of the stored material is an active research zone, and it is still a matter of dispute among researchers. Figure 1-10 shows the collapse of a slender steel silo after the seismic swarm occurred in the Emilia–Romagna, Northern Italy, in 2012. Also, visible buckling dam-ages in the high-

ly stressed areas were observed on the other three silos of the group (Butenweg et al., 2017).



Figure 1-10 Overturning and damages of steel silos due to a seismic swarm hit Emilia Romagna, Italy, 2012 (Butenweg et al., 2017).

Many strategies were introduced by the literature regarding the seismic risk mitigation of elevated (Kanyilmaz & Castiglioni, 2017) and flat-bottom ground supported silos or tanks (Basone et al., 2019). For instance, Basone et al. ( 2019) presented a study in which the seismic vibration-induced damage of ground supported fuel storage tanks was investigated. However, similar strategies could be extended for silos storing solid materials. In this study, new type of seismic isolation was adopted to mitigate the seismic risk, which was based on a finite locally resonant metamaterial concept. To this scope, four meta-foundations characterized by different layers and column heights were designed, exploiting properties of metamaterials and combining them with classical seismic isolation concepts by using the traditional construction materials (e.g., steel, concrete and wire ropes). The study was made in accordance with the Italian standards and considering the response spectrum for an active seismic site located in Sicily, Italy (peak ground acceleration, PGA, of 0.56 g for safe shut-down earthquakes and soil type B). Two tanks were evaluated by means of a performance index (PI), and an energy dissipation index (EDI). Time history analyses showed that base shear was reduced by 10%-15% for slender tank with one-layer meta-foundation. Nevertheless, it was observed that the case of two-layer meta-foundations presents low efficiency for this tank typology. On the other hand, in case of board tanks, the base shear is reduced by up to 30% with one-layer meta-foundation and about 10%-15% in case of two-layer me-ta-foundation. Moreover, the effectiveness of base isolation as passive control systems was presented by Paolacci

et al. (Paolacci et al., 2012), where the effectiveness of different isolation techniques on floating-roof steel storage tanks was investigated through numerical and experimental models of shaking table tests ("La Casaccia" Research Centre - Rome, Italy). Particularly, two alternative base isolation systems have been used: high damping rubber bearings devices (HDRB) and PTFE-steel sliding isolation devices with c-shaped elasto-plastic dampers (SIEPD). The test was performed on a reduced scale (1:14) physical model of a real steel tank (diameter 55m, height 15.6 m) typically used in petrochemical plants. The results affirmed the high efficiency of both the isolation systems and, at the same time, the reliability of lumped mass model for the prediction of the seismic response of isolated above-ground tanks. In the same context, a study presented by Kanyilmaz and Castiglioni (2017) investigated the efficiency of traditional base isolation techniques (curved surface slider) to reduce the seismic vulnerability of elevated steel silo group, taking a real case study located in Livorno (Italy) as a reference. A three-dimensional model was developed, by using the simplified approach proposed by Castiglioni et al. (Kanyilmaz & Castiglioni, 2017), where the silo content is simulated with static pressures and lumped-distributed masses. For the purpose of this study, a single curved surface slider was proposed (designed and optimized based on the horizontal stiffness and the friction parameters) and the seismic performance was compared after and before the retrofit interventions. Whereas the original system suffers from stress concentration, elastic deformation and yielding in the supporting structure, it was noted that all the response parameters were positively reduced after retrofitting. The different observations proofed the advantages of the suggested system in terms of inelastic deformation, global horizontal shear, inter-storey drift, isolator displacement and residual displacement.

Another cause of failure of silos is given by the mechanical phenomenon known as thermal ratcheting. This effect could develop in the metal silos, since steel is more sensitive to temperature fluctuation than the RC. In general, for a possible rise in internal/external temperatures, steel walls of the silo expand allowing the stored material to settle. However, when the temperatures drop, silo walls are subjected to a contract (or a shrink), which goes in contrast with the settled particles that cannot move if a

46

discharge phase is not taking place. Thus, the expansion becomes irreversible and thermal stresses accumulate, which in turn amplify the tensile stresses in the wall. This phenomenon is repeated over many and many thermal cycles and, eventually, this ends up in failure. This phenomenon could occur due to any cyclic swelling and shrinking conditions (e.g., moisture fluctuating) applied to the stored material, as shown in (H. V. Kebeli et al., 2000). One famous example of this kind of failure is reported when describing the collapse accident of a new brand steel silo containing thousands of tonnes of fly ash, shown in Figure 1-11, and located in southwestern United States (J. W. Carson & Holmes, 2003). The experts attributed the accident to the thermal ratcheting phenomenon, which was not considered in the design. Despite this, most of the main inter-national standards account for the thermal ratcheting effect, especially the European, the American and Australian ones. About this topic, scientific literature provides different detailed stress models to account for the phenomenon of thermal ratcheting, often opting for FE methods. On the other hand, a discrete element method (DEM) along with experimental tests approaches was defined by Sassine et al. ( 2018). This study investigated the effect of this phenomenon on the shell walls of tanks used in thermal energy storage systems (as essential parts in power plants). The investigated silos typically contain a thermal storage medium of solid material (e.g., steel, sand, gravel, or rock). The functionality of this kind of silos makes it exposed to differential expansion between filling and walls. DEM was used to simulate the stored material and two different thermal approaches were considered. Specifically, homogenous heating and vertical gradient heating along the wall's height were investigated as typical thermal configurations. The study revealed that higher stresses develop in silo walls in case of thermal gradient along the height. Moreover, the significant effect of slenderness ratio, the internal friction, and the solids-wall friction on thermal stresses was affirmed through the simulation of DEM. An increased radial stress was recorded and it was equal to 3 times the initial one after performing 108 cycles. In the same context, a statistical description of the pressure on the wall of silos storing hot material was introduced by Maj and Ubysz (Maj & Ubysz, 2020b).

The study employed an experimental and statistical approach to quantify the total load given by the combination of thermal loads and static loads on the walls of RC silo.
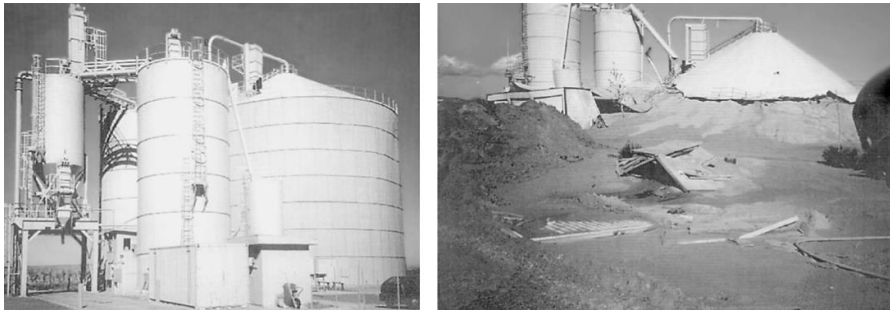


Figure 1-11 Steel silo of 24 m-diameter split apart about two weeks after its first full capacity filling (J. W. Carson & Holmes, 2003).

Still, in the context of extreme events threatening silos, an explosive atmosphere could be created inside the silo depending on the nature of the stored substances. The risk of fires and explosions is presented inside the silo (Eckhoff, 2009). For example, airborne organic/metal dust generated during loading and discharging, or gas generated within the container, such as bulk-emitted flammable gases during the storage or fermentation process (fodder) leading to methane generation. However, pressure loads exerted by industrial dust explosions are extremely complex to quantify and predicting their consequences by numerical models (depending on fundamental, physical and chemical principles) in general is beyond reach(Eckhoff & Skjold, 2016). Pineau et al. (Pineau & Masson, 2001), introduced a study about an accident of grain silo explosion, as shown in Figure 1-12, at Blaye, France, occurred in 1997 and causing 12 casualties. Particularly, the final report of the accident (Pineau & Masson, 2001) suggested that the explosion could be attributed to the generation of flammable dust-air mixture inside the silo along with existence of ignition sources (sparks or mechanical heating effects, static electricity, electrical sparks, or the self-ignition of a deposit of dust).

48

a                                                                                                     b

Figure 1-12 Explosion of RC silo Battery (a) before explosion, (b) after explosion, Blaye, France, 1998 (Pineau & Masson, 2001).

However, the explosion risk in silos could be eliminated by following the preventive measures: (a) avoid design for near horizontal internal surfaces where the dust may accumulate; (b) provide explosion relief vents or doors (Tascón, 2017); (c) select the proper electrical equipment to re-duce the risk of dust explosion according to the relevant standard, e.g., EN 61241-17 ( 2005); (d) classify the hazardous areas in relation to combustible dusts according to the relevant standards, e.g., EN 50281-3 (2002); (e) locate the electrical equipment or the sparks sources away from the hazardous areas; (f) provide lighting protection as an ignition hazard.

## 1.7. Assessment of existing steel silos

As last part of this chapter, it is essential to mention that despite of the fact that robust design methodologies can be improved to avoid the risks mentioned in Section 1.6, it is necessary to prevent losses by monitoring the conditions of existing silos aiming to assess the behavior under the realistic circumstances. Consequently, a safe and continuous operation of these structures and the relevant facilities must be guar-anteed. In fact, destructive (DTs) and non-destructive tests (NDTs) have been developed as tools to estimate the cylindrical shells efficiency, or as proof-testing of structure, or for the purpose of theoretical analysis validation. However, the common buckling tests have a destructive or terminal nature, as the loaded structure buckles with large plastic deformations. Thus, the same test cannot be repeated and definitely it is not suitable for silos in service. However, for more practical solution, several as-

sessment techniques were developed as NDTs applicable for existing silo structures. Generally, non-destructive methods can be classified to be whether dynamic or static and they could be employed for either direct determination of the buckling load and determination of the actual boundary conditions leading to better numerical determination of the buckling load. One of the first NDT to predict the buckling loads of steel structures is the Southwell approach, which was initially developed for a simple column (Vynne Southwell, 1914).

Later, this approach was extended to include cylindrical shell (Galletly et al., 1958), but the notable drawback of this approach is represented by the need of applying high loads, in order to come up with reliable prediction and this can threaten the non-destructive feature of the test (Kalnins et al., 2015). However, one of the most common NDT is the vibration correlation technique (VCT) that is being employed, now days, to predict the buckling capacity of shell structures used for several applications. In the following, this technique and its applicability for silos is presented. For purpose of vulnerability assessment, the vibration correlation method can be used. This method can be defined as an NDT used to estimate the buckling load from the pre-buckling stage of the structure, basing on the variation of the natural frequency with the applied loads. Historically, this approach was firstly derived for columns de-pending on the fact that the buckling modes and vibration modes are similar for a simple structure of a column. In other words, this method takes advantage from the similarity between the buckling behavior and the free vibration behavior of the relevant structures. The relationship between the squared frequency and the compressive load is nearly linear for columns with different boundary conditions (Lurie, 1950), while it is exactly linear in the case of simple supports columns, where the vibration mode is identical to the buckling mode:

$$\left(\frac{\omega_n}{\omega_{n0}}\right)^2 = 1 - \left(\frac{P}{P_n}\right)$$

1-2

In the equation, $\omega_n$ is the $n^{th}$ natural frequency of the loaded column, $\omega_{n0}$ is the $n^{th}$ natural frequency of the unloaded column, P is the applied load, and $P_n$ is the Euler buckling load corresponding to $n^{th}$ vibration mode. Later, VCT was further developed

to address plates (Arbelo, de Almeida, et al., 2014) and shells (Skukis, Ozolins, Kalnins, et al., 2017). The main feature of this method is the ability to estimate the destructive buckling behavior of relevant structure from a simple vibration test, where results are obtained by subjecting the addressed structure (e.g., cylindrical shell) to compressive loads with-out reaching the instability point. This technique was thus extended for plates by Lurie (Lurie, 1950), which declared that VCT is reliable only when it is applied on specimens having small initial imperfections. This fact was also confirmed by Chailleux et al.(Chailleux et al., 1975), identifying a re-markable deviation from linearity in the case of plate structures with relatively significant initial imperfection. Some attempts to exploit the concept of VCTs for cylindrical shells were firstly proposed in 1970s (Rosen & Singer, 1976), for the purpose of aerospace applications. In this application, VCT was used for determining the actual boundary conditions in numerical calculation of stringer-stiffened shells, as based on laboratory-type and on realistic boundary conditions. Currently, several researchers attempt to further exploit VCT for the purpose of erected cylindrical shell assessment. For instance, Arbelo et al. (Arbelo, de Almeida, et al., 2014) identified the range of applicability of the VCT for unstiffened cylindrical shells, showing the efficiency of the technique applied to these structures. In addition, authors demonstrated the advantages given by the results of the FE modelling, considering the realistic boundary conditions obtained by VCT in conjunction with an actual measurement of the initial geometric imperfections. On this base, in (Arbelo, de Almeida, et al., 2014) a new methodology to estimate the buckling load of unstiffened cylindrical shells using the VCT was proposed. An experimental verification of this approach was presented by Kalnins et al. (Kalnins et al., 2015), which measured the first natural frequency of vibration and the related mode shape by using a 3D laser scanner on two composite laminated cylindrical shells and two stainless steel cylinders. The authors recommended the monitoring of the first and second vibration modes, as this latter can provide a better prediction when compressive loads increase. In addition,  (Arbelo, de Almeida, et al., 2014) suggested that the maximum load to be adopted in the VCT should be limited to 50% of the buckling load as non-destructive test. Still, the investigated approach presented in (Kalnins et

al., 2015) returned a very good correlation when the ratio of the test applied load to the experimental buckling capacity is higher than 80%. This fact was also demonstrated by a further experimental work presented by Skukis et al.( 2017), which addressed unstiffened cylindrical shells loaded in axial compression and two laminated composite cylinders loaded repeatedly up to instability point. The study concluded that tests up to 65% of the buckling load can give a 90% fidelity in estimation of buckling load. Moreover, the applicability the modified VCT, presented in(Arbelo, de Almeida, et al., 2014), has been investigated by Skukis et al. (Skukis, Ozolins, Andersons, et al., 2017) for the thin-walled isotropic cylindrical shells with and without circular cut-outs. The study concluded that VCT provides a reliable estimation of the buck-ling load of uncut shells and when the global failure mode is governing the collapse. On the other hand, the study stated that using VCT for shells with a cutout is invalid due to developing of local buckling. The study suggested that the global failure mode and the reliability of the VCT estimation could be enabled for these shells by using reinforcement with a ring of the same material, adhesively bonded around the cutout. In addition, using an analytical approach, (Franzoni et al., 2019)et al. demonstrated the reliability of the approach suggested in (Arbelo, de Almeida, et al., 2014) for isotropic unstiffened cylindrical shell. The study defined the basis of numerical modelling for which the second-order relationship be-tween the applied load and the squared natural frequency holds. Re-cent studies examine the effectiveness of VCT for steel silos. Zmu-da-Trzebiatowski and Iwicki (żmuda-Trzebiatowski & Iwicki, 2021) presented a study in which a steel silo was analyzed. The investigated silo was made through a corrugated wall and stiffened with cold-formed columns. Aiming to evaluate the impact of imperfections on the VCT effectiveness, both imperfect and perfect geometries were taken into account with different imperfection amplitudes. Particularly, the impact of such imperfections on relation between squared natural frequencies and compressive forces was evaluated. Although imperfections were measured in experimental models to investigate similar issues (Kalnins et al., 2015), that paper numerically addressed a part of a real structure (the steel silo segment schematized in Figure 1-13). In other words, an artificial substitute of the geometric

imperfections (eigen-mode imperfection) was adopted to account for the focused effect, by using different amplitudes of the first buckling mode and the first vibration mode. The buckling load was determined both by means of the VCT and non-linear static analysis. The outcomes of the study showed that a VCT allows to predict the right buckling load for the perfect structure of the silo segment and a limited load in the case of the imperfect structure. Hence, VCT precision decreases as the geometrical imperfection magnitude increases. Moreover, the relationship between squared natural frequencies and the applied load is governed by the magnitude of the applied loads, while considerable non-linearity is observed if the applied load become close to the minimum buckling load or the limit loads.
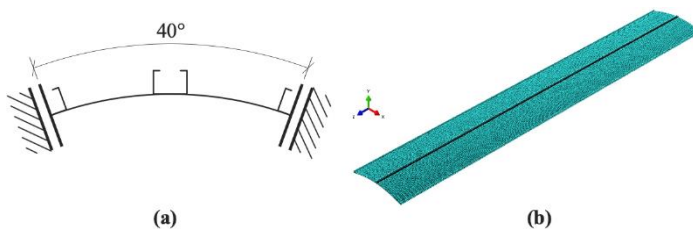


Figure 1-13 The studied silo segment: (a) scheme of boundary conditions (simplified); (b) numerical model (Żmuda-Trzebiatowski & Iwicki, 2021).

The geometric imperfections, in terms of the amplitude and form, are vital to the assessment of the structural buckling strength of a thin steel silo. The imperfection measurement of existing silos is another practical approach. However, it is efficient to employ a professional scanning method for the purpose of quantifying the realistic geometric imperfections. Ding et al. (Ding et al., 1996a) proposed one of the first comprehensive measuring techniques using conventional survey instrumentation, and specifically designed surface profile measurement apparatus. Mainly, the system consists of measuring trolley and the relevant software package. Through the study introduced by Ding et al. (Ding et al., 1996b), the developed technique in  (Ding et al., 1996a) was practically used for the imperfection assessments of three real full-scale metal silos of 10,000 tonne capacity in New South Wales, Australia. Authors analyzed the measured data using a double Fourier series to determine dominant imperfection modes. The results offered notable advantages (in terms of accuracy, labor intensity,

and cost) over the traditional measuring methods existed in that time(Ding et al., 1996b). However, the data released by measurement techniques can be adopted both for assessment and design by correlating the measurement results with buckling predictions and tests. Teng et al.(Teng & Song, 2001) analyzed extensive data on imperfection characterization, by providing a full identification of the possible imperfection set. In this context, the authors concern was to provide a reliable estimate of buckling in shell structures, avoiding any simplified assumptions. In the end, as shown on many occasions, the risks to which silos are subjected are elevated, especially as shown after hazardous events as earthquakes, which can cause serious accidents in the industrial plants with catastrophic consequences. For instance, in Italy, about 30% of industrial plants are situated in regions with a high seismic risk, and they are exposed to more hazards and more likely to fail. The collapse of a single silo can get out of order the entire industrial location. Thus, the silo seismic vulnerability assessment is of fundamental importance. For example, a very recent study introduced by Morelli et al. (Morelli et al., 2018)presented a performance-based earthquake assessment of a real case study of an elevated steel silo structure group with a regular plan dimensions 37.80 m × 16.94 m and total height 29.64 m. The supporting structure is of 10.80 m height and equipped with different typologies of lateral loads resisting systems (e.g., moment resisting frame, inverted V bracings, and diagonal bracings). Nonlinear static pushover and nonlinear response history analyses were used to evaluate the seismic performance of the structure under investigation. Aiming at identifying suitable techniques to select and scale natural ground motions for 3D analysis, two sets of natural ground motions were selected, one coherent with the uniform hazard spectrum and one with the conditional mean spectrum. The study suggested to use unscaled ground motions consistent with uniform hazard spectrum as the most suitable technique to obtain reliable results through a limited number of analyses.

## 1.8. Final remarks

This chapter highlights the behavior and the performance of silos used in the industrial sector, employed to store a wide range of bulk solid material with capacity up to thousands of tonnes. This review has covered research topics on structural configuration and be-haviour, seismic response, bulk material properties and behavior, loads imposed according to the standards, failure modes/causes, and assessment of silos in existing. As thin-walled shell structures, silos have an inherent sensitivity of structural configuration and these structures undergo unconventional loads and conditions depending on the nature of usage. Consequently, unusual silos failure modes were observed in many industrial locations leading to out-of-use or full collapse of the silo. Still, these structures are exposed to several hazards mobilized by different factors, such as dis-charging disturbance phenomena, stored material behavior, fluctuation due to bulk properties variance and anisotropy/asymmetry, seismic excitations, soil failure, misuse/maintenance errors, thermal ratcheting, dust explosion, lack of knowledge. The deficiency in the international design standards in considering complex loading conditions, such as those caused by the asymmetric flow of stored materials, have contributed to the proposal of new and oversimplified design approaches. Several hazard sources have been defined and different strategies to improve and retrofit silos, aiming to mitigate the vulnerability, were outlined throughout this article. For instance, de-pending on the risk nature and the addressed part of the silo, the suggested solutions in the literature could be classified into: (i) structural integrity upgrading and mechanical strengthening techniques; (ii) seismic isolation technique; (iii) bulk material behavior enhancement. The multiplicity of hazards sources acting on silos raised a concern about risk assessment approaches connected to these structures. Risk assessment of industrial silos has significant importance, and it is urgent to develop reliable proposals aiming to reduce the overall vulnerability, and eventually, preserve integrity and operational continuity of the silo and the relevant facilities. Future developments consist in the refinement on the available risk assessment methodologies in pursuit of more adaptable framework considering the relevant hazards associated to the operation of these structures, accounting for the and

quantification of the impact of different hazardous event on the overall silos' vulnerability.

Advanced seismic modeling and analysis of flat-bottom cylindrical steel silos interacting with stored granular-like materials.

# 2. A numerical procedure to estimate seismic fragility of cylindrical ground-supported steel silos containing granular-like material.

**Abstract**: The chapter presents a study on the evaluation of seismic fragility of cylindrical ground-supported steel silos intended for storing solid material. Silos are a key facility in industrial processes. For example, cylindrical steel silos constitute the main structural component for several industrial activities, such as the ones aimed at the production of food and beverage, and seismic actions can cause high economic losses and long functionality interruptions. Thus, the main goal of the study presented in this chapter is to propose a numerical procedure aimed to assess the seismic fragility of different cylindrical steel silos, accounting for varying geometries and service conditions (i.e., filling level of granular-like material), and observing different failure modes. In detail, a set of smooth steel silos was selected, considering different geometrical configurations (i.e., varying from squattest to slenderest structures). Different service conditions were simulated, with the aim to observe the behaviour of empty and filled silos (30%, 60%, and 90% of filling degree with respect to the maximum capacity). For each configuration, a detailed numerical model was developed under proper boundary conditions, adequately simulating the shell structure, the solid material inside, and the interactions between them. After validating the numerical models against existing literature data, three different failure modes were identified and assessed, accounting for the most recurrent post-elastic buckling type (i.e., elephant foot) and considering the possible occurrence of the elastic ones (i.e., diamond or similar shape failures at the middle and top of the structures). Both static and dynamic analyses were performed to identify the most probable failure modes and evaluate the probability of exceeding each one. As the output of the proposed approach, the seismic performance of each silo under a specific limit state was provided in the form of fragility curves. The results highlight some novel aspects, starting from the role that

service conditions assume in the silos seismic performance up to the possible differences in terms of failure modes for different silos geometrical structural configuration.

**Keywords**: Steel Silos, Granular-Like Material, Filling Degree, Industrial Facilities, Seismic Performance, Fragility Curve.

## 2.1. Introduction

The continuous development of industrial activities has highlighted the vulnerability of relevant facilities under hazardous events, both man-made and natural ones (e.g., earthquake, flood, tsunami, blast). Industrial sites inherently exhibit a complex configuration consisting of heterogeneous structural and non-structural components, which can suffer widespread damages under exceptional actions, causing enormous losses on several levels, e.g., human lives, economic, environmental issues, interruptions. Thus, the safety of the different industrial components under seismic events deserves high attention in earthquake-prone countries. For instance, in Italy, about 30% of industrial plants are located in regions with a high seismic hazard (Paolacci et al., 2012). In this framework, typical assets of industrial plants are the storage systems. A main classification of storage systems can be made, by distinguishing tanks storing liquid and silos storing solid materials. While the seismic vulnerability of tanks has been deeply investigated in the scientific literature (Bakalis et al., 2019; O'Rourke & So, 2000), fewer contributions are available for silos, despite their relevance in food and chemical industry sectors and the high seismic vulnerability observed in recent severe seismic events (e.g., 2023, Turkish Earthquake(Hu et al., 2023); 2012, Emilia Earthquake (Brunesi et al., 2015)).

This study aims to investigate the seismic behavior of flat-bottomed ground-supported silos used for storing granular-like material. However, limitations should be acknowledged regarding the structural typology of the silos under investigation. The silos considered in this study are of smooth walls that are unstiffened neither in the vertical nor in the horizontal direction. Although not the most widespread typology in practice, their behavior under seismic excitation is of a great interest as they exhibit a

higher vulnerability to buckling phenomena comparing to the other silos with corrugated and/or stiffened steel walls. Despite new silos for storing granular-like material could be of different typologies (e.g., corrugated, stiffened), several companies still propose this kind of silos (see Figure 2-1) as the most traditional and consolidated ones in the practice. Therefore, the proposed procedure aims to investigate seismic behavior of new and, above all, existing structures characterized by similar features.



Figure 2-1. Examples of new unstiffened smoothed walls steel silos (from left to right, phots are retrieved from the website of the companies Cepi Spa and Technobins, respectively).

In the same context, unstiffened smooth wall silos were investigated in the literature under different loading conditions (e.g., Butenweg et al., 2017; Mehretehran & Maleki, 2018; Sadowski & Rotter, 2011c; Silvestri et al., 2016). However, in the light of the state-of-the-art presented in Section 2.2, it is evident that the most influencing parameters on the seismic response of these structures are: (a) the geometry of the structure (i.e., height, diameter, walls thickness); (b) the silo functionality (i.e., filled or empty); (c) the intensity and characteristics of the ground motion. However, additional aspects also need to be investigated in detail. First of all, since silos are thin-walled shell structures, under dynamic excitations steel walls can develop different Buckling Modes (BMs), such as the elephant foot bucking at the base of the structure and the diamond or similar shapes failures at the middle and top of the structures.

60

Secondly, silos could show a different seismic behaviour when different filling levels of the stored granular-like material are considered, situation that aims to reproduce the possible real service conditions when the unexpected seismic event occurs.

With these goals in mind, this study proposes a numerical procedure (in the framework of the performance-based earthquake engineering, PBEE) to derive fragility curves of steel silos storing solid materials, accounting for different geometrical configurations, different service conditions, and different failure modes. In detail, a set of smooth and unstiffened steel silos was selected, varying two main geometrical aspects, that is, radius-to-thickness and height-to-diameter ratios. A specific granular-like material was considered, according to the detailed information provided by Moya et al. (2013). In the analyses, different levels of filling material were investigated, namely 90%, 60%, and 30% of the maximum capacity level, as well as the empty condition. Moreover, different BMs (also named throughout the chapter as failure modes) were considered. For each combination of the involved parameters, detailed numerical models were proposed, and after a phase of modelling validation, static and dynamic analyses were carried out. As the output of the proposed procedure, fragility curves were derived for each specific geometry of the silo storing an assigned level of filling material and looking at a particular BM. The results show in probabilistic terms the likely BM occurring as the seismic intensity varies, providing some insights on the influence of the accounted parameters.

## 2.2. Background

### 2.2.1. Seismic behavior of ground-supported steel silos

Steel silos are more commonly adopted types of storage facilities than reinforced concrete (RC) ones, since they provide an efficient solution with limited dimensions, weight, and cost. Among existing silos, a first classification can be made distinguishing the elevated silos resting on a framed structure (Jansseune et al., 2016; Kanyilmaz and Castiglioni, 2017), and the ground-supported ones (Butenweg et al., 2017; Sadowski and Rotter, 2011a). Referring to ground-supported steel silos,

different structural configurations and typologies exist, usually aimed at different functions. Basically, two main categories of flat-bottomed ground-supported steel silos can be identified: (a) smooth silos, composed of thin-walled isotropic plain rolled sheets, with stepped or constant wall-thickness (e.g., Iwicki et al., 2014; Mehretehran & Maleki, 2021; Sadowski & Rotter, 2011c, 2011d; Song, 2004; Song & Teng, 2003); (b) corrugated silos, composed of stiffened (e.g., Iwicki et al., 2015, 2016, 2019; Rejowski et al., 2023; Wójcik et al., 2017) or unstiffened (e.g., Kuczyńska et al., 2015) corrugated shell.

Focusing on smooth and unstiffened ground-supported silos containing solids, and on their behaviour under seismic actions, early investigations trace back to the second half of the last century, when the quantification of the seismic loads, the dynamic characteristics, and the distribution of the response acceleration along the height were the key matters. Different approaches, including experimental (Jing, Chen, et al., 2022; Shimamoto et al., 1984; Silvestri et al., 2016; Yokota et al., 1983), numerical (Butenweg et al., 2017; Demir & Livaoglu, 2023; Hardin et al., 1996; Holler & Meskouris, 2006; Mehretehran & Maleki, 2018; Rotter & Hull, 1989; Sasaki & Yoshimura, 1988; Shimamoto et al., 1984; Yokota et al., 1983), and analytical (Lee, 1981; Pieraccini et al., 2015; Trahair et al., 1983; Veletsos & Younan, 1998; Younan & Veletsos, 1998) studies, were proposed and adopted. Turning to more recent literature contributions, the focus was aimed at identifying the most influencing parameters governing the seismic behaviour of ground-supported steel silos, such as the slenderness ratio (Holler and Meskouris, 2006; Mehretehran and Maleki, 2018; Nateghi and Yakhchalian, 2012; Rotter and Hull, 1989; Veletsos and Younan, 1998; Younan and Veletsos, 1998), the properties of stored material (Hardin et al., 1996; Shimamoto et al., 1984; Yokota et al., 1983), the effective mass (Lee, 1981; Sasaki and Yoshimura, 1992; Silvestri et al., 2012), the additional normal pressure (Holler and Meskouris, 2006; Silvestri et al., 2012; Trahair et al., 1983), the compaction of the solids (Silvestri et al., 2022), the soil-structure interaction (SSI) (Butenweg et al., 2017; Holler and Meskouris, 2006), and the wall-solids interaction (Holler & Meskouris, 2006; Mansour, Silvestri, et al., 2022; Nateghi & Yakhchalian, 2012).

Discussing the available literature in chronological order, one of the first contributions about the seismic response of ground-supported silos was provided by Rotter and Hull (1989) in which the authors assessed, based on finite element (FE) approach, the critical seismic stresses in squat silo walls and derived the corresponding analytical expressions. A uniform horizontal acceleration was adopted (as quasi-static horizontal body force), and the stored solid material was characterized as an isotropic and homogenous mean with a specific elastic modulus. The results stated that the membrane stress developed in the shell walls are proportional to the height-to-diameter ratio. Sasaki and Yoshimura (1992) evaluated the effective mass pushing on the silo wall under an earthquake based on a numerical model of a tested scaled silo. Hardin et al. (1996) evaluated the seismic response of a real scale steel wheat-silo. The stress-strain distribution, the acceleration history, and the amplification of the horizontal acceleration were recorded. In their work, a composite shear-beam model was employed to simulate the investigated grain-silo system. Younan and Veletsos (Veletsos and Younan, 1998; Younan and Veletsos, 1998) provided an analytical formulation to describe the seismic response of ground-supported silos considering the effect of the slenderness ratio and walls flexibility, where the ensiled material was simulated as a linear viscoelastic solid.

The above-mentioned works represent milestones about seismic response of ground-supported silos, which were followed by the drafting of the current European standard, EN 1998-4-2006 (2006) and a series of subsequent studies. With this regard, it is worth mentioning that the guidelines in EN 1998-4 (2006) employed a static equivalent approach to provide a practical method for seismically designing the silos structure. In fact, seismic loads are considered by defining an effective mass horizontally applied on the silo walls, determined as a percentage of the total mass. Following this approach, Holler and Meskouris (2006) investigated the behaviour of steel silos containing granular material and, in the study, they considered the effect of the aspect ratio, the grain-wall interaction, the SSI, and the granular material nonlinearity. The results suggested to apply a reduction to the effective mass proposed by the code for squat silos (and not for slender ones) to achieve a more realistic design. Yakhchalian

and Nateghi (2012) presented a numerical investigation to assess the influence of the aspect ratio on the seismic behaviour of ground-supported steel silos. The study quantified the additional normal pressures over the silo height and compared the results with those obtained by the application of a constant distribution of accelerations. The authors concluded that this distribution was conservative for squat silos and non-conservative for slender silos. A physically based estimation of the effective mass of grain-silo systems was presented by Silvestri et al. (2012) and later refined by Pieraccini et al. (2015). The works provided a set of analytical formulations aimed at estimating the pressures on the silo walls. Based on the obtained results, authors emphasized that the approach proposed by the code about squat silos is conservative. In the same context, Silvestri et al. (2016) presented an experimental study with a shaking table test for a reduced-scale silo filled with granular material. The result of the experimental campaign revealed a significant effect of the wall-friction coefficient on the overturning moment at the silo base. Further investigation on the simplified approach of the static equivalent load adopted by the code was presented by Butenweg et al. (2017), who compared the code method with a more sophisticated approach, based on the time history analysis and nonlinear FE modelling. The proposed FE model considered the solid nonlinearity, the solid-wall interaction, and the SSI. The study revealed that the application of static equivalent loads on slender silos can be too conservative if a simplified linear acceleration along the wall height is considered. Instead, the use of an acceleration profile based on the multimodal analysis of a simplified beam yields more realistic result. Similarly, the study stated that the simplified static equivalent approach is also conservative in case of squat silos (as stated by Holler and Meskouris, 2006; Silvestri et al., 2012). However, the authors attributed this circumstance to the fact that the equivalent static approach does not precisely consider the likely stress reduction caused by the friction of the bulk material in case of squat silos. In the end, the study suggested to opt for nonlinear numerical modelling as it leads to more realistic and economic silo design. Durmus and Livaoglu (2015) introduced an analytical solution based on a simplified model consisting of a single-degree-of-freedom flexural cantilever beam with a lumped mass. The findings

based on the proposed approach were compared to those obtained from a more sophisticated numerical FE modelling, showing the soundness of the proposal. The study also concluded that the SSI effect has a negligible contribution to the seismic behaviour of the system and can be ignored in practical applications. Mehretehran and Maleki (2018) investigated the dynamic buckling behaviour of steel silos by implementing incremental dynamic analysis (IDA) with 10 ground motion records. In this case, the investigated silos were assumed filled up to 90% of the maximum capacity and the Elephant Foot Buckling (EFB) was the solely investigated damage pattern. The main findings of this study indicated that slender silos are more vulnerable to buckling failure, while squat silos presented a considerably higher resistance under same conditions. Recently, the same authors extended their findings to include the stepped wall steel silos under seismic conditions (Mehretehran and Maleki, 2021) and observing different buckling modes. Particularly, local diagonal shear wrinkles were found to be dominant for squat and intermediate slender silos, while EFB damage was observed at the base of slender ones. Recently, Silvestri et al. (2022) performed an experimental study in which the seismic behaviour of a full-scale flat-bottom steel silo filled with wheat was investigated on a shaking table. The aim was to estimate several parameters of interest, such as the static pressure, the dynamic characteristics, and the dynamic overpressure. The study, moreover, reported the role of the compaction degree of the granular material and its effect on the acceleration profile along the silo wall and within the fillings. Another experimental study was presented by Jing et al. (2022), whose purpose was the assessment of the favorable effect provided by the existence of the granular material on the energy dissipation of the grain-silo system. The effect of different level state on the acceleration vertical profile and on the fundamental frequency was also mentioned. For the sake of synthesis, the state-of-the-art herein reported is limited to the ground-supported steel silos, which characterize the subject of this work. More information about silo structures and their behaviour under different conditions is presented in the first chapter of this dissertation.

### 2.2.2. Possible failure modes of steel silos under earthquakes

Failure of structures can be defined as the state beyond which the structure (or a part of it) does not satisfy the design performance requirements. In the case of steel silos, structural failure is governed by specific damage patterns. When talking about earthquake effects on steel silos, failure modes depend on several parameters, such as the geometry, the presence or absence of filling material, and the ground motion intensity. BMs can be generally associated to a specific damage scenario that is observed on the shell body of the silo. Looking at the post-earthquakes site inspections on industrial sites (e.g., Brunesi et al., 2015; Buratti & Tavano, 2014; Niwa & Clough, 1982) a wide variety of possible failure modes and mechanisms under earthquake can be noted. However, this study focuses on the damage state associated to the instability phenomena in the silo walls, which is commonly associated to the shell buckling damages and that can anticipate any other type of collapse. As a matter of fact, under a seismic event, the silo walls undergo additional normal pressures (EN 1998-4, 2006). However, the increased internal pressure can provoke buckling in the shell wall and, considering the complex grain-wall interaction, different buckling phenomena can develop in different positions of the wall. In this view, three BMs can be identified: (a) the elasto-plastic buckling named Elephant Foot Buckling and known as EFB (Rotter, 2006b) (Figure 2-2a); (b) the elastic Top-of-Wall Damage (TWD) buckling (Malhotra et al., 2018; Mehretehran & Maleki, 2021; J. Virella et al., 2006) (Figure 2-2b); (c) the elastic wall deformation occurring near to the middle part of the silo, known as Elastic Buckling (EB) (Virella et al., 2008) (Figure 2-2c), and recalling the diamond (or similar) shape buckling. Importantly, although the BMs under consideration are practically more relevant to tanks storing liquids as depicted in Figure 2-2, this study consider investigating the possibility to experience each of the three BMs in case of silos storing solids as silos and tanks share similar structural configuration and similar functionality as storage system, especially in the light of the lack of post-earthquake inspection of silos which implies vagueness in the seismic damage patterns for silos in contrast to tanks.
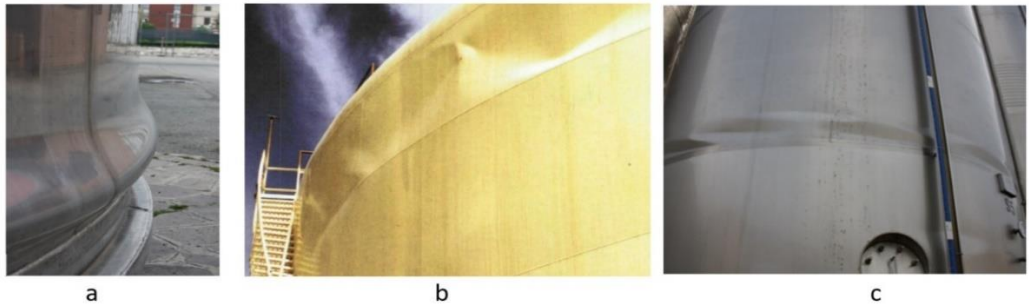
Figure 2-2 Possible BMs observed after earthquake events: (a) EFB (Brunesi et al., 2015); (b) TWD (Malhotra et al., 2018); (c) EB (Brunesi et al., 2015).

The EFB, which was well investigated by Rotter (2006), is a BM usually induced by the combination of axial compressive stress exceeding the critical shell stress and the circumferential tensile stress close to yield strength. EFB is described by an outward bulge, near to the base, which extends around the circumference of the wall. In general, EFB is the most likely phenomenon when considering seismic actions on silos. On the other hand, elastic phenomena as TWD and EB must be considered for the case at hand, as observed in several post-earthquake inspections for similar structures, such as tanks (e.g., Buratti and Tavano, 2014; Malhotra et al., 2018). In addition, the TWD damage was numerically studied by Mehretehran and Maleki (2021) for silos storing granular material under seismic conditions. Instead, the EB was investigated by Sadowski and Rotter (2011a, 2011b) for silos containing solids and, despite this BM was attributed to the normal pressure induced by discharge loading, it is typical of shell structures and could occur also in case of dynamic excitation.

All three BMs are investigated through this chapter, with the twofold aim to provide a specific Engineering Demand Parameter (EDP) for each failure mode and to explore the conditions in which EFB can be anticipated by the elastic BMs (i.e., TWD and EB).

## 2.3. Proposed numerical procedure

The proposed numerical procedure is illustrated in Figure 2-3, and is composed by four consecutive steps, which are aimed to derive fragility curves for ground-supported steel silos with different geometries and different service conditions, i.e., different filling levels of stored material. Based on PBEE approach, fragility curves are derived, accounting for the silo geometries, the service conditions, and the possible BMs.
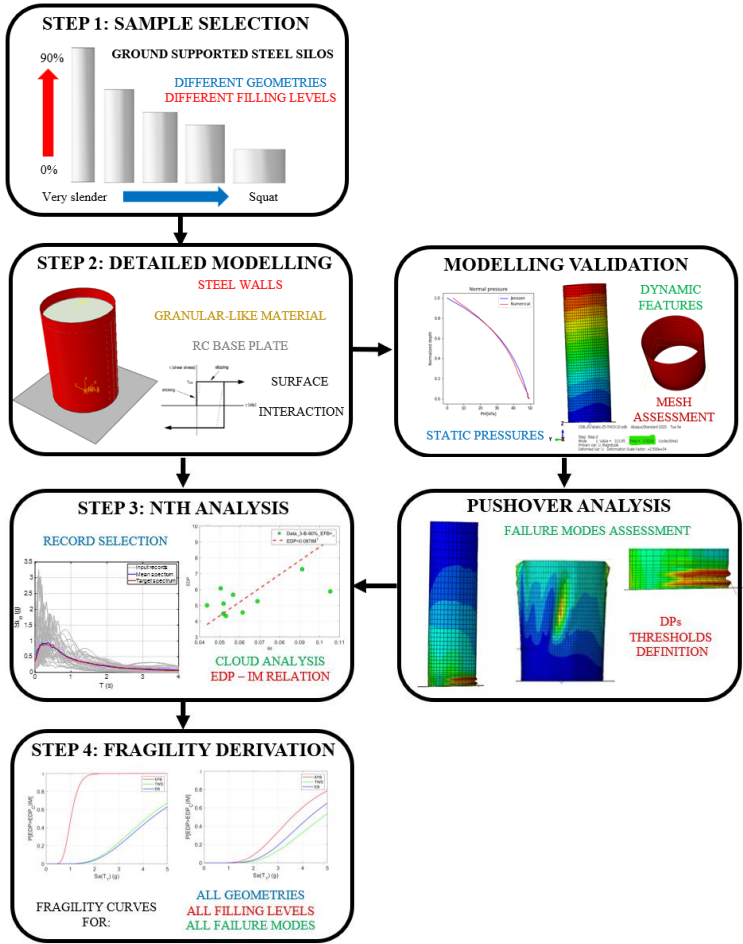


Figure 2-3 Flowchart outlining the proposed numerical procedure.

The first step consists in the selection of a set of representative cases of steel silos, which can cover a wide range of possible conditions, according to a combination of the main influencing parameters the seismic behavior. Assuming as focus of this study only the ground supported smooth steel silos, different geometries must be considered, ranging from very slender (low radius-to-thickness and high height-to-diameter ratios) to squat cases (high radius-to-thickness and low height-to-diameter ratios). To adequately consider the influence of the stored material and the occurrence of seismic events in any condition, different filling levels must be considered in the investigation ranging from the near-full level to the empty case.

The second step consists in the detailed modelling of the considered samples. Given the boundary conditions and the applied loads, complex models are strongly suggested to reproduce the peculiar structural behavior that is mainly ruled by the steel walls (as shells elements), the stored material, and the interaction between the two above elements. For the scope of the proposed procedure, the focus is on the steel walls, whereas adequate modelling simplification can be applied on the filling material, which can be simulated through an elastic approach. Obviously, dealing with shell structure, an adequate mesh must be defined, in order to accurately simulate the failure modes. For such a numerical approach, a validation process is required to assess the basic parameters against real-life (or experimental) case studies. As minimum requirements, models should be assessed in terms of static conditions (e.g., controlling the pressure on the walls and comparing it to the analytical solutions) and dynamic conditions (e.g., computing the eigen frequencies and comparing them to existing or experimental benchmark cases). In relation to steps 1 and 2, it is worth noting that, to account for uncertainties in the generation of the sample, the variation of several parameters should be considered, such as the mechanical parameters of the structural steel and the physical properties of filling material. Nevertheless, it is worth remarking that to perform a more comprehensive parametric analysis on this type of structures, a less detailed modelling approach than the one proposed here should be considered. Therefore, for the proposed procedure, specific geometrical configura-

tions and physical properties of the stored material are considered, reserving more intensive analyses for further developments.

Once numerical models are available, the third step consists in the analysis campaign. To probabilistically characterize the seismic performance of the silos, nonlinear time history analyses (NTHAs) are required, and for this purpose, several parameters must be defined: (a) selection of ground motion records; (b) EDP and intensity measure (IM) to characterize the demand-intensity relationship; (c) possible failure modes and thresholds identifying their achievement; (d) type of analysis approach to employ. Concerning the ground motion selection, specific hazard-consistent records can be considered, selected according to a specific hazard curve or to a response spectrum for the site of interest (Kohrangi et al., 2017). In a PBEE-based approach, record selection should be performed by selecting a range of ground motion wide enough to cover any type of IM and to ensure sufficiency (Luco & Bazzurro, 2007). Nevertheless, given the complexity of the proposed modelling approach and the absence of specific code prescriptions, a set of 11 records (analogously to the idea developed in Ruggieri et al., 2021) spectrum-compatible with the reference site was employed (record selection is to be processed according to the Eurocode 8 prescriptions (EN 1998-1, 2004), while a higher number of records than Eurocode provisions is suggested). The evident simplification in terms of record selection (i.e., possible high dispersion in the EDP-IM relationship, with probable issues in terms of regression analysis and high epistemic uncertainties) is balanced by an important advantage: a reduction of the computational analysis cost, which could be very expensive when a very detailed modelling approach is employed.

In respect of the EDP selection, several parameters could be employed, such as displacements or an index of the stress/strain relationship. Nevertheless, considering that the aim of the study is to characterize the failure of steel silos looking at different buckling phenomena, which can occur in different zones along the height, a typical representative parameter can be the rotation of the wall with respect to the base, $\theta_{W,BM}$ (the subscript BM oversees all failure modes and then, according to the specific failure mode, it is replaced throughout the text with the proper acronym, i.e., EFB, TWD,

70

EB) expressed as the ratio between the horizontal displacement in the likely buckling zone (at the top: $\delta_{W,TWD}$; in the middle: $\delta_{W,EB}$; close to the base:, $\delta_{W,EFB}$) and the height of the identified zone from the silo base (at the top: $h_{W,TWD}$; in the middle: $h_{W,EB}$; close to the base: $h_{W,EFB}$):

$$\theta_{W,BM} \rightarrow \theta_{W,EFB} = \frac{\delta_{W,EFB}}{h_{W,EFB}} ; \theta_{W,TWD} = \frac{\delta_{W,TWD}}{h_{W,TWD}} ; \theta_{W,EB} = \frac{\delta_{W,EB}}{h_{W,EB}} \qquad \text{2-1}$$

The use of $\theta_{W,BM}$ is suitable for all BMs, as it is an unbiased parameter neutralizing the position of the buckling zone and then, is effective for the purpose of the procedure. Figure 2-4 graphically illustrates the EDP calculation with reference to the EFB case as an example. With respect to the IM selection, and as a principle, the IM should be chosen to well describe the severity of the ground motion on the structure. For instance, the peak ground acceleration, peak ground velocity, peak ground displacement, and the spectral acceleration (PGA, PGV, PGD) are examples of the non-structure specific IMs that can be employed for fragility analysis, while the first mode spectral acceleration Sa(T1) fall into the category of structure specific IM. The PGA is the most widely used IM parameter for the seismic risk analysis of similar structures. Nevertheless, the severity of the ground motion on the structure is relative to the structure itself and it depends on its dynamic characteristic in addition to the features of the ground motion. Thus, the PGA might not be the best parameter to measure the severity of the ground motion in this case, especially that we have different silos with different characteristics. Alternatively, the spectral acceleration Sa(T1) corresponding to the fundamental vibration mode is adopted as IM since it may provide a more rational representation (relevant to the structure) of the intensity of the ground motion. However, the most widely used IMs are: peak ground acceleration (PGA), which is adopted in several research works (Buratti & Tavano, 2014; Kildashti et al., 2018; Mehretehran & Maleki, 2021; O'Rourke & So, 2000; Salzano et al., 2003; Sobhan et al., 2017; J. Virella et al., 2006), or spectral acceleration of the first vibration mode (Sa($T_1$)). It is worth noting that, unlike tanks, silos storing granular-like materials do not have a convective response, which represents a limit in the use of Sa($T_1$) because the first vibration period ($T_1$) cannot accurately describe the effective acceleration. For

the case at hand, instead, if compaction phenomena of the stored granular material are neglected, $T_1$ tends to be invariant for a given condition of functionality and $Sa(T_1)$ can provide a better quantification of the seismic effect on the couple grain-silo system than PGA. Still, considering that the solid filling material represents an additional mass for the system, the values of $T_1$ are expected to fall in the spectral range of linear-constant acceleration (plateau).
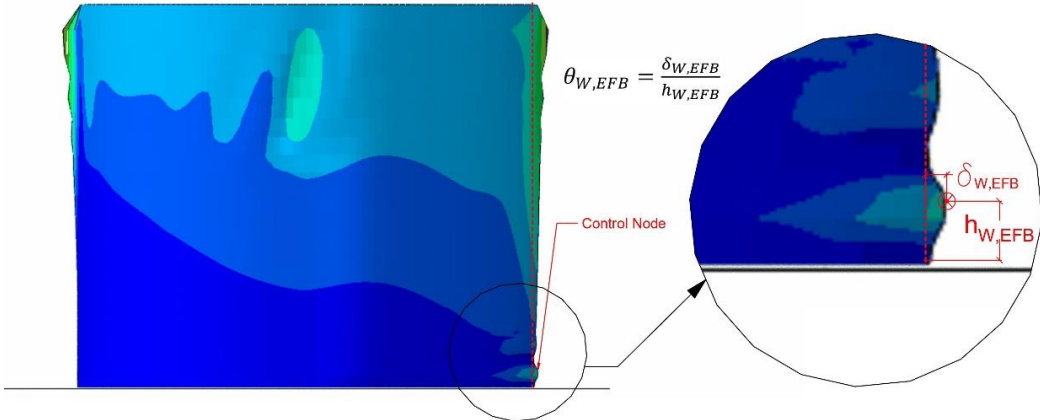


Figure 2-4 EDP calculation for the sample of silos (e.g., Q silo, 60% filling level for EFB)

Once EDP-IM quantities are defined and given the failure modes defined in Section 2.2.2, BMs thresholds ($EDP_{C,EFB}$, $EDP_{C,TWD}$, $EDP_{C,EB}$, where the subscript C stands for the capacity) can be quantified by using pushover analysis. In detail, all numerical models can be investigated under a specific load profile defined as a vector of forces proportional to the nodal masses of the silo wall. This load profile is preferred to the one proportional to the first vibration mode, considering that in some cases the participating mass for the main vibration mode could be lower than a reasonable value, and therefore not representative of the dynamic behavior of the structure. The results of the pushover analysis are used to capture the $\theta_{W,BM}$ values characteristic of the zones where the BMs occur (i.e., base, middle, and top of the wall). These values can be directly observed on the pushover curves expressed in terms of base shear ($V_b$) vs. $\theta_{W,BM}$. In particular, in the case of EFB mode, which is an elasto-plastic failure mode, the threshold can be identified by the point identifying the transition from the elastic to

72

the post-elastic zone (i.e., yielding-like point of the capacity curve). When observing EB and TWD modes, which are elastic failure modes, two possibilities are available: (i) identify the change of stiffness in the capacity curve (i.e., change of slope); (ii) record the final point of the curve, which corresponds to the final step of the pushover and indicates the collapse of the structure. The latter could also merely correspond to a numerical convergence problem, which can however be easily discarded by observing if a real failure mechanism is activated at the end of the analysis. At this point, is worth specifying two aspects. Firstly, by considering different service conditions, at a first glance, different thresholds values could be recorded. Nevertheless, considering that the focus of the study is the structural behaviour of the wall, it is necessary that the threshold value, which is the lower limit behind which the relevant BM is observed, is established independently of the filling level. Secondly, the pushover analysis can clarify the occurrence of different failure modes that anticipate the EFB occurrence (considering EFB the most likely failure mode in silos under earthquakes).

Once defined the thresholds values, NTHAs can be performed according to a proper methodology capable of characterizing the distribution of EDP|IM (or IM|EDP). One can optimally choose among IDAs (Vamvatsikos & Allin Cornell, 2002), multi stripe (Bazzurro et al., 1998; Jalayer & Cornell, 2009) or cloud analysis (Bazzurro et al., 1998; Jalayer, 2003) and in line with the necessity to reduce the computational demands, cloud analysis is considered. Undeniable are the uncertainties related to the regression analysis, which could even require the implementation of logistic regression, especially in the case of elevated number of collapses. Nevertheless, some advantages over IDAs can be mentioned, such as the computational efficiency (that is fundamental for the proposed numerical modelling) and the possibility to employ a local fit in the IM-band of interest. In the end, it is worth noting that, given the axial-symmetry of the proposed models, NTHAs can be run on half models, provided that proper boundary conditions are imposed on the symmetry plan, so to ensure realistic mechanical conditions of the structure, i.e., displacements in the perpendicular direction to the symmetry plan and rotations in the main directions on the symmetry plan are not allowed. Results in the EDP-IM plane can be processed through the probabil-

istic seismic demand model proposed by Cornell et al. (2002). Thus, for each BM, it can be expressed as:

$$EDP_{BM} = \alpha_{BM} IM^{\beta_{BM}}$$ 
<div align="right">2-2</div>

where $\ln(\alpha_{BM})$ is the intercept and $\beta_{BM}$ is the slope of the regression line in the log-space, both evaluated using the least square method.

The last step of the proposed procedure consists in the definition of the fragility curves, aimed to define the probability for the silos of exceeding specific BMs. Fragility functions are mathematically defined as the cumulative distribution function (CDF) that describes the relation between the IM and the probability of collapse ($P_f$) according to a certain BM:

$$P_f(EDP \geq EDP_C | IM) = \Phi\left(\frac{\ln(x/\mu_{BM})}{\sigma_{BM}}\right)$$
<div align="right">2-3</div>

where x is the generic IM value, and $\mu_{BM}$ and $\sigma_{BM}$ are the median and the dispersion of the CDF, respectively. For the case at hand, the fragility of the silos has been estimated for all geometries and all service conditions (i.e., filling level), and the governing fragility function is the one corresponding to the BM having the higher $P_f$.

$$P_f = max\big(P_f(EFB), P_f(TWD), P_f(EB)\big)$$ 2-4

## 2.4. Selection of the sample of ground-supported steel silos and description

To reflect the variety in the geometry of the existing silos used in the practice, a set of five different structural configurations with different geometries were considered. The set was the same designed by Sadowski and Rotter (2011a) according to the Eurocode prescriptions (EN 1993-1-6, 2007)(EN 1993-1-6, 2007), and it was investigated under different conditions of discharge loading. Figure 2-5 graphically depicts the variation in terms of geometry among the considered cylindrical silos, which differ in terms of 3 main characterizing parameters: height, diameter, and thickness.
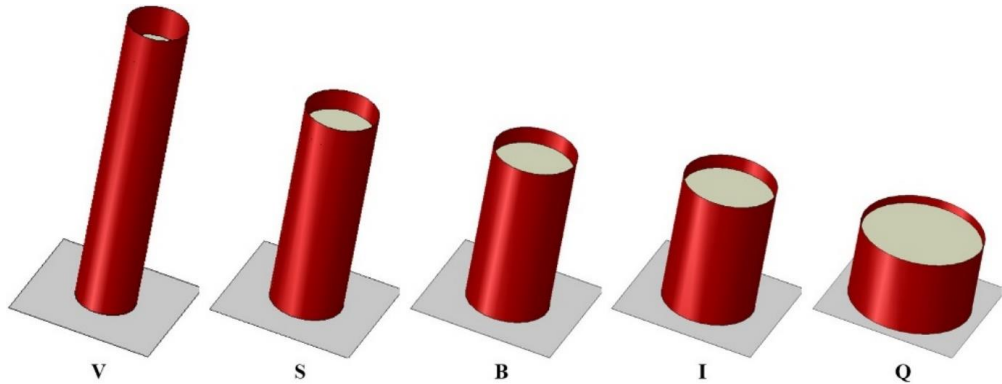
Figure 2-5 Schematic representation of the five considered silos, drawn to scale.

In the design of a typical silo, the relevant geometrical parameters are usually expressed through two ratios: (i) height-to-diameter ratio (h/D) and radius-to-thickness ratio (R/t). The choice of the sample set of case studies aims to cover a wide range of typologies, including very slender (V), slender (S), boundary (B), intermediate squat (I) and squat (Q) silos. Regarding the design roles, h/D reasonably assumes a value ranging from 0.65 to 5.2, while R/t ranges from 357 to 1667 (corresponding to the most economic design values). In the proposed sample set, the storage capacity is constant and equal to 510 m3. The geometric features of the set are reported in Table 2-1, describing the slenderness type, the silo acronym, the height (h), the diameter (D), the thickness (t) and the abovementioned design ratios.

Table 2-1 Geometric characteristics of the considered set of silos.

| Slenderness | Acronym | h (m) | D (m) | t (mm) | h/D | R/t |
|---|---|---|---|---|---|---|
| Very slender | V | 26 | 5.00 | 7 | 5.2 | 357 |
| Slender | S | 18 | 6.00 | 6 | 3 | 500 |
| Boundary | B | 14 | 6.80 | 6 | 2 | 567 |
| Intermediate | I | 11.2 | 7.60 | 5 | 1.47 | 760 |
| Squat | Q | 6.5 | 10.0 | 3 | 0.65 | 1667 |

With respect to the service conditions, the presence of the filling material has a favorable impact on the lateral stiffness and imperfection amplitude (Buratti and Tavano, 2014), and then on the structural strength. The existence of the granular material, in fact, represents an elastic lateral support for the shell wall, and prevents buckling. The

reduction of the filling load could be an efficient approach to reduce the seismic demand in earthquake-prone zones since the stored solids contribute to the greater part of the seismic mass of the silo. From this first discussion, it can be deduced that the filling level is a crucial factor governing the failure mechanism of silos under earthquakes. In order to investigate and quantify the effect of the filling level on the dynamic capacity of the silo under earthquake excitation, each silo of the sample set was investigated considering different possible filling levels, expressed in percentage terms of the maximum storage capacity. The considered values are 90%, 60%, and 30%, while also the empty condition was considered for the sake of completeness. Combining the different silos typologies and the different filling levels, 20 specific cases were investigated.

## 2.5. Numearical Modelling

For all the silos of the set, three-dimensional (3D) numerical models were developed by means of the FE software ABAQUS (Simulia, 2012). According to the software philosophy, three numerical parts were identified to form and assemble each FE model: (a) the cylindrical steel silo (modelled through Four-nodes shell elements S4R); (b) the bulk material stored in the silo (modelled through 8 node linear brick elements C3D8R); (c) the RC base (modelled through quadrilateral shell elements S4R). Fixed boundary conditions were applied to the steel wall bottom, by considering the radial, the circumferential, and the meridian displacements fixed to the RC base. Same considerations were employed for the rotations (constraints were applied around the circumference, at uniformly spaced points, in order to reproduce a fully fixed base). The detail of the roof structure was neglected in the model since the primary interest of the study is the behaviour of the shell wall. However, a rigid body constraint, connecting the nodes of the upper edge of the silo wall to a master point, was considered to reproduce the restricting effect of the roof on the out-of-roundness displacement at the upper boundary of the silo shell wall. On this subject, it is worth noting that a ring beam placed at the very top of the silo wall is often used in the practice to avoid the out-of-roundness displacements at the silo top. 4-node shell ele-

ments with reduced integration (S4R) were adopted to model the steel silo wall. S4R is classified as a general-purpose and three-dimensional 4-nodded shell element that considers the finite membrane strains and uses both displacement and rotational degrees of freedom (Simulia, 2012). However, with S4R elements, the change of the shell thickness as a function of in-plane deformation is accounted for. This element can be employed to model the behaviour of thin and thick shell structures under different loading conditions. The filling material was modelled by using eight-node classical brick element with reduced integration (C3D8R element), and the RC base foundation was considered as a fully stiff element, restrained to the ground. It is worth nothing that the shell failure is very sensitive to the imperfection amplitude, when considering under axial compression (Jansseune et al., 2016). Since the focus of this work is the behavior of silo shell wall under horizontal loads, it is more convenient to override the effect of the imperfection with reasonable simplification. In fact, for the case at hand the horizontal pressure is the most predominant action to consider and the not investigation of other vertical actions (e.g., vertical component of the seismic motion) reduces the impact that imperfection amplitude can provoke on the silos behavior (Buratti and Tavano, 2014).

Concerning the mesh, a specific investigation was performed for each silo, under different analysis conditions. For the case at hand, as modelling strategy, a higher number of elements was considered in the zones in which the variation of stress rate was high (i.e., bottom part of the silos). According to this modelling strategy, a mesh size ranging from 125 to 1000 mm was considered for the shell of the silo wall. For the mesh of the filling material, a stepwise graded approach was considered in the radial direction. Particularly, a finer mesh size of 250 mm was used at the interface near the wall to ensure a proper developing of the friction interaction between the filling material and the wall, while a coarser mesh size of 1000 mm was adopted for the inner part of the filling solid. A mesh size ranging from 250 to 500 mm was used for circumferential and meridian directions. An example of the employed mesh strategy is reported in Figure 2-6, which shows the FE models of the silos' walls and the filling material.
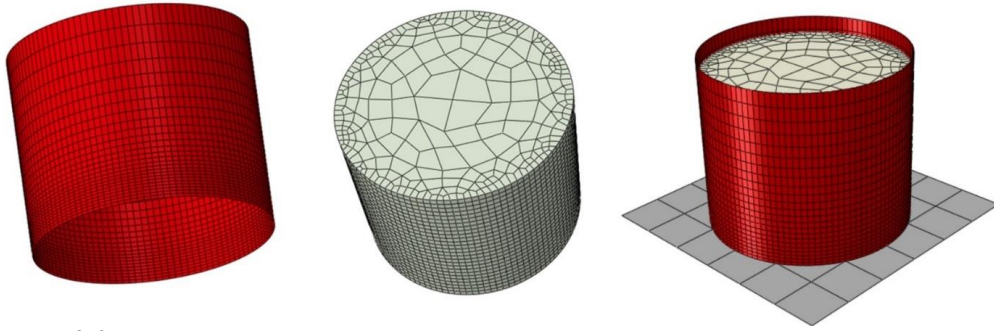
Figure 2-6 Modelling and meshing approaches for the considered sample of silos. From left to right, steel wall, granular material and complete model with base plate are reported.

Regarding the constitutive laws of employed materials, the steel of shell walls was assumed with an elastic-hardening behavior and the Von Mises yield criterion was accounted for. The features of the steel are: Elastic Modulus, $E_s$, equal to 210 GPa; Poisson's ratio, $v_s$, equal to 0.3; yield strength, $f_{s,y}$, equal to 275 MPa; ultimate strength, $f_{s,u}$, equal to 430 MPa; strain hardening modulus, $E_t$, equal to 3880 MPa; density, $\rho$ equal to 7850 kg/m3. The considered silos are filled with 'Camacho' wheat having a density of 8.36 kN/m3; the coefficient of friction was assumed equal to 0.19 for the steel wall and 0.42 for the RC base. Other specific properties of the used filling material are reported in Table 2-2 according to (Moya et al., 2013), where relevant information derived by experimental investigations are provided. It is worth noting also that only the elastic properties of the filling material were considered, neglecting the insight about the nonlinear behavior, which is not the objective of the study. However, seeking more realistic modelling approach, the effect of the granular material nonlinearity could be accounted for, by considering more sophisticated constitutive material models (e.g., the hypoplastic material law as adopted by Butenweg et al. (2017) or the extended Drucker-Prager law as used by Mehretehran and Maleki (2018)) that can more accurately capture the solids behavior and its impacts on the silo walls, in terms of additional pressures. Obviously, this would strongly increase the computational demand to achieve convergence in the numerical model and, for this reason, any type of granular material nonlinearity was neglected in the numerical model.

Concerning the interaction between the filling material and the structure, a Coulomb frictional model was assumed, by defining the critical shear stress (threshold) between the two contact surfaces. According to this model, the slip between the two surfaces occurs after that the shear stress between them exceeds the threshold. The critical shear stress is mainly proportional to the normal pressure on the contact surface and the friction coefficient between the two materials. While the normal pressure on the contact surface is calculated based on the numerical analysis, the coefficient of friction, as it was derived from Moya et al., (2013), was manually inserted by the authors as input of the FE model.

Table 2-2 Mechanical properties of the stored material ('Camacho' wheat) (Moya et al., 2013)

| Angle of internal friction (°) | Apparent cohesion (MPa) | Coulomb friction coefficients (Steel and RC) | | Dilatancy angle (°) | Young's modulus (MPa) | Poisson's ratio | Density (kg/m3) | Unit weight (KN/m3) |
|---|---|---|---|---|---|---|---|---|
| 22.2 | 0.0095 | 0.19 | 0.42 | 23.1 | 19.658 | 0.37 | 836 | 8.36 |

## 2.6. Modelling approach assessment and validation

In order to assess the validity of the proposed modelling approach, a specific section is devoted to the aspects related to the appropriateness of the proposed mesh size and the type of FE selected from the software library (Section 2.6.1) and the validation with the existing literature (Section 2.6.2).

### 2.6.1. Mesh resolution and assessment of the FE type selection

The software ABAQUS accounts for the use of different FE elements from the available libraries, which could be used for detailing the numerical models. For the case at hand, it is relevant the modelling technique adopted for the structural part of the silos (i.e., steel walls) and for this reason some additional basic analyses were performed. However, for the granular-like material and the surface interaction, which are not the central focus, the used modelling approach can be assumed to be adequate. For modelling the steel of shell walls, ABAQUS allows to select more complex

FE types than the used one, such as the eight-node continuum shell element (SC8R element) or the eight-node continuum solid shell element (CSS8 element). Comparing to the S4R element, which is a 4-node quadrilateral shell element with reduced integration that allows transverse shear deformation, SC8R element is 8-node hexahedron continuum shell element with reduced integration that allows transverse shear deformation. Differently from the S4R, the SC8R is used to discretize an entire three-dimensional body, and from the modelling point of view, it is like a 3D continuum solid presenting kinematic and constitutive behaviour like conventional shell elements and with the thickness determined from the element nodal geometry. Still, CSS8 element is an 8-node linear solid shell brick, that is typically suggested for thin-walled structures, and it can fill the gap between incompatible mode elements, which use 3D constitutive laws but tend to exhibit locking in bending for large aspect ratios, and continuum shell elements, which present good bending response for large aspect ratios but are limited to two-dimensional plane stress constitutive behaviors.

To understand which of the above FEs (i.e., S4R, SC8R, CSS8) provides the better performance, higher accuracy and shorter time of analysis, a preliminary linear analysis was performed on an axially compressed cylindrical shell. In particular, the purpose was to estimate the buckling capacity ($N_{numerical}$) under axial meridian stresses by employing the three FE types and compare it to a classical analytical solution ($N_{analytical}$). For this new numerical experiment, the shell was assumed to be fixed at the bottom and with reduced degrees of freedom at the top, i.e., with possibility of free vertical displacements. The geometry of the numerical specimen presents D equal to 800 mm, h equal to 1200 mm, and t equal to 1 mm. For the steel, it was assumed having $E_s$ equal to 210 GPa, and Poisson ratio, $v$, equal to 0.3. The solution $N_{analytical}$ was estimated through the classical formulation of the elastic critical force applied to a shell under axial compression, that is, the Timoshenko formulation:

$$N_{analytical} = \frac{2 \cdot \pi \cdot E_s \cdot t^2}{\sqrt{3(1 - v^2)}} \quad \text{2-5}$$

Using the same values of the numerical benchmark, $N_{analytical}$ results in 798.58 kN. By excluding the geometrical imperfections from the evaluation of the numerical solution,

the results for $N_{numerical}$ are shown in Table 2-3, which also reports the percentage difference from $N_{analytical}$. Table 2-3 reports also the CPU time required for estimating $N_{numerical}$ through a workstation equipped with a Core i5 CPU, 4 GBs of RAM, and an INTEL HD Graphics 4000. Basing on the obtained results, the differences among the analytical and numerical solutions are quasi-negligible (element S4R provides a lower percentage difference, but also other models provide good results). Nevertheless, the main discriminant parameter is the time of analysis, which was sensibly lower for S4R and SC8R elements than CSS8. This first assessment demonstrated the reliability of the proposed modelling technique compared to the more complex FE types.

Table 2-3 Comparison among different FEs types for steel shell element, in terms of numerical results and CPU time

| Parameter | S4R | SC8R | CSS8 |
|---|---|---|---|
| $N_{numerical}$ (kN) | 803.149 | 831.51 | 903.61 |
| Difference $N_{numerical}$ - $N_{analytical}$ (%) | 0.57 | 4.12 | 13.15 |
| CPU time (s) | 174 | 182 | 844 |

### 2.6.2. Validation

For purpose of modelling approach validation, two different steps were performed: (a) a comparison among the numerical results in terms of static pressure imposed by the filling material on the silo walls and those obtained by analytical solutions based on Janssen's theory (Janssen, 1895), and modified Reimbert's theory (Reimbert and Reimbert, 1976); (b) a comparison among the fundamental frequencies provided by the proposed numerical models, the ones obtained by experimental investigations on a reduced-scale silo reported in (Silvestri et al., 2016), and the numeral investigations of a full-scale silo reported in Mehretehran and Maleki (2018).

Concerning to the first validation step, horizontal (or normal) pressure (Ph) and frictional (or vertical) traction (Pw) imposed by the filling on the walls were numerically computed for all models with grain material inside, i.e., 15 cases over 20, excluding the empty cases. For the cases V, S and B, Janssen's theory (see Equation 2-6) was applied, while for I and Q cases, modified Reimbert's theory (see Equation 2-7) was employed, according to the following expressions:

$$P_h(z) = P_{h0}\left(1 - e^{-z/z_0}\right)$$  2-6

$$P_h(z) = P_{h0}\left(1 - \left\{\left(\frac{z - h_0}{z_0 - h_0}\right) + 1\right\}^n\right)$$

2-7

where $P_{h0}$ is a pressure proportional to the lateral pressure ratio, the unit weight of the granular solid and $z_0$; $h_0$ is the height between the equivalent surface of the solid and the highest solid to wall contact; $z$ is the height of a generic point of the silo; $z_0$ is the ratio between the silo radius and a quantity proportional to the wall friction coefficient between the granular solid and the wall and the lateral pressure value. Then, the values of $P_w$ are defined as a fraction of $P_h$, as:

$$P_w = \mu_F P_h$$

2-8

where $\mu_F$ is the coefficient of friction.

It is worth remembering that both theories are currently adopted by most of the international standards such as the European ones (EN 1991-4, 2006). Figure 2-7 shows the comparison between numerical and analytical results in terms of $P_h$ and $P_w$ against the normalized height, $h_{norm}$, for the 5 different geometries of silos with 90% filling ratio. The static pressures numerically computed (red lines) are in good agreement with those provided by the theoretical solutions (blue lines), even though some discrepancies can be observed in the bottom parts of the silos, as also reported in (Ayuga et al., 2001) and in (Mehretehran & Maleki, 2018).
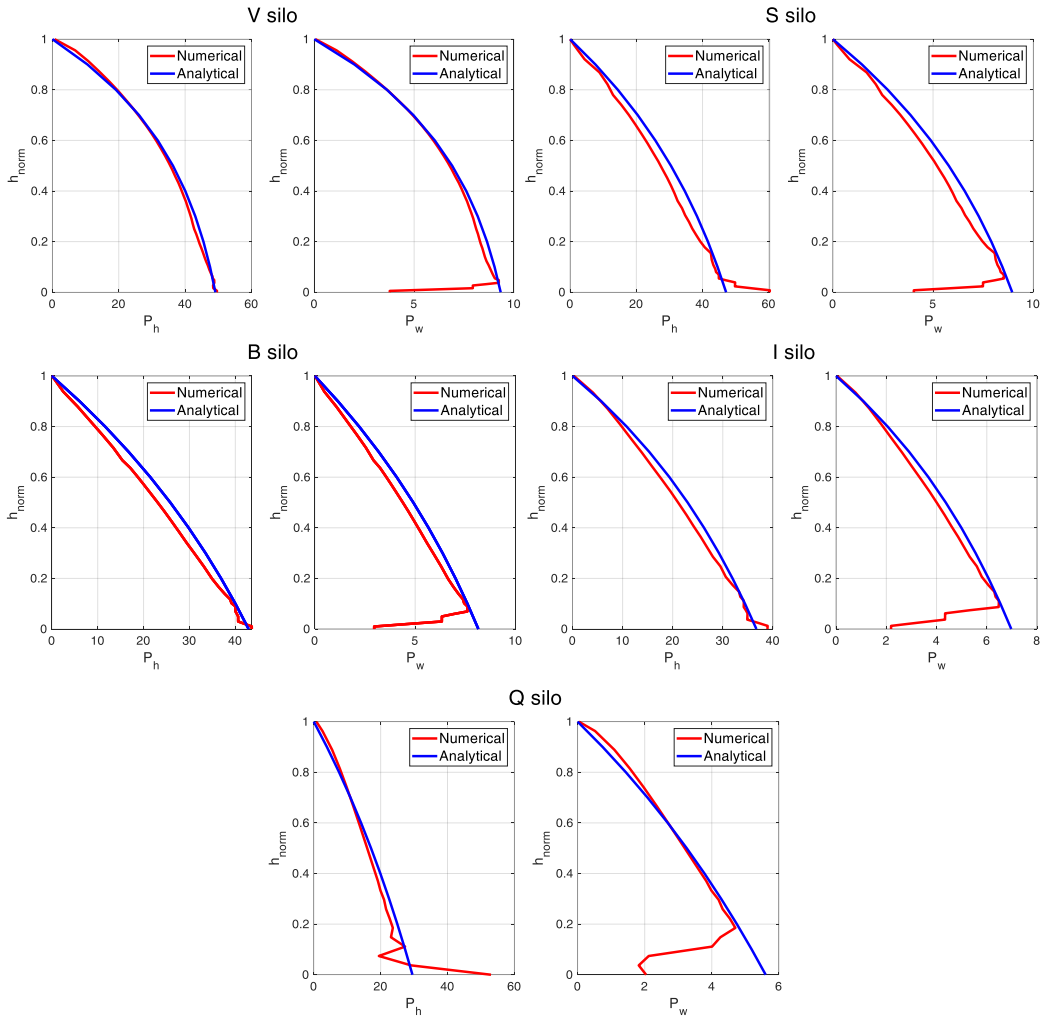
Figure 2-7 Comparison among numerical and analytical values of Ph and Pw for all silos geometries with 90% filling level.

In order to verify the dynamic characteristics of the FE models, the second validation step was performed by considering the experimental results on a reduced-scale benchmark silo manufactured in laboratory and subjected to dynamic excitations (Silvestri et al., 2016). The benchmark silo was numerically reproduced by employing the proposed modelling approach, and modal analysis was performed to compare outputs with the experimental results. The numerical results showed a good agreement with the experimental ones, where the first and second natural frequencies

calculated by the FE model were 15.65 Hz and 43.79 Hz, respectively, while the ones identified in Silvestri et al. (2016) after shaking table tests were declared in the ranges of 12.7-14.1 Hz and 43.9-44.9 Hz, respectively. It is also worth mentioning that due to the axial-symmetry, the model showed duplicated mode shapes in two main directions. Figure 2-8 reports the two lowest-frequency modes of vibration corresponding to a global cantilever flexural mode in the translational directions.
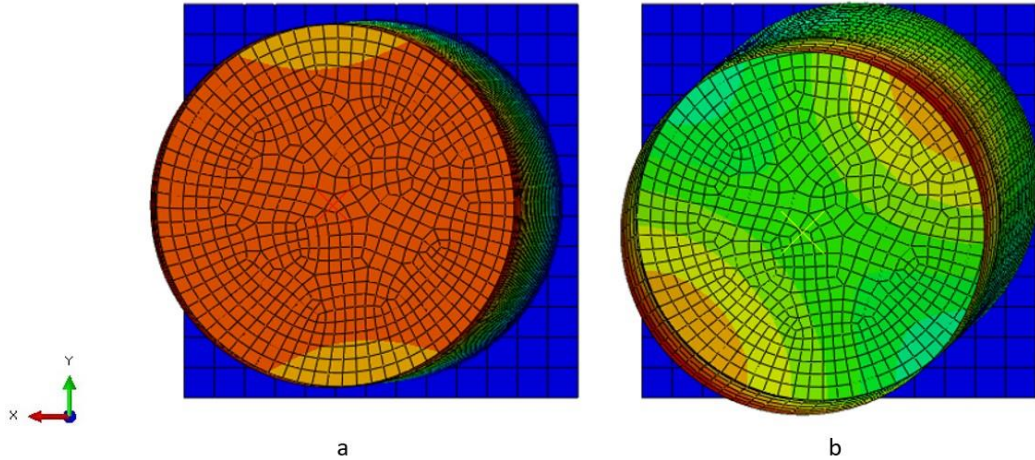


Figure 2-8 Model of the benchmark silo in (Silvestri et al., 2016) and vibration modes (a) the first vibration mode 15.65 Hz; (b) the second vibration mode 43.79 Hz.

To complete the second validation step, a second FE model was developed, for reproducing the outcomes of the numerical model of a full-scale silo presented in Mehretehran and Maleki (2018) in terms of modal analysis and static pressures. This silo presents t equal to 10 mm, h equal to 25 m, D equal to 10 m, while steel material was modelled with a $f_{y,s}$ equal to 250 MPa, $E_s$ equal to 210 GPa, $v$ equal to 0.3, and density equal to 7850 kg/m3. Using these data, modal analysis was carried out on the FE model and the frequency of the first vibration mode was found to be equal to 2.8 Hz, which was identical to the one obtained by Mehretehran and Maleki (2018).

84

## *2.7. Seismic analysis of the selected silos*

### *2.7.1. Modal analysis*

For the selected set of silo models, modal analysis was performed, aimed at calculating $T_1$ and the related participating mass (M[%]) as the geometry changes from V to Q, and as the percentage of filling level varies from 90% to the empty case. The results are reported in Table 2-4, in which it can be observed that the two varied parameters provide different results. Obviously, duplicated $T_1$ values were obtained in the two main orthogonal directions, due to the axial-symmetry of the structure. For a same filling level, going from the V to Q silo, the value of $T_1$ reduces at the same filling level, which is due to an increment of stiffness among silos (higher values of R/t provide a decrease in $T_1$, as well as occurs for lower values of h/D). For the same geometry, going from the 90% filling level to the empty case, the value of $T_1$ reduces, which is due to a gradual decrease of the total mass.

Table 2-4 Variation of the fundamental periods (T1) and the related participating mass (M[%]), according to the silos' geometry and percentage of filling level.

| Geometry | Filling level 90% | | Filling level 60% | | Filling level 30% | | Filling level 0% | |
|:---:|:---:|:---:|:---:|:---:|:---:|:---:|:---:|:---:|
| | $T_1$(s) | M[%] | $T_1$(s) | M[%] | $T_1$(s) | M[%] | $T_1$(s) | M[%] |
| *V* | 0.52 | 63.3 | 0.27 | 61.9 | 0.14 | 53.6 | 0.07 | 62.7 |
| *S* | 0.27 | 66.6 | 0.16 | 68.7 | 0.08 | 61.0 | 0.06 | 65.0 |
| *B* | 0.19 | 69.9 | 0.12 | 71.1 | 0.07 | 62.9 | 0.04 | 65.7 |
| *I* | 0.15 | 72.0 | 0.11 | 71.6 | 0.08 | 63.8 | 0.03 | 71.5 |
| *Q* | 0.12 | 73.4 | 0.10 | 72.1 | 0.07 | 67.2 | 0.02 | 77.0 |

Looking at the dispersion of $T_1$ for a same geometry, as the filling level varies, a high dispersion can be observed for the cases V and S, while a lower dispersion was obtained for the cases I and Q. This observation reveals that the squattest geometries are less sensitive to the filling level parameter, while the slenderest geometries have an opposite behavior. Different considerations can be provided for the values of M[%]. In general, values of M[%] range from 55% to 75% and for all service conditions, the M[%] increases going from the slenderest to the squattest configurations. Observing the service conditions, different outcomes can be derived. In fact, going

from 90% to 30% of filling level, the values of M[%] decrease for the same geometry. Instead, different trend from the filled silos is observed for empty silos, where the values of M[%] are higher than the ones obtained in 30% and 60% filled silos, and similar to the ones obtained in 90% filled silo.

## 2.7.2. *Pushover analysis and the threshold definition*

Once modal analysis results have been derived, pushover analysis was performed. As stated in Section 2.3, this step has two objectives: (a) predefine the most vulnerable buckling zones, which should be monitored when running NTHAs; (b) derive the values of proper thresholds, $EDP_{C,BM}$, beyond which the structure is considered to be failed exhibiting a specific BM. With these goals in mind, all silos were investigated, and the evolution of the deformed configurations was recorded. Pushing the structures, accumulation of stress was observed in different zones of the silo wall. In the squattest configurations, EFB anticipated EB and TWD, confirming the available literature. Also the structures with 90% and 60% filling ratio showed a similar outcome. When coming to the slenderest configurations and to the empty (or near-empty) cases, it was observed that the first occurring buckling mode is not always the EFB but can be the EB or the TWD. As a physical interpretation of the obtained results, in the case of the empty or 30% filling level, the development of elastic failures such as EB can be attributed to the absence of the stored solids, which could be imagined like an elastic lateral support against buckling. A summary of these outcomes is graphically outlined in Figure 2-9 and Figure 2-10, where the evolution of the deformation under horizontal static loads is shown in terms of displacement for the Q silo, 0% filling level, and for the Q silo, 60% filling level, respectively. In particular, for the case in Figure 2-9, the first BM developed is the EB in the middle zone of the silo, while EFB does not appear. Instead, in Figure 2-10, despite a hint of EB occurs, the main developed BM is the EFB. In both cases, due the application of the forces, TWD can be observed, and they are more or less accentuated depending on the analysis step. These observations assume high relevance, because they confirm that the combination between geometry and service condition governs the BM development

under horizontal actions. Still, the failure modes assumed at the base of this study are confirmed.
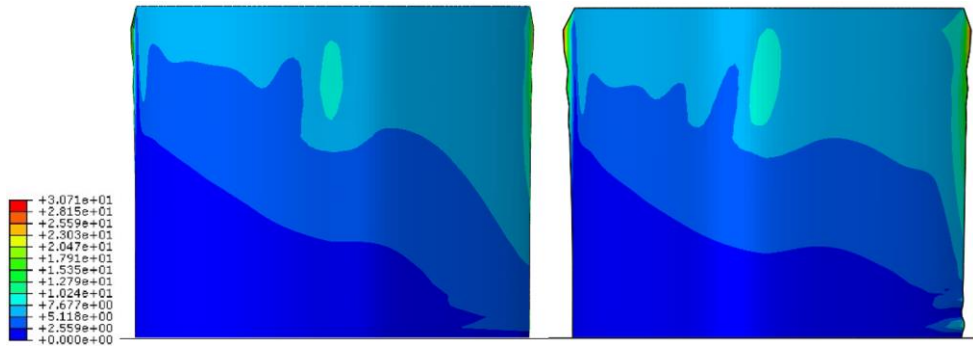


Figure 2-9 Evolution of the deformation in terms of displacements (from left to right) under pushover analysis of Q silo, 0% filling level.
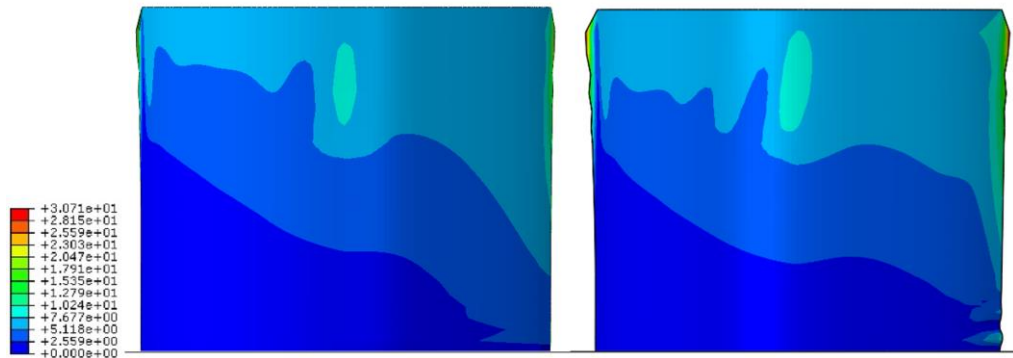


Figure 2-10 Evolution of the deformation in terms of displacements (from left to right) under pushover analysis of Q silo, 60% filling level.

The second step of the pushover analysis is the definition of the deformation limit beyond which the buckling phenomena develops (i.e., capture the thresholds) and the identification of the specific zone to monitor during NTHAs. After running the analyses, it is worth noting that while for EFB and TWD at the bottom and upper parts of the structures can be well identified, for the EB failure mode there is not a specific position to consider (e.g., a position that, for all silos, could be representative if normalized over the height). Thus, EB failure needs to be observed case-by-case, to define a

specific height of the zone. Table 2-5 reports the obtained thresholds values, $\theta_{W,BM}$, and the related quantities for estimating the EDP.

Table 2-5 Thresholds values for the considered silos, in terms of $\theta_{W,BM}$, $\delta_{,W,BM}$, $h_{W,BM}$.

| Silos | $\vartheta_{W,EFB}$ | $\vartheta_{W,TWD}$ | $\vartheta_{W,EB}$ | $h_{W,EFB}$ | $h_{W,TWD}$ | $h_{W,EB}$ | $\delta_{W,EFB}$ | $\delta_{W,TWD}$ | $\delta_{W,EB}$ |
|---|---|---|---|---|---|---|---|---|---|
| | (-) | (-) | (-) | (mm) | (mm) | (mm) | (mm) | (mm) | (mm) |
| V | 0.0048 | 0.0030 | 0.0035 | 259.60 | 25467.60 | 19860.60 | 1.246 | 76.403 | 69.512 |
| S | 0.0065 | 0.0030 | 0.0028 | 265.21 | 17542.30 | 13680.00 | 1.724 | 52.627 | 38.304 |
| B | 0.0072 | 0.0020 | 0.0030 | 27098 | 13527.40 | 6230.58 | 1.951 | 27.055 | 18.692 |
| I | 0.0080 | 0.0030 | 0.0022 | 254.72 | 10635.40 | 9094.59 | 2.038 | 31.906 | 20.008 |
| Q | 0.0097 | 0.0040 | 0.0010 | 249.75 | 7091.99 | 5741.89 | 2.423 | 28.368 | 5.742 |

As observed, for the values of $\theta_{W,BM}$ it is difficult to derive a trend among thresholds, considering that similar values occur for TWD and EB failure modes, while higher values were recorded for EFB. Looking at the other parameters, such as the $\delta_{W,BM}$, it can be observed that going from V to Q silos, the achievement of the EFB occurs at an increasing displacement, while the achievement of TWD and EB occurs at a decreasing displacement. Still, looking at the parameter $h_{W,BM}$, it was observed that the EFB occurs at the same height from the ground, while the TWD and EB failures occur at different heights, according to the type of considered silo.

Finally, it is useful to show how the values in Table 2-5 were estimated. For this scope, capacity curves in terms of $V_b$ vs. $\theta_{W,BM}$ are reported in Figure 2-11 for all silos, accounting for specific filling levels and monitoring different zones, that is to say, the base of the walls for the EFB and the middle of the walls for the EB. Thresholds are reported as black dots on each curve, according to the values in Table 2-5 and the criteria reported in Section 2.3. Regarding these latter, no cases can be mentioned in which convergence problems occurred and black dots reported in the final point of the curve. By varying the geometry of the silos and going from the slenderest to the squattest silos, the value of $V_b$ increases and the value of $\theta_{W,BM}$ decreases.

It is worth remarking that pushover analyses, here, are not employed with the objective of characterizing the seismic performance of silos, which is instead achieved by employing more reliable NTHA approach, as reported in Section 2.8.
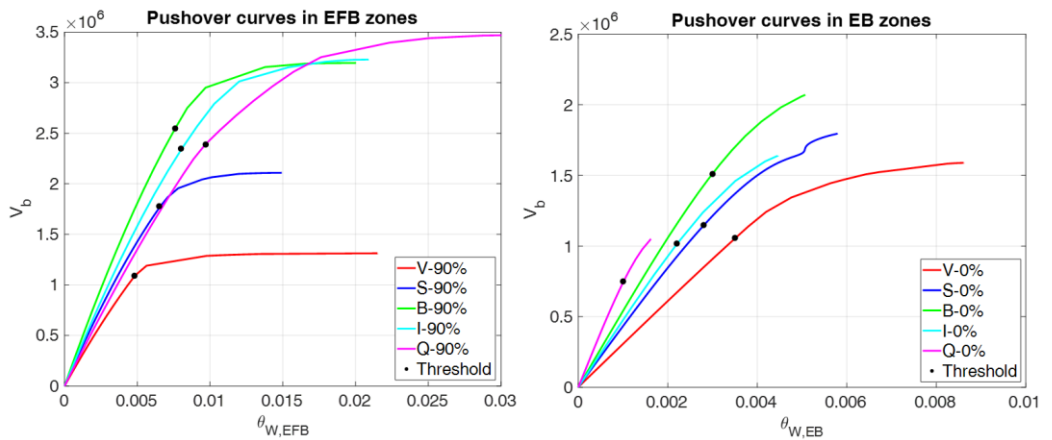
Figure 2-11 Pushover curves obtained by monitoring EFB and EB zones, for all silos with 90% and 0% filling level.

## 2.8. Record selection and cloud analysis

To run NTHAs on the silos, a proper record selection was firstly performed. For the case at hand, a set of 11 records was selected from the European-Strong-Motion-Database (Ambraseys et al., 2004), by referring to a target spectrum obtained from the municipality presenting the highest value of PGA in Italy (Ferla, Sicily), and by amplifying the spectrum according to a soil category of type C. The choice was performed, on one hand, in order to ensure high acceleration values on silos (and then, induce failures) and, on the other hand, to characterize the analysis in the country of the authors' universities. Following the prescriptions of Eurocode 8, records were selected in order to limit the difference between mean and target spectra to + 30 % and –10 % in a period range of interest for the investigated structures, that is, from 0 to about 1 s (low-medium range of periods) (Ruggieri & Vukobratović, 2023). The latter value was selected because it was twice larger than the maximum obtained $T_1$ value, which occurred for the V silo with 90% filling level. All elastic ground motion records (5% damping) are reported in Figure 2-12, with the indication of target and mean spectra.
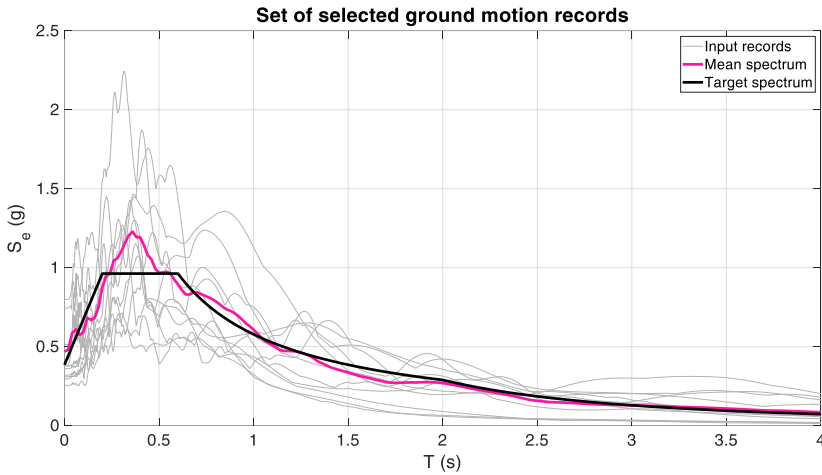
Figure 2-12 Set of selected records.

To reduce the effort of the analysis, considering the axial-symmetry of the structures, the numerical models developed were modified, opting for running NTHAs on half of the systems and by applying the adequate boundary conditions described in Section 2.3. It is worth noting that this approach was also employed by Mehretehran and Maleki (2018), with the purpose of running IDAs on complex numerical models. In the NTHAs, a damping ratio of 2% was considered for the models and the implicit time-integration technique provided by ABAQUS was used. It is worth mentioning that this selection of the damping ratio can be conservative. However, the material damping inherent in the system's material is complex, and in the case of granular material, it may vary depending on the internal structure of the granules. Generally, the structural of the granular material is very sensitive to dynamic excitation and this is attributable to the compaction phenomena imposing unfavorable impact on the damping ratio. In this regard, a deep investigation into the material damping is recommended for careful consideration of the damping ratio. Nevertheless, a selection of relatively low damping ratio appears to me more favorable, and it provides a margin of safety. Coherently with the modelling simplifications, accelerograms were applied in one direction, that is, the one in the symmetry plan. Nevertheless, it is worth mentioning that the vertical component of the seismic action could be crucial for the silo safety (Butenweg et al., 2017), considering an additional acceleration on the silos mass, which yields addi-

90

tional dynamic pressures. This could be important especially for the slender or elevated silos (since it particularly relevant for the vertical pressure on the hopper in case of elevated silos).

From the observation of the first outputs, silos behaved as expected, exhibiting an EFB failure mode, especially when 90% and 60% of filling material was considered. This effect is graphically shown in Figure 2-13, which reports the development of EFB for the Q (from left to right, the first two images) and S silos (from left to right, the last two images), under a randomly chosen record among the above-mentioned set.
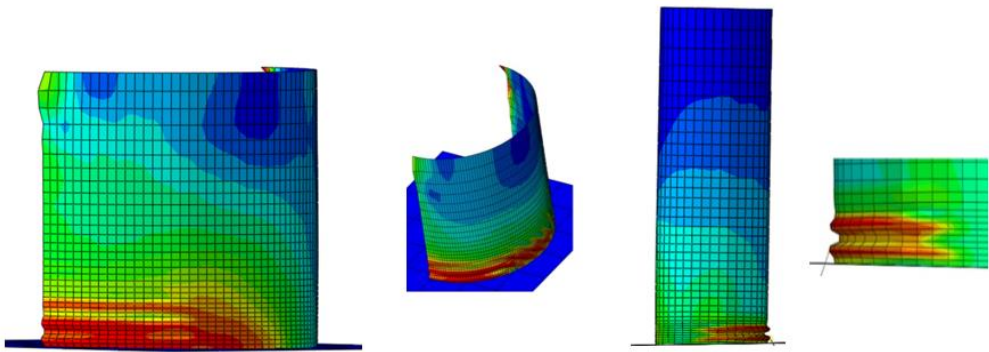


Figure 2-13 Numerically predicted EFB for Q (from left to right, the first two images) and S (from left to right, the last two images) silos, subjected to a randomly chosen ground motion record from the selected set.

The NTHAs campaign was performed in the form of cloud analysis, without performing record scaling. Figure 2-14 shows a couple of examples reporting the distribution of cloud points in the EDP-IM space and the global power law fit. Some comments can be provided about the obtained results. Firstly, as expected, the points are dispersed, which means that on the base of the performed regression, the values at higher IM could deviate from the near reality. Thus, other approaches could provide substantial improvements, such as by opting for IDAs or by scaling the ground motions to better capture the effective BMs. On the other hand, it is worth considering manifold aspects that justify our analysis simplifications. First of all, an undeniable computational effort reduction can be mentioned, considering that for running 220 analyses (20 silos with 11 records) on the detailed models, using a more powerful

workstation than the one described in Section 2.6.1 (Core i9-13900HK CPU, 64 GBs of RAM, and an NVIDIA GeForce 3090 GPU equipped with 24 GBs or VRAM), more than 1 month was spent. Anyway, with the selected suits of input, no collapses occurred, which means that all the planned EDP-IM points were obtained for the global fitting. Moreover, taking into account the combination between the input records and the selected IM, the analyses performed have covered a band from about 0.5g to about 2-2.2g in the low-medium range of periods, providing an EDP-IM relationship in an IM-band consistent with the existing literature and accounting for a seismic intensity able to bring the considered structures to failure (Mehretehran and Maleki, 2018). An important consideration should be provided about the obtained results in Figure 2-14. Considering silos as short period structures, the obtained exponent of the power low is extremely lower than 1, which is not properly correct if considering an expected value close or greater than 1. This numerical aspect, due to the extremely scattered results, confirms once again the necessity to increase the number of analyses to run. Finally, although the results obtained could be not so accurate for some parts of the EDP-IM space, our investigation provides clear information on the most likely (dominant) failure mode at the variation of the geometry and service conditions.
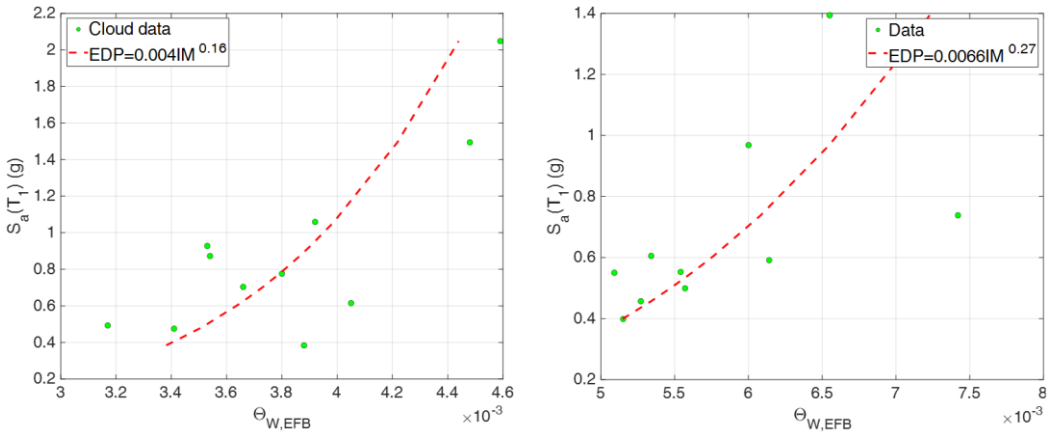


Figure 2-14 Cloud analysis and power law regression for the Q silo with 90% filling level (left) and I silo with 60% filling level. IM is Sa(T1), expressed in unit of g, while EDP is θW,EFB.

## 2.9. Estimation of seismic fragility and discussion of results

From the previous results, fragility curves can be derived according to the approach described in (Bakalis & Vamvatsikos, 2018) for all silos, accounting for the combination of all geometries, all service conditions, and all BMs. Results in terms of fragility curves are reported in Figure 2-15, while Table 2-6 reports the detailed values of $\mu_{BM}$ and $\sigma_{BM}$.
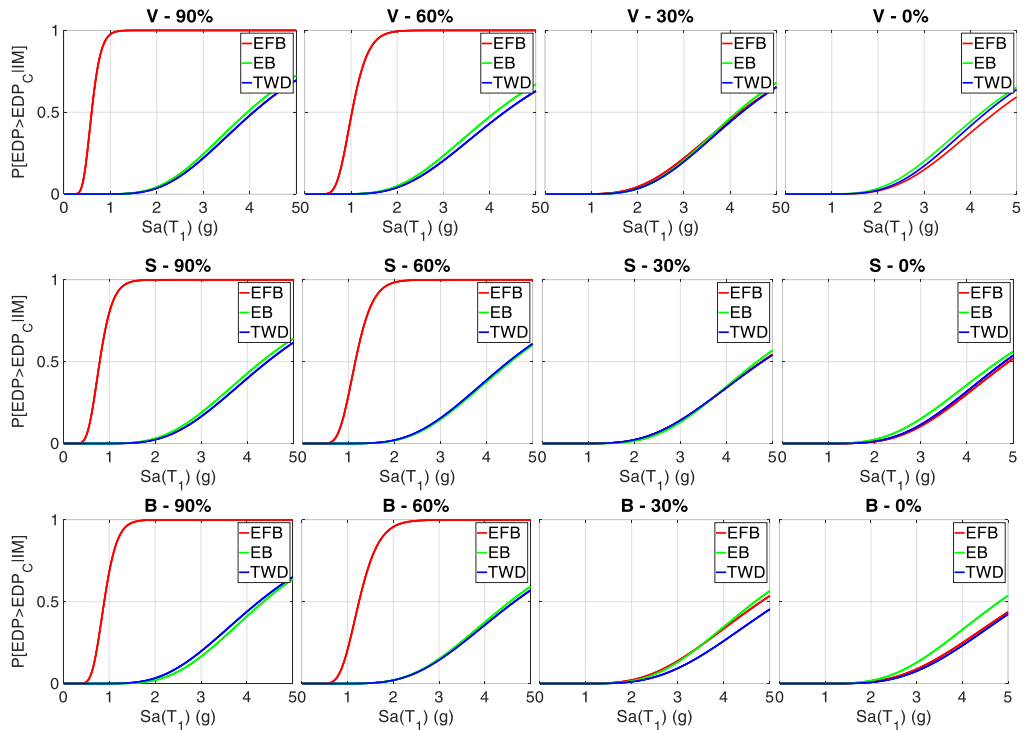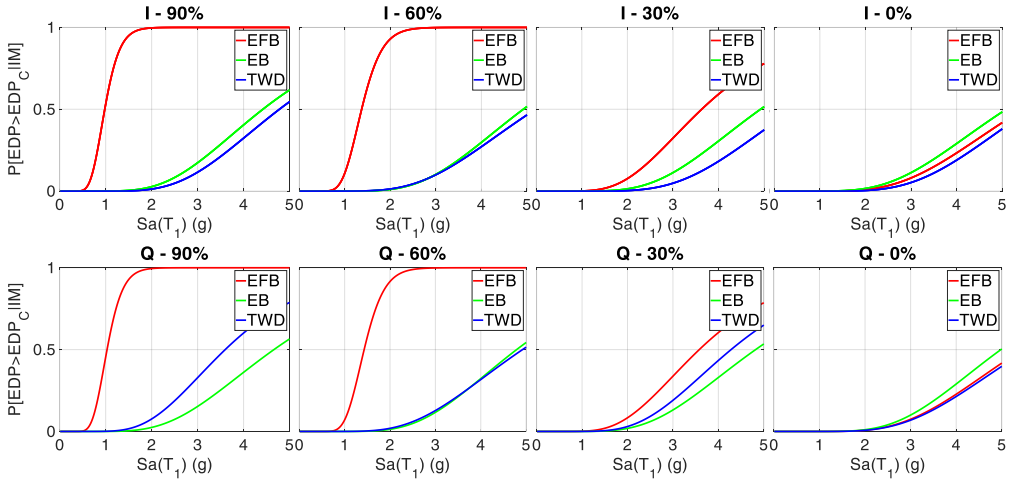
Figure 2-15 Fragility curves accounting for all silos geometries, all conditions of functionality and all BMs

As expected, the EFB is the most probable BM occurring on silos when dynamic excitation is applied, while the other BMs, i.e., TWD and EB, could occur in specific cases (quasi-empty and empty silos) and for high values of the seismic intensity, anticipating the EFB. Discussing in detail the results obtained from the point of view of service conditions, it can be observed that going from the filled to the empty cases, the EFB fragility curves reduce their $P_f$ ($\mu_{EFB}$ increases). The physical interpretation of this result can be given by considering that a reduction of the stored material induces a reduction of the mass excited under the earthquake, inducing a benign effect on the seismic performance of the silo. Looking at the EFB fragility curves for a given filling level, varying the geometry from the slenderest to the squattest silo the $\mu_{EFB}$ increase (an increment of about 40% was recorded, with an almost doubled median), which implies a better performance of squat silos under earthquake actions. As a matter of fact, silos with lower aspect ratio present higher performance than those with high aspect ratio under seismic actions, given the same service conditions. Moving to silos with 30% and 0% of filling level, EFB fragility curves shift to right, and the EB and TWD fragility curves can anticipate the previous one. Anyway, this estimate cannot be accurate for the reasons repeatedly discussed throughout the study: for high levels of seismic intensity, different BMs could occur and anticipate the usually

expected EFB. Also, this result assumes a physical sense, by considering that a low total mass characterizing an empty system implies a low fundamental period of vibration and then, a reduction of the seismic demand. The very high values of $\mu_{BM}$ for quasi-empty or empty cases suggest that a low seismic risk is connected to these kinds of structures (they can difficultly collapse under a natural seismic event) and that the most influent parameter in the overall fragility estimate are the stored material type, its level and its interaction with the structure.

Table 2-6 Values of $\mu_{BM}$ and $\sigma_{BM}$ for fragility curves, accounting for all geometries, all conditions of functionality and all BMs.

|  | $\mu_{EPB}$ | $\sigma_{EFB}$ | $\mu_{TWD}$ | $\sigma_{TWD}$ | $\mu_{EB}$ | $\sigma_{EB}$ |
|---|---|---|---|---|---|---|
| V - 0% | 4.55 | 0.40 | 4.25 | 0.42 | 4.35 | 0.39 |
| V - 30% | 4.21 | 0.44 | 4.15 | 0.40 | 4.25 | 0.41 |
| V - 60% | 1.02 | 0.27 | 4.12 | 0.44 | 4.32 | 0.44 |
| V - 90% | 0.60 | 0.26 | 3.95 | 0.40 | 4.08 | 0.40 |
| S - 0% | 4.91 | 0.39 | 4.68 | 0.43 | 4.82 | 0.40 |
| S - 30% | 4.77 | 0.43 | 4.67 | 0.39 | 4.78 | 0.43 |
| S - 60% | 1.15 | 0.26 | 4.52 | 0.39 | 4.48 | 0.40 |
| S - 90% | 0.79 | 0.28 | 4.31 | 0.41 | 4.44 | 0.40 |
| B - 00% | 5.35 | 0.43 | 4.81 | 0.42 | 5.41 | 0.41 |
| B - 30% | 4.81 | 0.43 | 4.68 | 0.40 | 5.25 | 0.42 |
| B - 60% | 1.25 | 0.27 | 4.55 | 0.40 | 4.65 | 0.41 |
| B - 90% | 0.89 | 0.25 | 4.36 | 0.38 | 4.26 | 0.41 |
| I - 0% | 5.46 | 0.43 | 5.09 | 0.44 | 5.63 | 0.39 |
| I - 30% | 3.63 | 0.42 | 4.92 | 0.41 | 5.65 | 0.38 |
| I - 60% | 1.37 | 0.26 | 4.92 | 0.39 | 5.19 | 0.43 |
| I - 90% | 0.98 | 0.26 | 4.42 | 0.41 | 4.78 | 0.39 |
| Q - 00% | 5.45 | 0.41 | 4.98 | 0.40 | 5.57 | 0.42 |
| Q - 30% | 3.58 | 0.42 | 4.82 | 0.42 | 4.28 | 0.40 |
| Q - 60% | 1.43 | 0.24 | 4.79 | 0.39 | 4.92 | 0.43 |
| Q - 90% | 1.03 | 0.26 | 4.66 | 0.43 | 3.60 | 0.41 |

## 2.10.  Final remarks

This chapter presents a numerical procedure to derive seismic fragility of cylindrical ground-supported steel silos storing granular-like material. The procedure

aims to investigate the influence of three main aspects on the seismic behaviour of these kinds of structures: (a) the geometry of the silos wall; (b) the service conditions, that is, the filling level of the stored material; (c) the type of failure mode. With this goal in mind, the procedure has been articulated in four consecutive steps. The first step consists in the selection of a set of smooth steel silos, which cover a large range of possibilities. The set was selected by assuming different geometries (e.g., varying from slender to squat silos) and different filling level of stored materials (from filled to empty case), obtaining a number of 20 cases. The second step consisted in the detailed modelling of the generated set of silos, which was performed through the software ABAQUS. Three-dimensional numerical models were created for simulating the behaviour of steel shell walls, the physical properties of a granular like material and the interaction between the above components. Some validations with data from the existing literature and the available analytical solutions were carried out, by assessing the numerical results in terms of static pressures and dynamic features. Considerations were provided about the mesh of the detailed numerical models, in order to ensure effective solutions of the successive analysis. The third step consists in the analysis campaign, which was based on the combination of static and dynamic nonlinear analyses. The role of static analyses is double: (a) the assessment of the possible failure modes occurring on steel silos under seismic actions, i.e., Elephant Foot Buckling in the bottom part of the wall, Elastic (diamond or similar shape) Buckling in the middle part of the wall, Top Wall Damage in the upper part of the wall; (b) the definition of likely thresholds to define the achievement of all the considered buckling modes. Instead, nonlinear time history analyses have been developed in order to define the probabilistic relationship between demand and capacity, assuming specific parameters for this purpose. With this regard, a set of 11 records was suggested to excite structures through a cloud analysis, and a regression analysis was performed through the power law fit. Although the number of analyses performed was reduced (to limit the computational cost for analyzing the models), the fourth step consists in the derivation of fragility curves for all silos geometries, all filling levels and all possible failure modes. The obtained results highlight some novel aspects. Accounting for

the influence of the silo geometry, the results have revealed that silos storing solids are more vulnerable to the elephant foot buckling, and this is emphasized when structures are filled with 90% and 60% of the maximum capacity. Looking at the median of fragility curves, going from squattest to slenderest silos, the probability of failure for same seismic intensity increases, which means that squattest silos show better performance than the slenderest ones under seismic actions (a difference of about 40% was recorded). With regard to the effect of the ensiled material, results indicated that Elephant Foot Buckling is the governing failure mode for filled silos (90% and 60%) while, in case of quasi-empty or empty (i.e., 30% and 0%), all three investigated failure modes present comparable probability of failure, despite high median values are obtained. Still, empty (or quasi-empty) silos exhibit very high seismic capacity, regardless of the failure mode, which means that in these service conditions there is a low probability of failure for silos, especially under ordinary natural seismic events.

Further developments of the work will be aimed to extend the investigation to different kinds of silos (e.g., stiffened, corrugated), and to consider different types of stored materials. In addition, a refinement of the numerical models could be performed, by considering additional physical factors for the granular solid material, such as the compaction of it under earthquakes actions. From the fragility curves derivation point of view, different approaches from the simple one herein used should be employed, by opting for using more records and by involving other analysis techniques (e.g., IDA).

# 3. Assessment of dynamic overpressure in flat bottom steel silos through a detailed modelling approach

**Abstract**: This chapter presents a study dealing with the assessment of the dynamic overpressure induced by earthquakes in flat bottom steel silos. In particular, silos represent a fundamental character of industrial plants, as part of an intricate network of mechanical and structural components. The safety of silos is a focal point in industrial processes, especially when the action of hazardous events (e.g., earthquakes) can mine their structural stability and, subsequently, the stored material. In this view, a robust and reliable design approach is crucial for civil engineering professionals, which need to properly understand and predict the dynamic conditions to which silos are subjected, especially under seismic excitations. The current Euro-pean standard, EN 1998-4-2006, suggests a static approach, by using equivalent loads to emulate an additional seismic pressure as seismic overload. However, a more realistic estimation of additional seismic overpressure could yield a more rational steel wall analysis and design for new structures and assessment for existing structures. With this goal in mind, this part of dissertation presents detailed numerical analyses to estimate the dynamic overpressure experienced by silos wall under seismic excitation. In detail, nonlinear finite element, FE, models were created for two geometries of silos, i.e., slender and squat and nonlinear time history analyses were carried out. The detailed models accounted for geometrical and material nonlinearity of steel silos and of stored granular-like solid material. This latter was simulated by employing hypoplasticity as constitutive model. The output of the analyses allowed to quantify the additional dynamic pressure, which was compared to the one provided by the European

standards (i.e., equivalent static approach). From the comparison, the main differences were highlighted, showing the need of modifying current code-based approach.

**Keyword**: Steel silos · Granular-like material · Hypoplasticity · Industrial facilities · Seismic performance · Dynamic Overpressure · Equivalent static loads.

## *3.1. Introduction*

Industrial plants are large and non-homogeneous complex of different structural and mechanical units. Ensuring the safety and ongoing operations in the production processes implies a reliable design and construction of the relevant structures (Alessandri et al., 2018). A fundamental part of industrial plants is characterized by storage systems, such as steel silos, aimed at containing granular solids covering a wide range of substances such as flour, iron ore pellets, cement, chemical and agricultural materials. From the geometrical point of view, steel silos feature a circular plan shape, although different structural configurations can be adopted (Wójcik & Tejchman, 2015). Still, a primary categorization of silos can be provided, by distinguishing the flat-bottom ground supported silos (Butenweg et al., 2017), from elevated substructure-supported silos (Kanyilmaz & Castiglioni, 2017). As thin-walled shell structures, steel silos are inherently susceptible to buckling phenomena under extreme load conditions, as demonstrated by latest seismic events, e.g., 2023 Turkey-Syria Earthquake (Hu et al., 2023), 2012 Emilia Earthquake (Brunesi et al., 2015), which also showed the effects of dynamic excitations and the related damage patterns.

Nevertheless, from the static behavior point of view, silo walls are typically subjected to horizontal and vertical frictional pressures, which can be estimated through the Janssen theory (Janssen, 1895). However, under dynamic conditions, the silo walls are subjected to additional dynamic pressure (named, dynamic overpressure), which could significantly impact the structural integrity of silo walls. Thus, to assess the entity of the dynamic overpressure and to ensure a rational shell wall analysis and design, a more realistic simulation is required, especially considering that the current

100

state of the art is base of the provisions given by technical standards, e.g., Eurocode, (EN 1998-4, 2006). This latter proposes an equivalent static approach, illustrated in section 3.1.3, for representing the dynamic overpressure on the silo walls that, although simplified and easy to implement, could hide some approximations that over-/under-estimated the real matter.

On this basis, the aim of this study is to assess the reliability of the equivalent static approach suggested by the European standards (EN 1998-4, 2006), by verifying its assumptions and outcomes in terms of intensity and the distribution of overpressure given by seismic events. The verification process involves a comparison between pressure pattern produced in accordance with the European standards specifications and an overdetailed finite element method (FEM) solution, based on a numerical sophisticated modelling approach. The numerical model takes into account the behavior and the dynamic response of the silo structure and the stored particulate solid material. Nonlinear behavior of filling material was simulated, as well as the shell wall and the interaction between the above components. For the granular-like material, a hypo-plasticity constitutive model was employed to accurately reflect the behavior of filling under dynamic excitation and to capture its realistic impact on the silo wall. Two different geometries were considered, that is, slender and squat silos. Nonlinear time-history analyses (NTHAs) were run on both geometries, in order to simulate the abovementioned effects of seismic excitation. The comparisons between the detailed numerical model and the equivalent static loads were presented and discussed, with the aim to improve the current code-based practice.

### 3.1.1.  Silo seismic behavior

Although the scientific literature proposes different studies on the diverse components in industrial sites, such as tanks (Gabbianelli et al., 2022; Gian Michele Calvi & Roberto Nascimbene, 2023), piping systems (Vathi & Karamanos, 2018), framed structure   especially with reference to different hazardous sources (e.g., earthquakes, blast loading, and strong winds), the study of the behavior of silos and the related interaction with the stored material were poorly investigated in the past.

Nevertheless, the dynamic characteristics and the principal dynamic behavior of silos were investigated by the scientific literature since the middle of the last century. In this context, Lee (1981) presented an analytical estimation of the effective mass, the portion of mass of the grain which pushes on the silo walls under dynamic excitation. Trahair et al. (1983) introduced simple and conservative expressions to quantify the pressures applied on the silo wall under horizontal dynamic excitation representing the seismic response effect of the stored material on the shell wall. Yokota et al. (1983) employed the finite element techniques to model the cylindrical shell and the ensiled material, assuming coal as an ensiled material. The FE model yielded in natural frequencies that are 30-40% larger than those reported by the corresponding experimental findings. Similarly, Shimamoto et al. (Shimamoto et al., 1984) studied the dynamic response of silo containing coal based on the FE model, using conical shell elements. However, the numerical solution represented by the resonance curves were compared with those obtained based on the tested silo specimens. Rotter and Hull (1989) studied the response of squat circular ground-supported silos based on elastic FE analysis where stresses induced, in the silo wall, by the seismic action were calculated and relevant expressions were provided. The study concluded that the membrane stresses in the shell are proportional to R/t and to H/R ratios (R is the radius of the silo, t is the wall thickness and H is the height). The seismic load was represented by quasi-static horizontal body force considering a uniform horizontal acceleration. Sasaki and Yoshimura (1992) evaluated the effective mass, which pushes on the silo wall under an earthquake, through a numerical model reproducing a tested scaled silo. Hardin et al. (1996) reported on the acceleration history the am-plification of the horizontal acceleration, and the stress-strain distribution of a large-scale steel silos storing wheat based on numerical studies. In that work, the structure was accelerated by real earthquake record and the grail-silo system was modelled by the means of composite shear-beam model. Later, Younan and Veletsos (1998a; 1998b), examined based on analytical investigation cylindrical silos storing linear viscoelastic solids and subjected to earthquake-induced ground motions. The aim of the study was to provide an analytical formulation to describe the seismic response of the filled

silo, accounting for the parameters of slenderness ratio and the wall flexibility. Knoedel et al. (1995) discussed different approaches of modelling imperfections in steel silos based on experimental and numerical work. Knoedel and Ummenhofer (2016) addressed the imperfections in the aluminum silos tackling the discrepancy between the outcomes of the scientific research and the corresponding equations in EN 1999-1-5 (EC9)(2009). Holler and Meskouris (2006) characterized the effect of the different component (e.g., the variation of some key parameters, such as the grain-wall interaction, the aspect ratio, the nonlinearity of the granular material, and soil-structure interaction) on the silo seismic behavior. The study adopted the linear elastic wall behavior, grounding on the basis of FE numerical modelling. The study concluded that a substantial portion of the ensiled weight does not participate in the horizontal pressures, in case of squat silos, as it is transferred directly to the ground.

Nateghi and Yakhchalian (2012) presented further investigating on the influence of the aspect ratio on the seismic response of ground-supported silos. Based on numerical observations, the study emphasized the influence of the aspect ratio and concluded that assuming a constant value of acceleration distribution leads to conservative design for a squat silo but, on the other hand, this assumption holds fair for a slender one. However, only one artificial earthquake record was considered in this study. Silvestri et al. (2012) investigated the effective mass pushing on the silo wall under seismic action. Grounding on a new physical-based analytical approach, subsequently refined by Pieraccini et al. (2015), this study underscored the conservatism of Eurocode provisions (EN 1998-4, 2006) with regards to squat silos. Within the same context, a series of shaking table tests were performed by Silvestri et al. (2016), on scaled silos made of polycarbonate sheets and containing granular-like material. This experimental work unveiled the substantial effect of the coefficient of wall-friction on the base overturning moment, aligning with the analytical approach introduced in (Silvestri et al., 2012). However, this effect is disregarded by the cur-rent Eurocode provisions, conservatively estimating the base overturning moment. Butenweg et al. (2017) investigated the static equivalent loads by comparing it to a sophisticated approach based on the time history analysis. The study revealed that considering an ac-

celeration profile determined based on multimodal analysis of a simplified beam is more realistic than adopting a simplified linear acceleration along the height. The comparison involved assessing stresses generated in the silo wall, calculated based on the different approaches. Moreover, the study recommended using the nonlinear numerical modelling as it leads to more economical design than the equivalent static load approach in case of squat silos, as also suggested by (Holler & Meskouris, 2006). Durmus and Livaoglu (2015) presented a simplified silo model represented by a single degree of freedom flexural cantilever beam with a lumped mass. The study aimed at estimating the base shear force, the dynamic pressure, the fundamental frequency of vibration and the soil structure interaction effect. The results obtained by this analytical solution were compared with those obtained based on the numerical simulation. This study stated concluded that the effect of soil structure interaction has negligible contribution, especially in case of squat silo, and can be ignored in practical applications. Knoedel et al. (2022) presented an investigation on the behavior factor of elevated silos, this study recommended a two-step approach to substitute the single behavior factor for the overall structural system with an advantage of avoiding any sudden buckling of the shell wall prior to developing plasticity at the sub-structure. Mehretehran and Maleki (2018) studied the dynamic buckling behavior of steel silos with a constant wall thickness. The silos were assumed to be filled up to 90% of the maximum capacity. The study estimated the seismic buckling capacity, by means of incremental dynamic analysis, of the relevant silo by the peak ground acceleration PGA that initiate the buckling. Where the elephant foot buckling was the only observed damage pattern. The results indicated that slender silos exhibit higher vulnerability to buckling failure, whereas squat ones demonstrated a considerably higher resistance under same conditions. Same authors extended their findings to include the stepped wall steel silos under seismic conditions ( Mehretehran and Maleki, 2021) asserting that the vertical component of the seismic excitation is of a quite marginal effect for ground supported silos. Silverstri et al. (2022) reported a series of shaking table tests on a full scall flat-bottom steel silo (3.64 m-diameter 5.50 m-height) with corrugated walls, filled with wheat. The study provided an experimental insight into the static

pressure, the dynamic properties, and the dynamic overpressure. Regarding dynamic behavior, the re-search found that the fundamental frequency is influenced by acceleration and grain compaction. Additionally, dynamic amplification increases vertically within the silo, reaching its maximum at the top of the ensiled content, and the additional normal pressure rises with depth. Furinghetti et al., (2024)discussed on the efficiency of seismic base-isolation application on the same silos specimen, the study revealed a notable 30-80% reduction in the dynamic response, i.e., acceleration amplifications and the dynamic overpressures, of the system under isolated-base conditions. Jing et al. (Jing, Wang, et al., 2022) conducted a combined numerical and experimental work on silos concluding that the horizontal pressure incremented with higher peak ground acceleration and silo height, with the maximum dynamic horizontal pressure observed at the top of the silo. Another experimental study was presented by Jing et al. (Jing, Chen, et al., 2022) based on shaking table tests and considering different real and artificial earthquake excitations. The study highlighted the positive impact of the presence of granular material on the energy dissipation of the grain-silo system. In the end, For the sake of conciseness, the state-of-art overview above is limited to the ground-supported steel silos which aligns closely with the focus of this work. However, more elaborated state-of-art about the silo structure and their behavior under different conditions is presented in chapter 1 of this dissertation.

### 3.1.2.  Hypoplastic constitutive model

Hypoplasticity constitutive model was employed to represent the behavior of the ensiled material. To describe hypoplasticity, principle of continuum mechanics can be used, by referring to the mechanical behavior of an ensiled material, in a confined body. This approach, usually theorized for simulating more precisely the cyclic behavior of the granules through describing the mechanical behavior of granular materials by assuming grains as aggregated to a simple granular skeleton. The first version of hypoplasticity was developed in Karlsruhe University by von Wolffersdorff, (1996). In detail, hypoplasticity consists in the relation associating the strain rate to the stress rate, where the inelastic behavior is modeled by using the modulus of the strain rate. The nonlinear behavior is modeled by the stress dependence of the stiff-

ness. The rate-type hypoplasticity formulation ensures a realistic modelling of loading and unloading paths, therefore the hypoplasticity can simulate the nonlinear behavior of the relevant granular material. Although Von Wolffersdorff's constitutive law well performs in the simulation of the deformation due to the grain skeleton rearrangements, it exhibits some issues when modelling cyclic stressing or deformation with small-amplitude deformations. In this regard, ratcheting is the most striking drawback. Ratcheting can be defined as the excessive accumulation of deformation predicted for small stress cycles. To overcome this shortcoming, intergranular strain was added to the hypoplasticity constitutive model by Niemunis & Herle, (1997), which introduced additional parameters to better simulate the deformation of the interface layer between the grains. Other options of hypoplastic theory can be also mentioned, such as the modified versions using time history analysis function according to Bauer (1992) and Braun (1997), and Gudehus (1996) formulation. However, according to (Butenweg et al., 2017) hypoplasticity with the intergranular strain approach proved to be the most realistic approach to simulate the time dependent cyclic behavior of granular material when comparing with soil mechanic cyclic tests. Consequently, Von Wolffersdorff's hypoplasticity constitutive model, extended by the intergranular strain approach is adopted in this study.

The general stress-strain relation in the hypoplastic model considering the intergranular strain concept is:

$$\dot{T} = \mathcal{M} : D \qquad \qquad \text{3-1}$$

where $\dot{T}$ is the objective Jaumann stress rate, $D$ is stretching rate, and $\mathcal{M}$ is a fourth-order tensor representing stiffness. The intergranular strain $\delta$ is obtained by the accumulation of $D\Delta t$. The term $\rho$ is the normalized magnitude of $\delta$ and it is defined as:

$$\rho = \frac{\|\delta\|}{R} \qquad \qquad \text{3-2}$$

where R is the intergranular strain parameter used to define the strain range of active intergranular strain, the $\|\ \ \|$ is the Euclidean norm of a tensor, and $\|\delta\| = \sqrt{\delta_{ij}\delta_{ij}}$. However, the material stiffness can be calculated from the expression of $\mathcal{M}$:

$$\mathcal{M} = [\rho^x m_T + (1 - \rho^x)m_R]\mathcal{L} + \begin{cases} \rho^x(1 - m_T)\mathcal{L}:\widehat{\delta}\widehat{\delta} + \rho^x N\widehat{\delta} & for\ \widehat{\delta}:D > 0 \\ \rho^x(m_R - m_T)\mathcal{L}:\widehat{\delta}\widehat{\delta} & for\ \widehat{\delta}:D \le 0 \end{cases} \qquad \text{3-3}$$

where $\widehat{\delta}$ represents the direction of the intergranular strain and is defined as

$$\widehat{\delta} = \begin{cases} \delta/\|\delta\| & for\ \delta \ne 0 \\ 0 & for\ \delta = 0 \end{cases} \qquad \text{3-4}$$

The evolution equation for the intergranular strain tensor $\delta$ is:

$$\dot{\delta} = \begin{cases} (\ell - \widehat{\delta}\widehat{\delta}\rho^{\beta r}):D & for\ \widehat{\delta}:D > 0 \\ D & for\ \widehat{\delta}:D \le 0 \end{cases} \qquad \text{3-5}$$

where $\mathcal{L}$ is a fourth-order tensor and $N$ is a second-order tensor. $\mathcal{L}$ and $N$ tensors are functions of stress and void ratio according to equations 3-6 and 3-7

$$\mathcal{L} = f_b f_e \frac{1}{\widehat{T}:\widehat{T}}(F^2\ell + a^2\widehat{T}\widehat{T}) \qquad \text{3-6}$$

$$N = f_d f_b f_e \frac{Fa}{\widehat{T}:\widehat{T}}(\widehat{T} + \widehat{T}^*) \qquad \text{3-7}$$

in which $\ell$ is the unit tensor of the fourth-order. Defining $T$ as the stress tensor and $1$ is the unit tensor of second order, it can be estimated as

$$\widehat{T} = T/trT \qquad \text{3-8}$$

$$T^* = T - 13\ 1 \qquad \text{3-9}$$

$$a = \frac{\sqrt{3}(3 - \sin \varnothing_c)}{2\sqrt{2}\ \sin \varnothing_c} \qquad \text{3-10}$$

$$F = \sqrt{\frac{1}{8}\tan \psi^2 + \frac{2 - \tan \psi^2}{2 + \sqrt{2}\ \tan \psi \cos 3\theta} - \frac{1}{2\sqrt{2}}\tan \psi} \qquad \text{3-11}$$

$$\tan \psi = \sqrt{3}\|\widehat{T}^*\| \qquad \text{3-12}$$

$$\tan 3\theta = -\sqrt{6}\frac{tr(\widehat{T}^{*3})}{[tr(\widehat{T}^{*2})]^{3/2}} \qquad \text{3-13}$$

In the above-mentioned equations, tensors of the second-order are denoted with bold letters. In addition, different kinds of tensorial multiplication are used such as:

$$[\mathcal{M}:D = \mathcal{M}_{ijkl}D_{kl}, \qquad \widehat{\delta}\widehat{\delta} = \widehat{\delta}_{ij}\widehat{\delta}_{kl}, \qquad N\widehat{\delta} = N_{ij}\widehat{\delta}_{kl}, \qquad \widehat{\delta}:D = \widehat{\delta}_{ij}D_{ij}]$$

$$f_e = \left(\frac{e_c}{e}\right)^\beta \qquad \text{3-14}$$

$$f_d = \left(\frac{e - e_d}{e_c - e_d}\right)^a$$

3-15

$$f_b = \frac{h_s}{n}\left(\frac{1 + e_i}{e_i}\right)\left(\frac{e_{i0}}{e_{c0}}\right)^{\beta}\left(\frac{-trT}{h_s}\right)^{1-n} \times \left[3 + a^2 - a\sqrt{3}\left(\frac{e_{i0} - e_{d0}}{e_{c0} - e_{d0}}\right)^a\right]^{-1}$$

3-16

$e_i$ is the void ratio during isotropic compression at the minimum density, $e_c$ is the critical void ratio, $e_d$ is the void ratio during isotropic compression at the maximum density. These functions take into account the influence of the density and mean pressure.

$$\frac{e_i}{e_{i0}} = \frac{e_c}{e_{c0}} = \frac{e_d}{e_{d0}} = exp\left[-\left(\frac{-trT}{h_s}\right)^n\right]$$

3-17

There are seven material constants in von Wolffersdorff's model. These constants are closely related to the geometric and mechanical properties of the grains. However, Niemunis's extension requires incorporate five additional constants. Three of them have a clear physical meaning, which are the size of the elastic range and two ratios of characteristic stiffness. Two exponents appear to be universal as exponents used in the physics of second-order phase transition. Using the above concepts, the numerical model was developed and further details regarding the hypoplasticity parameters set in this study are provided in section 3.2.

### 3.1.3. Eurocode approach

Eurocode 8 part 4 (EN 1991-4, 2006) outlines two different approaches for designing and assessing silos under earthquake actions: (i) Dynamic Analysis Approach, which consists of analyzing the silo response to seismic forces by means of NTHAs; (ii) Equivalent Static Analysis Approach, which assumes that the seismic forces acting on the silo walls can be represented by an equivalent static load profile named "additional normal pressure/overpressure". The first approach requires a detailed model of the silo and the granular material, including the near-full characterization of the material properties and the geometry of the silo. Although the dynamic analysis approach is the most accurate method for designing a silo, it is surely the most computationally intensive and time-consuming. These aspects push engineers of referring to static analysis technique given its simplicity and intuitiveness.

Following the static approach, the Eurocode suggest that the additional normal pressure on the wall can be defined as a system of horizontal radial pressure. In circular silos, the additional normal pressure on the wall can be calculated as

$$\Delta_{ph,s} = \Delta_{ph,so} \cdot \cos\theta \qquad \qquad \text{3-18}$$

$$\Delta_{ph,so} = \alpha(z) \cdot \gamma \cdot \min(r_s^*, 3x) \qquad \qquad \text{3-19}$$

Where $\Delta_{ph,s}$ is the static equivalent pressure applied on the silo walls, $\Delta_{ph,so}$ is the reference pressure, $\theta$ is the angle between direction of the horizontal component of the seismic action and the radial line to the point of interest on the wall, $\alpha(z)$ is the response acceleration of the silo at a depth z from the equivalent surface of the fill mass [g], $\gamma$ is the unit weight of the bulk. The parameter $r_s^*$ $r_s^* = \min(h_b, d_c/2)$ is defined as $r_s^* = \min(h_b, d_c/2)$, where $h_b$ is the overall height of the silo, from the silo base to the equivalent surface of the stored content, $d_c$ is the inside dimension of the silo parallel to the horizontal component of the seismic action (silo diameter in case of circular silos), and x is the vertical distance of the point of interest to the silo base.
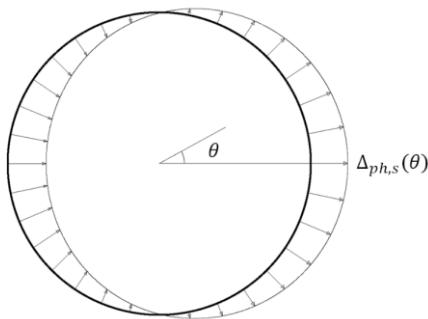


Figure 3-1 Equivalent static pressure distribution in the plan - cylindrical silos (Eurocode 8-4 (EN 1998-4, 2006))

According to the equations 3-18 and 3-19, the distribution of the additional normal pressure along the silo height is dictated by the function of the response acceleration $\alpha(z)$, while the horizontal distribution is only governed by the cosine function, as shown in Figure 3-1. Thus, the global distribution of the pressure on the walls is highly dependent on these two underlying assumptions. Usually, for simulating the response acceleration profiles, different options could be exploited, even though the Eurocode does not provide a precise indication. In the framework of this study, two different re-

sponse acceleration profiles are considered: (i) constant acceleration profile (named CA profile); (ii) variable acceleration profile, assuming linear variation over the heigh of the acceleration (named LA profile). Both load profiles were considered as likely shapes representing the additional normal pressure to account for designing or assessing silos.

## 3.2. FE numerical modelling and analysis

In order to assess the reliability of the standard overpressure profiles, detailed FE modelling of different geometries of silos was carried out. The choice of the sample of silos aimed to cover the most spread geometries in the practice: (i) the slender silo (S-silo), having height (h) = 18 m, diameter (D) = 6 m, and a constant wall thickness (t) = 6mm; (ii) the squat silo (Q-silo) having h = 6.5 m, D = 10 m, and t = 3 mm. The peculiarity of the proposed silos is that, despite they present different geometries, they have the same storage capacity (i.e., of 510 m3), assuming a near-full operative service condition (i.e., filling level) of 90% of the maximum capacity. The three-dimensional (3D) models were assembled in Abaqus software (Simulia, 2012), by combining three parts representing: (i) the silo shell wall; (ii) the bulk solids; and (iii) the reinforced concrete base. Four-node thin shell elements with reduced integration S4R were employed to model the silo shell wall and the base of the structure, while eight-node brick elements C3D8 were used to simulate the filling solid. It is worth noting that S4R elements are three dimensional shell elements employing both displacement and rotational degrees of freedom and consider a finite strain of the membrane (Simulia, 2012). These elements are effective in simulating the behavior of both thin and thick shells under dynamic or static conditions, where the in-plane deformation and the change of the shell thickness is accounted for. C3D8 elements are solid elements, used to model a continuum homogeneous-material body for linear and nonlinear analysis and accounting for aspects like contact, plasticity, and large deformations (Simulia, 2012).

Various considerations were adopted for the meshing strategy. Notably, the mesh resolution of the wall shell was increased in the bottom of the silo, near to the base,

110

where the variation of stress is of high rate. In addition, a stepwise graded mesh in the radial direction was adopted for the bulk solids. Thus, finer mesh was considered at the interface, in order to ensure more realistic simulation of the interaction between the silo wall and the filling material. For S-silo, the minimum size of the shell element was $125 \times 250$ mm2, and the maximum size was $125 \times 450$ mm2, while the minimum size of the brick solid element was $500 \times 260 \times 250$ mm3, and the maximum size was $500 \times 1000 \times 800$ mm3. The total number of finite elements was 5228, subdivided among 1596 for the silo wall, 3488 for the filling granular material, and 144 for the silo base. For Q-silo, the minimum size of the shell element was $250 \times 250$ mm2, and the maximum size was $250 \times 640$ mm2, while the minimum size of the brick solid elements was $200 \times 200 \times 250$ mm3, and the maximum size was $500 \times 475 \times 675$ mm3. In this case, the total number of finite elements was 10396, subdivided among 1264 for the silo wall, 8988 for the filling granular material, and 144 for the silo base.

In the 3D models, the roof structure was neglected since the primary interest of the study was to investigate the behavior of the shell wall and the pressure imposed on it under seismic conditions. In this regard, the effect of the roof on the structural behavior of the wall was simulated by considering a rigid body constraint, connecting the nodes of the upper edge of the silo wall to a master point. Thus, the out of roundness displacement was restricted (i.e., by simulating the effect of a ring beam at the top of the silo wall, as occurs in the practice).

It is noteworthy that imperfections type and amplitude implies a non-negligible impact on the silo shell wall behavior, especially under axial vertical compression forces as discussed in (Jansseune et al., 2016). On the other hand, given that the major focus of this work is the horizontal pressure imposed on the silo wall under lateral dynamic excitation, the effect of imperfection was reasonably eliminated. In addition, the horizontal pressure on the structure wall can make a favorable impact by reducing the imperfection amplitude according to (Buratti & Tavano, 2014).

Moving towards structural materials, the steel of the shell wall was assumed to be of an elasto-plastic with hardening behavior, with yield strength, $f_{s,y}$ = 275 MPa; ultimate strength, $f_{s,u}$ = 430 MPa; elastic modulus, $E_s$ = 210 GPa; Poisson's ratio, $v_s$ = 0.3; strain hardening modulus, $E_t$ = 3880 MPa; and density, $\rho$ = 7850 kg/m3. The Von Mises yield criterion was accounted for defining the material yielding. The silos are assumed to be filled with sand having a density of 15.0 kN/m3; a coefficient of friction of 0.4 for the steel wall and 0.7 for the RC base. In this regard, C3D8 elements were employed incorporating the hypoplastic constitutive law. Other specific hypoplasticity parameters and intergranular strain parameters that are implemented in the constitutive low of the filling material are reported Table 3-1. The relevant parameters are derived by experimental investigations and provided according to (Holler & Meskouris, 2006).

Table 3-1Hypoplasticity mechanical properties of the stored material

|  | Notation |  | Parameter value |
|---|---|---|---|
| Hypoplastic material parameters | $\phi_c$ | Critical friction angle | 37° |
|  | $h_s$ | The granular hardness determined form oedometer test | 11700 MPa |
|  | n | determined form oedometer test | 0.43 |
|  | $e_{do}$ | Conventional minimum void ratios | 0.532 |
|  | $e_{c0}$ | Conventional maximum void ratios | 0.69 |
|  | $e_{io}$ | Maximum possible void ratio | 0.8 |
|  | $\alpha$ | Angle to be calculated form the triaxial peak friction angle | 0.105 |
|  | $\beta$ | Angle to be calculated form the triaxial peak friction angle | 1.0 |
| Intergranular strain parameters | $\beta_r$ | Determined by the cyclic oedometer test to smooth the stiffness change following the load reversals | 1.0 |
|  | $\xi$ | Determined by the cyclic oedometer to smooth the stiffness change following the load reversals | 1.0 |
|  | $m_R$ | Used to describe the change of stiffness for each load reversal in 180 degrees | 1.5 |
|  | $m_T$ | Used to describe the change of stiffness for each load reversal in 90 degrees | 12.0 |
|  | R | Used to define the strain range of active intergranular strain | $5 \times 10^{-5}$ |

112

Taking into consideration the geometrical nonlinearity, an implicit time integration scheme available in ABAQUS/Standard was used to solve the equations of motion in case of NTHAs. On the other hand, incorporating the hypoplasticity model would strongly highly elevate the computational demand to achieve convergence in the numerical model. This is the cost of the assumptions at the base of this study, where the trade-off between accuracy and time analysis should bring substantial advantages, presenting a realistic insight into the additional normal pressure on the silo wall when subjected to a seismic excitation. Still, considering that many people can ask for always more detailed numerical models, the hypoplasticity with the inter-granular strain approach can definitely prove to be the most effective and accurate approach when simulating the behavior of granular materials under a cyclic loading. To conclude the modelling definition, Coulomb frictional model was employed for simulating the interaction between the bulk solids and silo steel wall, and between the bulk solids and the RC silo base. Coulomb fiction model is based on the concept of critical shear stress between the two surfaces in contact, where the slipping between the two surfaces develops when the shear stress intensity exceeds the critical shear stress. However, the critical shear stress is a function of the normal stresses on the contact surface and the friction coefficient between the two materials.

### 3.3. Numerical model validation

In order to validate the proposed modelling approach, two main checks were performed: (i) verification of the 3D model dynamic characteristics; (ii) verification of the effectiveness of the hypoplasticity constitutive model. To accomplish the first objective, the fundamental frequencies yielded by employing the proposed numerical approach were compared with those derived from other existing experimental and numerical studies, including a shaking table test on a scaled silo presented in (Silvestri et al., 2016) and numerical model of a full scall silo by (Mehretehran & Maleki, 2018).

The reduced-scale prototypical silo, manufactured in laboratory and subjected to dynamic excitations (Silvestri et al., 2016), was numerically modeled and reproduced

according to the proposed modelling approach elaborated in section 3.2. Modal analysis (eigenvalue analysis) was preformed, and the outputs were compared with the experimental outputs in terms of fundamental frequencies. The frequencies of the first two dominant vibration modes were 15.65 Hz and 43.79 Hz, while the corresponding frequencies from the numerical tests ranged from 12.7 to 14.1 Hz for the first mode and from 43.9 to 44.9 Hz for the second mode. Results showed a good agreement with the experimental work, as shown in Figure 3-2, which reports the vibration mode shapes corresponding to the aforementioned two frequencies (aligning with global cantilever flexural mode in the translational directions). It was noticed that the model exhibited duplicated mode shapes in two main directions, X and Y, however, attributed to the axial-symmetry of the structure.
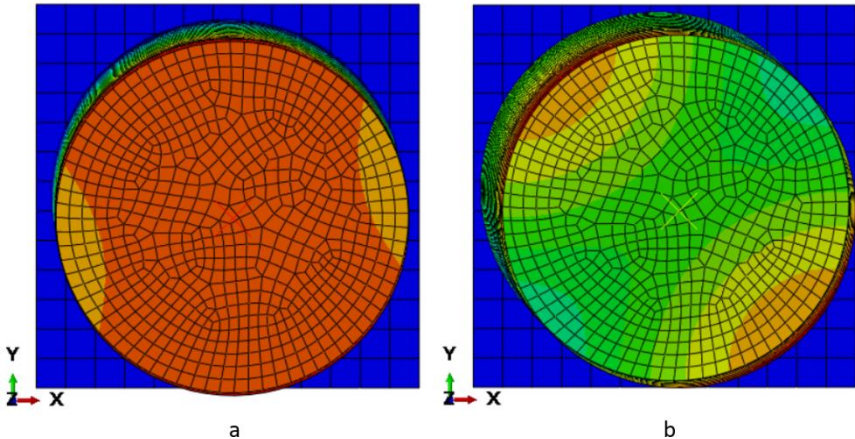


a                                          b

Figure 3-2The FEM solution of the prototypical silo after shaking table test (Silvestri et al., 2016), (a) 1st vibration mode shape, in Y direction, with 15.65 Hz; (b) 2nd vibration mode shape, in X direction, with 43.79 Hz

The dynamic characteristics yielded by the proposed modeling approach were further verified by producing the FE model of a full-scale silo (h = 25 m, D = 10 m, t = 6mm) investigated numerically in (Mehretehran & Maleki, 2018). Subsequently, modal analysis was performed where the frequency of the fundamental vibration mode was equal to 2.8 Hz and it was found identical to the corresponding one presented by the original study.

In pursuit of the second objective, a comparative assessment was performed on the values of static pressure, i.e., the normal horizontal pressure imposed by the bulk solids on the silo wall. In this regard, the FEM-based solution was compared to the analytical solution computed in accordance with Jansen theory (Janssen, 1895), and described in equations 3-20, 3-21, 3-22.

$$P_h(z) = P_{h0}\left(1 - e^{-z/z_0}\right)$$   3-20

$$P_{h0} = \gamma K z_0$$   3-21

$$z_0 = \frac{1}{K\mu_F}\frac{A}{U}$$   3-22

In the above expressions, z is the depth below the equivalent surface of the solid; $\gamma$ is the unit weight of the granular solid; K is the lateral pressure ratio; $\mu_F$ is the friction coefficient between the granular solid and the wall; A is the silo plan cross section area, U is the silo plan cross section perimeter. Then, the values of Pw are defined as a fraction of Ph, as:

$$P_w = \mu_F P_h$$   3-23

The comparison between numerical and analytical results is reported in Figure 3-3 presenting Ph against the normalized depth, $z_{norm}$, of the bulk solids for both slender and squat silos. The results showed that the numerically computed static pressure, (red lines) was consistent with the one provided by the theoretical solutions (blue lines). It is worth specifying that Jenssen's theory presented better alignment than the modified Reimbert's theory (Reimbert & Reimbert, 1976) with the FEM hypoplasticity-based solution even in case of squat silo, although Eurocode (EN 1998-4, 2006) recommend the modified Reimbert's theory for calculating the static granular-induced pressure in case of squat silos (0.4 < h/D < 2)
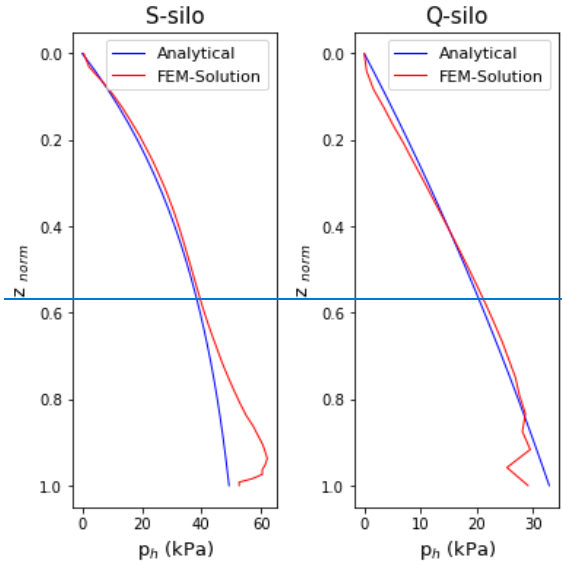
Figure 3-3 Comparison among numerical and analytical values of Ph for both slender and squat silos

### 3.4. Seismic analysis

Once validation was performed, for the two silos under consideration the eigenvalue analysis was performed, aimed at calculating dynamic characteristics of the structure. The first vibration period, $T_1$, for Q-silo was found equal to 0.12 sec, while $T_1$ for S-silo was equal to 0.32 sec. It can be observed that the variation in the geometry yields different dynamic properties, where S-silo exhibited longer $T_1$ than the Q-silo. Obviously, duplicated $T_1$ values were obtained in the two main orthogonal directions, due to the axial-symmetry of the structure.

To observe and quantify the overpressure applied on the silo wall under seismic conditions, NTHAs were conducted. To this purpose, a ground motion selection was preformed and, to reduce the effort of the analysis, given the axial-symmetry of the structures, the numerical models developed were modified, opting for running NTHAs on half of the systems and by applying adequate boundary conditions (i.e., displacements in the perpendicular direction to the symmetry plan and rotations in the main directions on the symmetry plan were restrained).

116

The considered seismic input consisted of 7 ground motion records, selected form the European-Strong-Motion-Database (Ambraseys et al. 2002). The number of records was established according to the provisions by Eurocode 8 (2004). Still, the selection was made with the respect to the Eurocode 8 (2004) provisions, considering that the limit differences between mean and target spectra amounted to $+30\%$ and $-10\%$. An elastic target spectrum with $a_g = 0.29$ g, soil amplification factor of 1.2 (Soil B) was used, resulting in the peak ground acceleration of 0.35 g. Figure 3-4 reports the elastic ground motion spectra for all individual records, their mean spectrum, and the target spectrum (T denotes the period, g is the gravity acceleration).
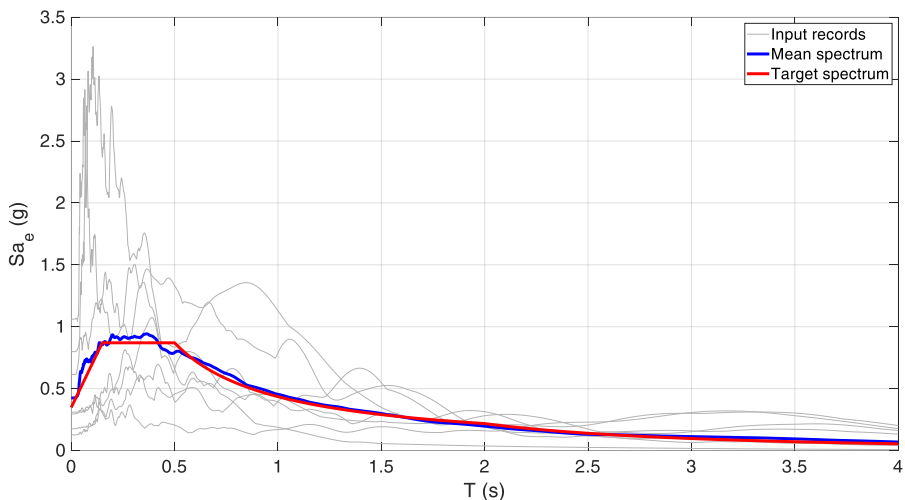


Figure 3-4 Elastic acceleration spectra (Sae) of the individual ground motion records, their mean elastic spectrum, and the target Eurocode 8 spectrum

Although the number or records could seem limited, it is worth specifying that the use of hypoplasticity requires high time. For the case at hand, using a machine equipped by a Core i9-13900HK CPU, 64 GBs of RAM, and an NVIDIA GeForce 3090 GPU with 24 GBs or VRAM, the convergence of 1 second of NTHAs was achieved in 24 hours. Hence, to run NTHAs with 7 records on 2 numerical models, a total of 5 months were spent, by exploiting the possibility of running analyses in parallel.

In running NTHAs, a damping ratio of 2% was considered for the models. Coherently with the modelling simplifications, accelerograms were applied in one direction, that

is, the one in the symmetry plan. Nevertheless, it is worth mentioning that the vertical component of the seismic action can be also critical for the silo safety (Butenweg et al., 2017), considering an additional acceleration on the silos mass, which yields additional dynamic pressures. This could be important especially for the slender or elevated silos (since it particularly relevant for the vertical pressure on the hopper).

Consequently, the dynamic pressure applied on the silo wall was recorded for each ground motion record and the dynamic overpressure was calculated. The obtained results are reported in Figure 3-6, 3-8, 3-9, 3-10 and deeply discussed in the next Section.

### 3.5. Dynamic overpressure and the equivalent static pressure

Under dynamic conditions, the overpressure exerted on the silo wall was systematically observed and compared to the corresponding equivalent static pressure scenarios, for both slender and squat silos. The observation involved in measuring pressure distribution and intensity, recorded upon silo failure. In line with the findings of chapter 2, silos under examination exhibited failure in accordance with the damage pattern of elephant foot buckling (EFB). EFB is an elasto-plastic buckling manifesting as an outward bulge near the silo base and extending around the circumference of the wall. However, this phenomenon is attributed to a combination of the axial compressive stresses exceeding the critical shell stress and the circumferential tensile stresses approaching yield limit (Rotter, 2006).

Seeking to articulate a thorough perspective on the overpressure variation and distribution, the dynamic pressure was observed and recorded along multiple paths of the silo shell wall, both horizontally and vertically. Giving the axial symmetry of the structure and the anticipated overpressure, the observed pressure paths pertained to a specific quarter of the silo wall body, displayed in red in Figure 3-5. To calculate the additional dynamic overpressure, the static lateral pressure was deduced from the total lateral pressure recorded upon failure.

Advanced seismic modeling and analysis of flat-bottom cylindrical steel silos interacting with stored granular-like materials.
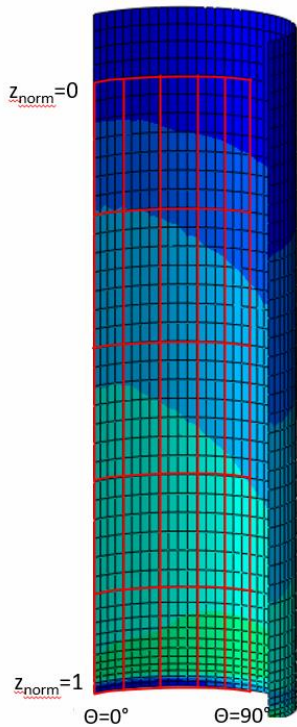


Figure 3-5 Horizontal and vertical paths along which the dynamic overpressure is observed (in red).

Subsequently, the overpressure profiles are illustrated in Figure 3-6 and Figure 3-8, reporting the pressure distribution of Q-silo across 6 vertical, and 6 horizontal paths, respectively. Each figure corresponds to the 7 ground motion records. Consequently, the overpressure mean is depicted alongside with the corresponding equivalent static pressure derived from CA and LA profiles.
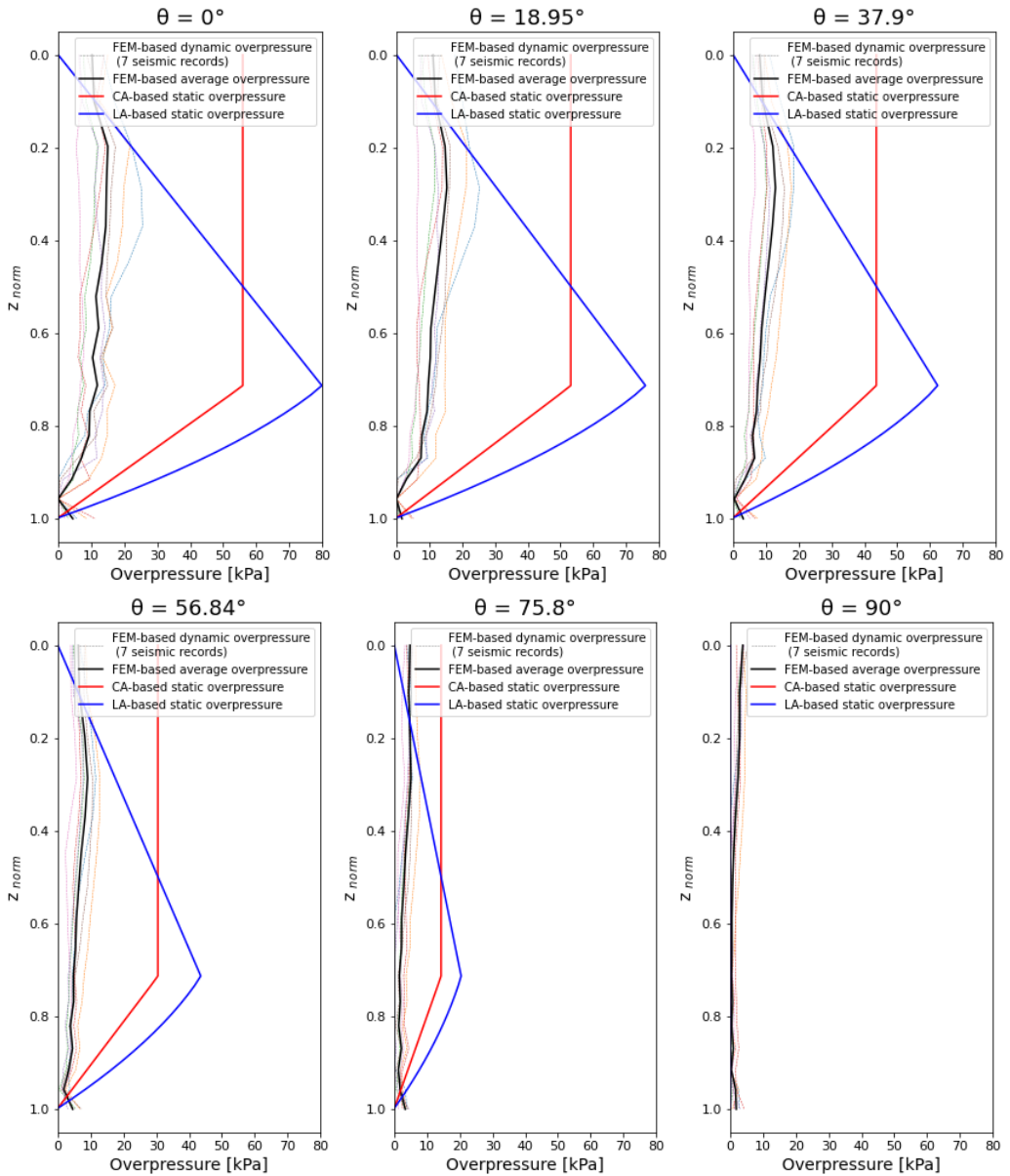
Figure 3-6 Overpressure vertical distribution of Q-silo depicting the FEM-based dynamic, and the equivalent static overpressure ( $0 \leq \theta \leq 90$ ).

120

As emphasized in Figure 3-6, the LA-based overpressure exhibits a high variation in the intensity between the top and the bottom, while the CA-based profile provides a more stable distribution of the overpressure along the height. By comparing the average FEM-based overpressure pattern with the one derived from the EC equivalent static approach, it can be to note that the CA-based overpressure pattern demonstrates higher compatibility than the LA-based overpressure with the FEM solution, in terms of pressure distribution. Nevertheless, both LA and CA-based solutions present a very high and conservative values, particularly when $\theta=0°$, with a safety factor ranging between 2 and 3. Conversely, the equivalent static approach presents unfavorable results especially when $\theta>75°$ with an overpressure intensity equal or lesser than the FEM solution prediction and diminishing to zero when $\theta=90°$.

As observed in Figure 3-8, the distribution of the FEM-based dynamic overpressure in the horizontal direction exhibits linear trajectory with a reduction in the overpressure intensity as $\theta$ increases ($z_{norm} < 0.8$), while it conforms to a uniform horizontal distribution at the bottom of silo ($z_{norm} > 0.8$), situation attributable to the compaction and settlement of the granular material due to the dynamic shaking. Figure 3-7 reports the evolution of compaction phenomenon of the granular solid material as a result of the dynamic excitation (a settlement of 157 mm was recorded at the top surface of the stored material after that the seismic excitation was applied). On the other hand, the static equivalent pressure follows a cosine function, suggesting a pronounced decline in the overpressure intensity as $\theta$ increases, and reaching zero value when $\theta=90°$. This stands in contrast to the non-zero FEM-based overpressure at the same point.

Still, as illustrated in Figure 3-8, and in comparison to the FEM-based solution, the fluctuation observed in the static overpressure yielded under the assumption of a LA profile, suggesting unfavorable results at the upper and lower extremities of the silo. At these points, static overpressure presents lesser intensity (static overpressure $= 0$ at $z_{norm} = 0$, $z_{norm} = 1$), or a near-perfect compatibility ($z_{norm} = 0.2$) with the dynamic FEM-based overpressure. However, this alignment ($z_{norm} = 0.2$) lacks practicality in the design process, as it is in contrast with the established safety considerations, especially where a safety factor is expected. Conversely, at the midsection of the silo

($z_{norm}$ = 0.4 - 0.8), LA static overpressure presents a high degree of conservatism. This discrepancy in the overpressure, in comparison to the FEM-based solution, entails unrealistic loading conditions, thus inappropriate shell wall behavior and design when considering the linear variation acceleration profile.
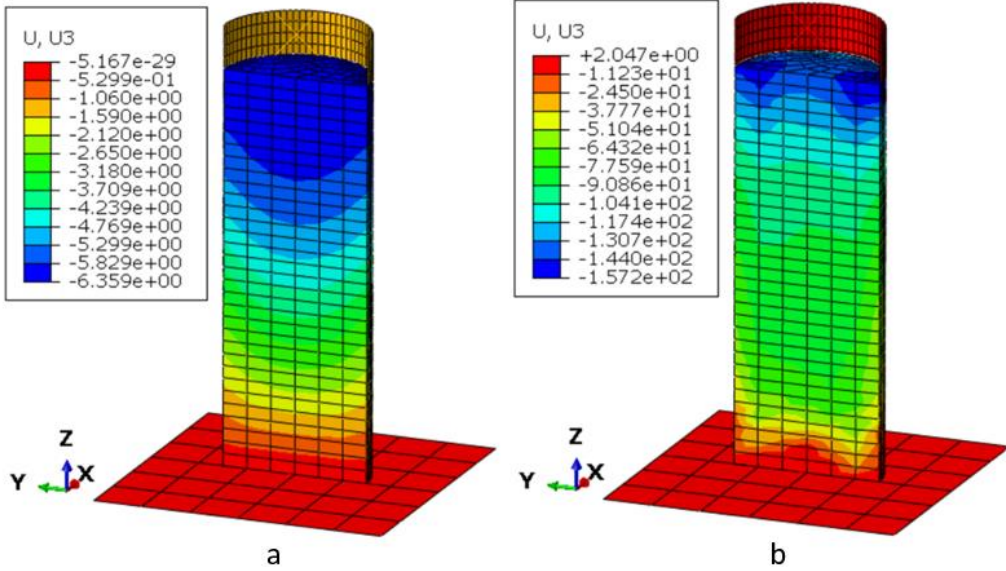


Figure 3-7 Evolution of the settlement in terms of vertical displacements of granular material (from left to right), (a) under static conditions; (b) under dynamic conditions. Values in the colored legend are expressed in mm.

On the other hand, the variation of static overpressure, yielded under the assumption of a CA profile, exhibits a certain level of conservatism along the silo height and inefficiency at the silo bottom ($z_{norm}$ = 1), as depicted in Figure 3-8. Otherwise, the CA-based static overpressure provides a relatively rational solution and more favorable results compared to the LA-based overpressure.

122

Advanced seismic modeling and analysis of flat-bottom cylindrical steel silos interacting with stored granular-like materials.
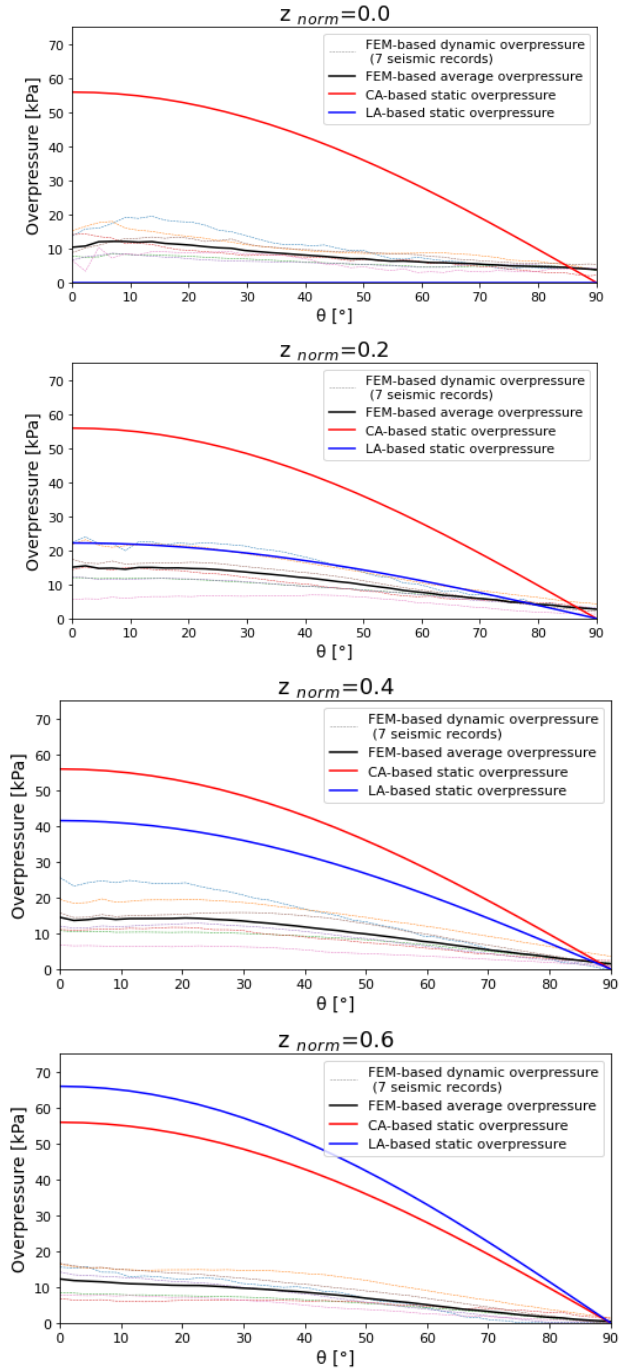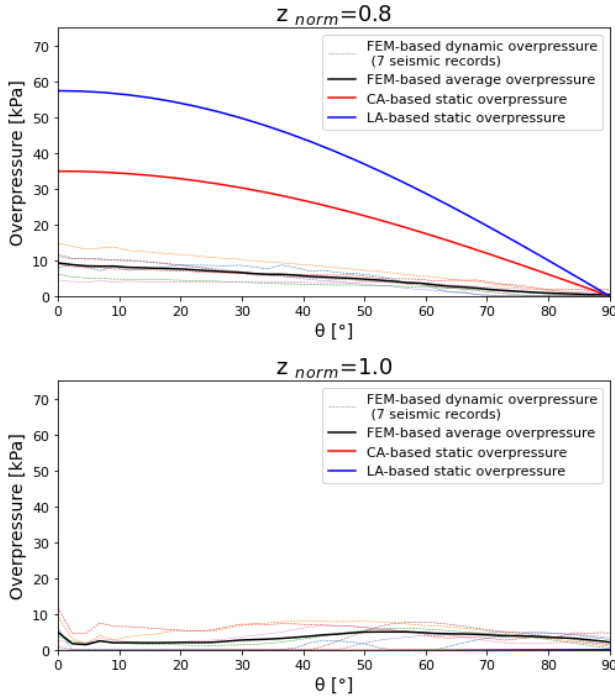
Figure 3-8 Overpressure horizontal distribution of Q-silo depicting the FEM-based dynamic, and the equivalent static overpressure ( $0 \leq z_{norm} \leq 1$ ).

Similarly, the overpressure profiles of S-silo are illustrated in Figure 3-9 and Figure 3-10, depicting the pressure distribution across 6 vertical, and 6 horizontal paths, respectively, and corresponding to the selected ground motion records.

Coherently with the findings concerning the vertical overpressure distribution of Q-silo (Figure 3-6), and as demonstrated in Figure 3-9, it can be noted that the CA overpressure pattern demonstrates higher compatibility with the FEM solution than the LA overpressure. The compatibility is noted in terms of pressure distribution, showcasing a pattern close to a uniform distribution. Also in this case, the equivalent static approach presents unfavorable results especially when θ>75° with an overpressure intensity equal or lesser than the FEM solution prediction and diminishing to zero when θ= 90°.

124

Advanced seismic modeling and analysis of flat-bottom cylindrical steel silos interacting with stored granular-like materials.
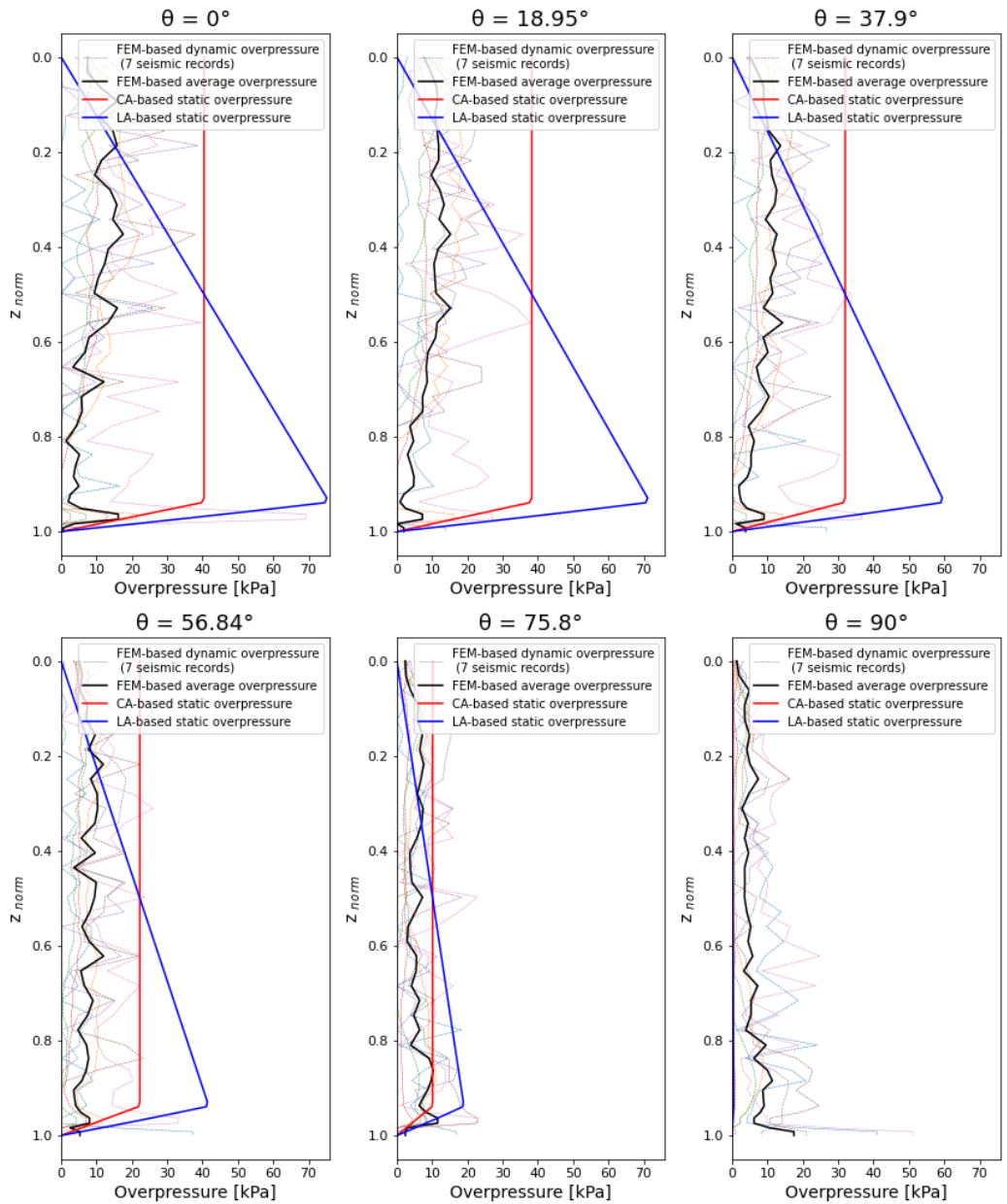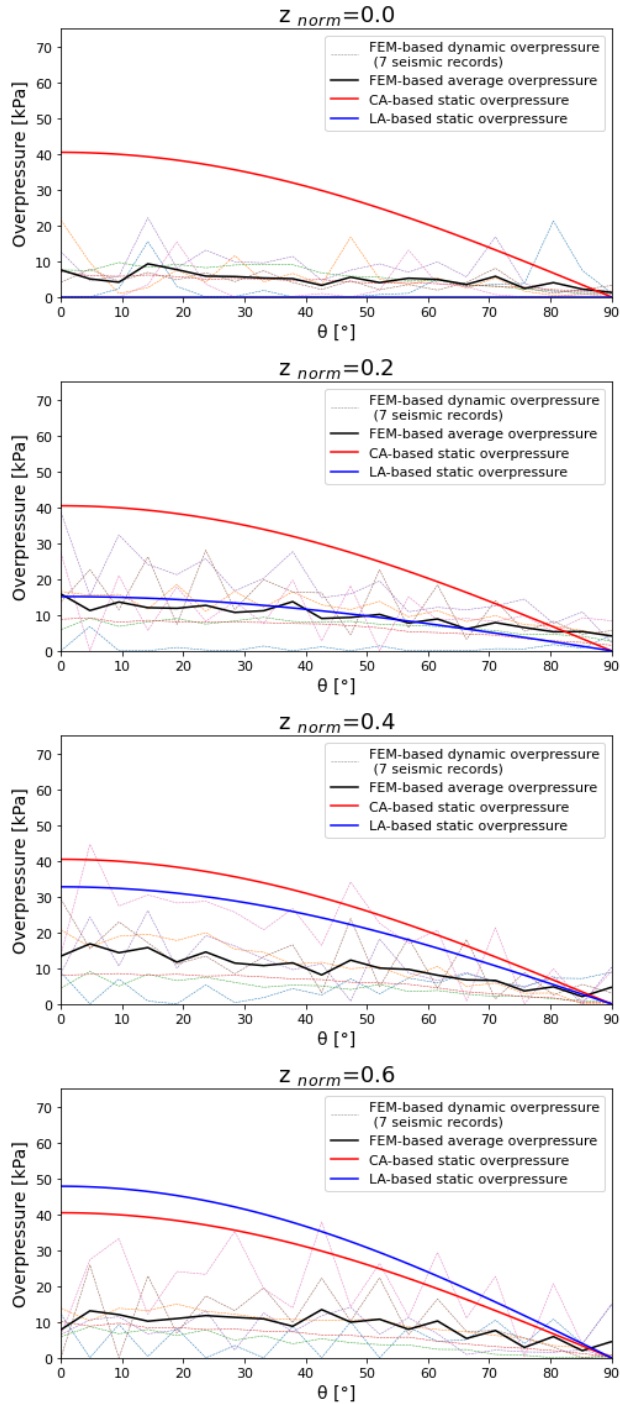


Figure 3-9 Overpressure vertical distribution of S-silo depicting the FEM-based dynamic, and the equivalent static overpressure ( $0 \leq \theta \leq 90$ ).

Regarding the overpressure horizontal distribution of S-silo, as observed in Figure 3-10, the distribution of the FEM-based dynamic overpressure in the horizontal direction follows a linear track with a marginal reduction in the overpressure intensity as $\theta$ increases, particularly at the middle and upper part of the silo ($z_{norm} < 0.6$), While a more uniform horizontal distribution at the lower parts of the silo wall ($z_{norm} > 0.6$) was observed, attributable to the compaction and settlement of the granular stored material, obtained by imposing a kind of symmetry in the pressure dynamic increment in the silo lower parts.

In addition, it is worth noting that the LA-based overpressure suggests unfavorable outcomes at the upper part and bottom of the silo. For instance, LA-based static overpressure presents lower intensity (at $z_{norm} = 0$, $z_{norm} = 1$), or a near-perfect unfavorable alignment ($z_{norm} = 0.2$) with the dynamic FEM-based overpressure. Conversely, at the middle and bottom of the silo ($z_{norm} = 0.4 - 0.8$), the LA static overpressure presents a high degree of conservatism. On the other hand, the CA static overpressure offers a relatively more favorable profile compared to the LA overpressure. In this regard, similar observations were reported for Q-silo emphasizing the consistency of these findings across different silo geometries.

Advanced seismic modeling and analysis of flat-bottom cylindrical steel silos interacting with stored granular-like materials.
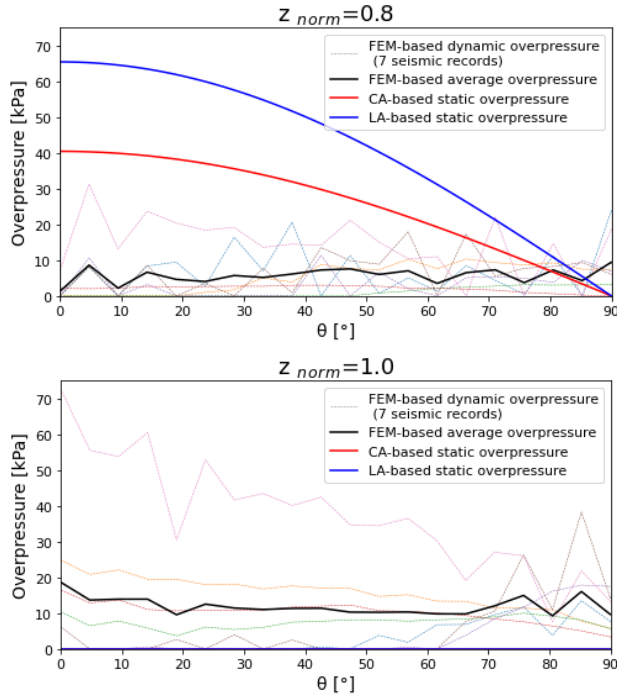
Figure 3-10 Overpressure horizontal distribution of S-silo depicting the FEM-based dynamic, and the equivalent static overpressure ($0 \leq z_{norm} \leq 1$).

## 3.6. Final remarks

This study provides an investigation on the earthquake-induced dynamic overpressure of flat-bottom steel silos interacting with the stored granular solids. Taking into account different silo geometries, an evaluation on the equivalent static approach, as prescribed by the European standards (EN 1991-4, 2006), was performed. A comparative analysis was presented between the Eurocode-like overpressure and the one generated based on the advanced numerical modelling. The modeling approach incorporates the hypoplasticity constitutive model for the filling material, in order to specifically simulate the cyclic behavior of the granules.

The numerical investigation revealed that the FEM-based overpressure pattern demonstrates a nearly uniform distribution in the vertical direction for both squat and slender silos. There is a noticeable reduction in the intensity of the overpressure at the

128

bottom of the silo, particularly in case of a squat silo. In addition, the distribution of the dynamic overpressure in the horizontal direction exhibits linear trajectory with a reduction in the overpressure intensity as θ increase, while it conforms to a uniform horizontal distribution at the silo bottom. In this context, a comparison be-tween the overpressure was derived from the different approaches, revealing that the equivalent static approach offers a better compatibility with the pressure pattern obtained by the dynamic FEM-based overpressure, especially when considering a constant accelera-tion profile along the silo height. Regarding the overpressure intensity, this static ap-proach leads to a significant margin of safety in terms of overpressure intensity, re-sulting in an economically inefficient design.

# CONCLUSIONS

This dissertation is centered on the seismic behavior of the ground-supported steel silos storing granular like material. The principal objectives of this work include outlining a numerical based procedure that allows to derive the seismic fragility curves of flat-bottom silos accounting for the interaction with the stored solids. In addition, this work aims to provide a comprehensive assessment of the dynamic over-pressure induced by the stored material on the silo walls under a seismic excitation.

An extensive review covering silos structural configuration and behavior, seismic response, bulk material properties, imposed loads according to standards, failure modes/causes, and assessment of existing silos is given in chapter 1.

Chapter 2 outlines the proposed procedure to derive seismic fragility of cylindrical ground- supported steel silos storing granular-like. The procedure aims to investigate the influence of three main aspects on the seismic behavior of these kinds of structures: (a) the geometry of the silos wall; (b) the service conditions, that is, the filling level of the stored material; (c) the type of failure mode. With this goal in mind, the procedure has been articulated in four consecutive steps: (i)selection of a set of smooth steel silos, which cover a large range of possibilities. Assuming different geometries (e.g., varying from slender to squat silos) and different filling level of stored materials (from filled to empty case), 20 cases were evaluated; (ii)detailed modelling of the considered silos was set and performed through the software ABAQUS. Three-dimensional numerical models were created for simulating the behaviour of steel shell walls, the physical properties of a granular like material and the interaction between the above components; (iii) preforming the analysis campaign, which was based on the combination of static and dynamic nonlinear analyses. The role of static analyses is double: (a) the as-assessment of the possible failure modes occurring on steel silos under seismic actions, i.e., Elephant Foot Buckling in the bottom part of the wall, Elastic (diamond or similar shape) Buckling in the middle part of the wall, Top Wall Damage in the upper part of the wall; (b) the definition of likely thresholds to define the achievement of all the considered buckling modes. Instead, nonlinear time history

analyses have been developed in order to define the probabilistic relationship between demand and capacity, assuming specific parameters for this purpose; (iiiv) deriving the fragility curves through a cloud analysis for all silos geometries, all filling levels and all possible failure modes. The obtained results highlight some novel aspects. Accounting for the influence of the silo geometry, the results have revealed that silos storing solids are more vulnerable to the elephant foot buckling, and this is emphasized when structures are filled with 90% and 60% of the maximum capacity. Looking at the median of fragility curves, going from squattest to slenderest silos, the probability of failure for same seismic intensity increases, which means that squattest silos show better performance than the slenderest ones under seismic actions (a difference of about 40% was recorded). With regard to the effect of the ensiled material, results indicated that Elephant Foot Buckling is the governing failure mode for filled silos (90% and 60%) while, in case of quasi-empty or empty (i.e., 30% and 0%), all three investigated failure modes present comparable probability of failure, despite high median values are obtained. Still, empty (or quasi-empty) silos exhibit very high seismic capacity, regardless of the failure mode, which means that in these service conditions there is a low probability of failure for silos, especial-ly under ordinary natural seismic events.

Chapter 3 provides an investigation on the earthquake-induced dynamic overpressure of flat-bottom steel silos interacting with the stored granular solids. Taking into account different silo geometries, an evaluation on the equivalent static approach, as prescribed by the European standards (EN 1991-4, 2006), was performed. A comparative analysis was presented between the Eurocode-like overpressure and the one generated based on the advanced numerical modelling. The modeling approach incorporates the hypoplasticity constitutive model for the filling material, in order to specifically simulate the cyclic behavior of the granules.

The numerical investigation revealed that the FEM-based overpressure pattern demonstrates a nearly uniform distribution in the vertical direction for both squat and slender silos. There is a noticeable reduction in the intensity of the overpressure at the bottom of the silo, particularly in case of a squat silo. In addition, the distribution of

the dynamic overpressure in the horizontal direction exhibits linear trajectory with a reduction in the overpressure intensity as θ increase, while it conforms to a uniform horizontal distribution at the silo bottom. In this context, a comparison between the overpressure was derived from the different approaches, revealing that the equivalent static approach offers a better compatibility with the pressure pattern obtained by the dynamic FEM-based overpressure, especially when considering a constant acceleration profile along the silo height. Regarding the overpressure intensity, this static approach leads to a significant margin of safety in terms of overpressure intensity, resulting in an economically inefficient design.

In this research direction, further developments of the work will be aimed to extend the investigation to different kinds of silos (e.g., stiffened, corrugated), and to consider different types of stored materials. In addition, a refinement of the numerical models could be performed, by considering different physical factors for the granular solid material. From the fragility curves derivation point of view, different approaches from the simple one herein used should be employed, by opting for using more records and by involving other analysis techniques (e.g., IDA).

# BIBLIOGRAPHY

ACI 313-16:2016. (2016). *Design Specification for Concrete Silos and Stacking Tubes for Storing Granular Materials and Commentary*. American Concrete Institute.

AIRY, W. (1898). THE PRESSURE OF GRAIN. (INCLUDING APPENDIXES). *Minutes of the Proceedings of the Institution of Civil Engineers*, *131*(1898), 347–358. https://doi.org/10.1680/imotp.1898.19213

Alessandri, S., Caputo, A. C., Corritore, D., Giannini, R., Paolacci, F., & Phan, H. N. (2018). Probabilistic risk analysis of process plants under seismic loading based on Monte Carlo simulations. *Journal of Loss Prevention in the Process Industries*, *53*, 136–148. https://doi.org/10.1016/j.jlp.2017.12.013

Ambraseys, N., Smit, P., Douglas, J., Margaris, B., Sigbjornsson, R., Olafsson, S., Suhadolc, P., & Costa, G. (2004). Internet-Site for European Strong-Motion Data; *BOLLETTINO DI GEOFISICA TEORICA ED APPLICATA*, *45*(3), 113–129.

Arbelo, M. A., de Almeida, S. F. M., Donadon, M. V., Rett, S. R., Degenhardt, R., Castro, S. G. P., Kalnins, K., & Ozoliņš, O. (2014). Vibration correlation technique for the estimation of real boundary conditions and buckling load of unstiffened plates and cylindrical shells. *Thin-Walled Structures*, *79*, 119–128. https://doi.org/10.1016/j.tws.2014.02.006

Arbelo, M. A., Degenhardt, R., Castro, S. G. P., & Zimmermann, R. (2014). Numerical characterization of imperfection sensitive composite structures. *Composite Structures*, *108*, 295–303. https://doi.org/10.1016/j.compstruct.2013.09.041

Askif, F., Hammadeh, H., Ubysz, A., & Maj, M. (2020). Numerical Modeling of Wall Pressure in Silo with and Without Insert. *Studia Geotechnica et Mechanica*, *43*(1), 22–33. https://doi.org/10.2478/sgem-2020-0009

Ayuga, F., Guaita, M., & Aguado, P. (2001). SE—Structures and Environment: Static and Dynamic Silo Loads using Finite Element Models. *Journal of Agricultural Engineering Research*, *78*(3), 299–308. https://doi.org/10.1006/JAER.2000.0640

Bakalis, K., Kazantzi, A. K., Vamvatsikos, D., & Fragiadakis, M. (2019). Seismic Performance Evaluation of Liquid Storage Tanks Using Nonlinear Static Procedures. *Journal of Pressure Vessel Technology*, *141*(1). https://doi.org/10.1115/1.4039634

Bakalis, K., & Vamvatsikos, D. (2018). Seismic Fragility Functions via Nonlinear Response History Analysis. *Journal of Structural Engineering*, *144*(10), 04018181. https://doi.org/10.1061/(ASCE)ST.1943-541X.0002141

Basone, F., Wenzel, M., Bursi, O. S., & Fossetti, M. (2019). Finite locally resonant Metafoundations for the seismic protection of fuel storage tanks. *Earthquake Engineering & Structural Dynamics*, *48*(2), 232–252. https://doi.org/10.1002/eqe.3134

Batikha, M., Chen, J.-F., & Rotter, J. M. (2018). Fibre reinforced polymer for strengthening cylindrical metal shells against elephant's foot buckling: An elasto-plastic analysis. *Advances in Structural Engineering*, *21*(16), 2483–2498. https://doi.org/10.1177/1369433218817139

Bauer, E. (1992). *Zum Mechanischen Verhalten Granularer Stoffe unter Vorwiegend ödometrischer Beanspruchungen*. Universität Fridericiana zu Karlsruhe.

Bazzurro, P., Cornell, C. A., Shome, N., & Carballo, J. E. (1998). Three Proposals for Characterizing MDOF Nonlinear Seismic Response. *Journal of Structural Engineering*, *124*(11), 1281–1289. https://doi.org/10.1061/(ASCE)0733-9445(1998)124:11(1281)

Bisagni, C. (2000). Numerical analysis and experimental correlation of composite shell buckling and post-buckling. *Composites Part B: Engineering*, *31*(8), 655–667. https://doi.org/10.1016/S1359-8368(00)00031-7

Błażejewski, P., & Marcinowski, J. (2013). Buckling resistance of vertical stiffeners of steel silos for grain storage. *Budownictwo i Architektura*, *12*(2), 189–196. https://doi.org/10.35784/bud-arch.2129

Braun, A. (1997). *Schüttgutbeanspruchungen von Silozellen unter Erdbebeneinwirkungen. Institut für Massivbau und Baustofftechnologie.* Karlsruhe Institute of Technology.

Brunesi, E., Nascimbene, R., Pagani, M., & Beilic, D. (2015). Seismic Performance of Storage Steel Tanks during the May 2012 Emilia, Italy, Earthquakes. *Journal of Performance of Constructed Facilities*, *29*(5). https://doi.org/10.1061/(ASCE)CF.1943-5509.0000628

Buratti, N., & Tavano, M. (2014). Dynamic buckling and seismic fragility of anchored steel tanks by the added mass method. *Earthquake Engineering & Structural Dynamics*, *43*(1), 1–21. https://doi.org/10.1002/EQE.2326

Butenweg, C., Rosin, J., & Holler, S. (2017). Analysis of Cylindrical Granular Material Silos under Seismic Excitation. *Buildings*, *7*(4), 61. https://doi.org/10.3390/buildings7030061

Carson, J. ., & Jenkyn, R. (1993). Load development and structural considerations in silo design. *Reliable Flow OfParticulate Solids II*.

Carson, J., & Craig, D. (2015). Silo Design Codes: Their Limits and Inconsistencies. *Procedia Engineering*, *102*, 647–656. https://doi.org/10.1016/j.proeng.2015.01.157

Carson, J. W., & Holmes, T. (2003). Silo failures: Why do they happen? *TASK QUARTERLY*, *7*(4), 499–512. http://www.bop.com.pl

Castro, S. G. P., Zimmermann, R., Arbelo, M. A., Khakimova, R., Hilburger, M. W., & Degenhardt, R. (2014). Geometric imperfections and lower-bound methods used to calculate knock-down factors for axially compressed composite cylindrical shells. *Thin-Walled Structures*, *74*, 118–132. https://doi.org/10.1016/j.tws.2013.08.011

Chailleux, A., Hans, Y., & Verchery, G. (1975). Experimental study of the buckling of laminated composite columns and plates. *International Journal of Mechanical Sciences*, *17*(8), 489-IN2. https://doi.org/10.1016/0020-7403(75)90013-2

Chen, Z., Wassgren, C., Veikle, E., & Ambrose, K. (2020). Determination of material and interaction properties of maize and wheat kernels for DEM simulation. *Biosystems Engineering*, *195*, 208–226. https://doi.org/10.1016/j.biosystemseng.2020.05.007

Cornell, C. A., Jalayer, F., Hamburger, R. O., & Foutch, D. A. (2002). Probabilistic Basis for 2000 SAC Federal Emergency Management Agency Steel Moment Frame Guidelines. *Journal of Structural Engineering*, *128*(4), 526–533. https://doi.org/10.1061/(ASCE)0733-9445(2002)128:4(526)

Demir, A. D., & Livaoglu, R. (2023). Simplified seismic response model for a bulk solid- silo-embedded foundation/soil system. *Soil Dynamics and Earthquake Engineering*, *165*, 107664. https://doi.org/10.1016/j.soildyn.2022.107664

DIN 1055-6-2005. (2014). *Actions on Structures – Part 6: Design Loads for Buildings and Loads in Silo Bins:* .

Ding, X., Coleman, R., & Rotter, J. M. (1996a). Surface Profiling System for Measurement of Engineering Structures. *Journal of Surveying Engineering*, *122*(1), 3–13. https://doi.org/10.1061/(ASCE)0733-9453(1996)122:1(3)

Ding, X., Coleman, R., & Rotter, J. M. (1996b). Technique for Precise Measurement of Large-Scale Silos and Tanks. *Journal of Surveying Engineering*, *122*(1), 14–25. https://doi.org/10.1061/(ASCE)0733-9453(1996)122:1(14)

Doerich, C., & Rotter, J. M. (2008). Behavior of Cylindrical Steel Shells Supported on Local Brackets. *Journal of Structural Engineering*, *134*(8), 1269–1277. https://doi.org/10.1061/(ASCE)0733-9445(2008)134:8(1269)

Dogangun, A., Karaca, Z., Durmus, A., & Sezen, H. (2009). Cause of Damage and Failures in Silo Structures. *Journal of Performance of Constructed Facilities*, *23*(2), 65–71. https://doi.org/10.1061/(ASCE)0887-3828(2009)23:2(65)

Durmuş, A., & Livaoglu, R. (2015). A simplified 3 D.O.F. model of A FEM model for seismic analysis of a silo containing elastic material accounting for soil–structure interaction. *Soil Dynamics and Earthquake Engineering*, *77*, 1–14. https://doi.org/10.1016/j.soildyn.2015.04.015

Eckhoff, R. K. (2009). Dust Explosion Prevention and Mitigation, Status and Developments in Basic Knowledge and in Practical Application. *International Journal of Chemical Engineering*, *2009*, 1–12. https://doi.org/10.1155/2009/569825

Eckhoff, R. K., & Skjold, T. (2016). Dust Explosions in the Process Industries: Research in the Twenty-first Century. *CHEMICAL ENGINEERING TRANSACTIONS*, *48*, 337–342.

Elishakoff, I., Manen, S. van, Vermeulen, P. G., & Arbocz, J. (1987). First-order second-moment analysis of the buckling of shells with random imperfections.

Advanced seismic modeling and analysis of flat-bottom cylindrical steel silos interacting with stored granular-like materials.

*AIAA Journal*, *25*(8), 1113–1117. https://doi.org/10.2514/3.9751

EN 1991-4. (2006). *Eurocode 1: Actions on Structures – Part 4: Silos and Tanks, CEN, Brussels.*

EN 1993-1-6. (2007). *Eurocode 3 - Design of steel structures - Part 1-6: Strength and Stability of Shell Structures. European Committee for Standardization*.

EN 1998-2. (2005). *Eurocode 8: Design of Structures for Earthquake Resistance – Part 2: Bridges, CEN, Brussels.*

EN 1998-4. (2006). *Eurocode 8: Design of Structures for Earthquake Resistance – Part 4: Silos, Tanks and Pipelines, CEN, Brussels, 2006.*

EN 1999-1-5. (2009). *Design of aluminium structures. Shell structures. 2007 + AC*.

EN 50281-3. (2002). *Equipment for Use in the Presence ofCombustible Dust-Part 3: Classification ofAreas where Combustible Dusts Are or May be Present; European Committee for Electrotechnical Standardization*.

EN61241-17. (2005). *Electrical Apparatus for Use in the Presence ofCombustible Dust-Part 17: Inspection and Maintenance ofElectrical Installations in Hazardous Areas (Other Than Mines); European Committee for Electrotechnical Standardization*.

Fajuyitan, O. K., & Sadowski, A. J. (2018). Imperfection sensitivity in cylindrical shells under uniform bending. *Advances in Structural Engineering*, *21*(16), 2433–2453. https://doi.org/10.1177/1369433218804928

Franzoni, F., Degenhardt, R., Albus, J., & Arbelo, M. A. (2019). Vibration correlation technique for predicting the buckling load of imperfection-sensitive isotropic cylindrical shells: An analytical and numerical verification. *Thin-Walled Structures*, *140*, 236–247. https://doi.org/10.1016/j.tws.2019.03.041

Furinghetti, M., Mansour, S., Marra, M., Silvestri, S., Lanese, I., Weber, F., & Pavese, A. (2024). Shaking table tests of a full-scale base-isolated flat-bottom steel silo equipped with curved surface slider bearings. *Soil Dynamics and Earthquake Engineering*, *176*, 108321. https://doi.org/10.1016/j.soildyn.2023.108321

Gabbianelli, G., Perrone, D., Nascimbene, R., & Paolacci, F. (2022, July 17). Seismic Vulnerability Assessment and Fragility Functions Derivation for Steel Storage Legged Tanks. *Volume 5: Operations, Applications, and Components; Seismic Engineering; ASME Nondestructive Evaluation, Diagnosis and Prognosis (NDPD) Division*. https://doi.org/10.1115/PVP2022-84416

Galletly, G. D., Slankard, R. C., & Wenk, E. (1958). General Instability of Ring-Stiffened Cylindrical Shells Subject to External Hydrostatic Pressure—A Comparison of Theory and Experiment. *Journal of Applied Mechanics*, *25*(2), 259–266. https://doi.org/10.1115/1.4011754

Gian Michele Calvi, & Roberto Nascimbene. (2023). *Seismic Design and Analysis of Tanks* (John Wiley & Sons (ed.)).

Gillie, M., & Holst, J. M. F. . (2003). Structural behaviour of silos supported on

discrete, eccentric brackets. *Journal of Constructional Steel Research*, *59*(7), 887–910. https://doi.org/10.1016/S0143-974X(02)00078-0

Gudehus, G. (1996). A Comprehensive Constitutive Equation for Granular Materials. *Soils and Foundations*, *36*(1), 1–12. https://doi.org/10.3208/sandf.36.1

Guo, K., Zhou, C., Meng, L., & Zhang, X. (2016). Seismic vulnerability assessment of reinforced concrete silo considering granular material-structure interaction. *The Structural Design of Tall and Special Buildings*, *25*(18), 1011–1030. https://doi.org/10.1002/tal.1295

H. V. Kebeli, R. A. Bucklin, D. S. Ellifritt, & K. V. Chau. (2000). MOISTURE-INDUCED PRESSURES AND LOADS IN GRAIN BINS. *Transactions of the ASAE*, *43*(5), 1211–1221. https://doi.org/10.13031/2013.3014

Hardin, B. O., Bucklin, R. A., & Ross, I. J. (1996). Shear-beam Analysis for Seismic Response of Metal Wheat Bins. *Transactions of the ASAE*, *39*(2), 677–687. https://doi.org/10.13031/2013.27552

Härtl, J., Ooi, J. Y., Rotter, J. M., Wojcik, M., Ding, S., & Enstad, G. G. (2008). The influence of a cone-in-cone insert on flow pattern and wall pressure in a full-scale silo. *Chemical Engineering Research and Design*, *86*(4), 370–378. https://doi.org/10.1016/j.cherd.2007.07.001

Holler, S., & Meskouris, K. (2006). Granular Material Silos under Dynamic Excitation: Numerical Simulation and Experimental Validation. *Journal of Structural Engineering*, *132*(10), 1573–1579. https://doi.org/10.1061/(ASCE)0733-9445(2006)132:10(1573)

Horabik, J., & Molenda, M. (2002). Properties of Grain for Silo Strength Calculation. In *Physical Methods in Agriculture* (pp. 195–217). Springer US. https://doi.org/10.1007/978-1-4615-0085-8_12

Horabik, J., Molenda, M., & Ross, I. (2002). Application of the anisotropy of mechanical properties of bedding of grain for reduction of silo load asymmetry resulting from off-center discharge. *Acta Agrophysica*, 49–60.

Horabik, J., Wiącek, J., Parafiniuk, P., Bańda, M., Kobyłka, R., Stasiak, M., & Molenda, M. (2020). Calibration of discrete-element-method model parameters of bulk wheat for storage. *Biosystems Engineering*, *200*, 298–314. https://doi.org/10.1016/j.biosystemseng.2020.10.010

Hu, G., Satake, K., Li, L., & Du, P. (2023). Origins of the Tsunami Following the 2023 Turkey–Syria Earthquake. *Geophysical Research Letters*, *50*(18). https://doi.org/10.1029/2023GL103997

Hühne, C., Rolfes, R., Breitbach, E., & Teßmer, J. (2008). Robust design of composite cylindrical shells under axial compression — Simulation and validation. *Thin-Walled Structures*, *46*(7–9), 947–962. https://doi.org/10.1016/j.tws.2008.01.043

Ismail, M. S., Purbolaksono, J., Andriyana, A., Tan, C. J., Muhammad, N., & Liew, H. L. (2015). The use of initial imperfection approach in design process and

138

buckling failure evaluation of axially compressed composite cylindrical shells. *Engineering Failure Analysis*, *51*, 20–28. https://doi.org/10.1016/j.engfailanal.2015.02.017

Iwicki, P., Rejowski, K., & Tejchman, J. (2015). Stability of cylindrical steel silos composed of corrugated sheets and columns based on FE analyses versus Eurocode 3 approach. *Engineering Failure Analysis*, *57*, 444–469. https://doi.org/10.1016/j.engfailanal.2015.08.017

Iwicki, P., Rejowski, K., & Tejchman, J. (2019). Determination of buckling strength of silos composed of corrugated walls and thin-walled columns using simplified wall segment models. *Thin-Walled Structures*, *135*, 414–436. https://doi.org/10.1016/j.tws.2018.11.018

Iwicki, P., Sondej, M., & Tejchman, J. (2016). Application of linear buckling sensitivity analysis to economic design of cylindrical steel silos composed of corrugated sheets and columns. *Engineering Failure Analysis*, *70*, 105–121. https://doi.org/10.1016/j.engfailanal.2016.07.013

Iwicki, P., Tejchman, J., & Chróścielewski, J. (2014). Dynamic FE simulations of buckling process in thin-walled cylindrical metal silos. *Thin-Walled Structures*, *84*, 344–359. https://doi.org/10.1016/J.TWS.2014.07.011

Jäger-Cañás, A., & Pasternak, H. (2017). 04.13: Influence of closely spaced ring-stiffeners on the axial buckling behavior of cylindrical shells. *Ce/Papers*, *1*(2–3), 928–937. https://doi.org/10.1002/cepa.133

Jalayer, F. (2003). *Direct Probabilistic Seismic Analysis: Implementing Non-Linear Dynamic Assessments*. Stanford University.

Jalayer, F., & Cornell, C. A. (2009). Alternative non-linear demand estimation methods for probability-based seismic assessments. *Earthquake Engineering & Structural Dynamics*, *38*(8), 951–972. https://doi.org/10.1002/EQE.876

Janssen, H. A. (1895). Versuche uber getreidedruck in silozellen. *Zeit. D. Ver. Dtsch. Ing.*, 1045–1049.

Jansseune, A., De Corte, W., & Belis, J. (2015). Elastic failure of locally supported silos with U-shaped longitudinal stiffeners. *KSCE Journal of Civil Engineering*, *19*(4), 1041–1049. https://doi.org/10.1007/s12205-015-0001-4

Jansseune, A., De Corte, W., & Belis, J. (2016). Imperfection sensitivity of locally supported cylindrical silos subjected to uniform axial compression. *International Journal of Solids and Structures*, *96*, 92–109. https://doi.org/10.1016/j.ijsolstr.2016.06.019

Jansseune, A., De Corte, W., & Van Impe, R. (2013). Column-supported silos: Elasto-plastic failure. *Thin-Walled Structures*, *73*, 158–173. https://doi.org/10.1016/j.tws.2013.08.005

Jiao, P., Chen, Z., Tang, X., Su, W., & Wu, J. (2018). Design of axially loaded isotropic cylindrical shells using multiple perturbation load approach – Simulation and validation. *Thin-Walled Structures*, *133*, 1–16.

https://doi.org/10.1016/j.tws.2018.09.028

Jing, H., Chen, H., Yang, J., & Li, P. (2022). Shaking table tests on a small-scale steel cylindrical silo model in different filling conditions. *Structures*, *37*, 698–708. https://doi.org/10.1016/j.istruc.2022.01.026

Jing, H., Wang, X., Yang, J., & Chen, H. (2022). Static and seismic pressure of cylindrical steel silo model with granular materials. *Journal of Constructional Steel Research*, *198*, 107515. https://doi.org/10.1016/j.jcsr.2022.107515

Kalnins, K., Arbelo, M. A., Ozolins, O., Skukis, E., Castro, S. G. P., & Degenhardt, R. (2015). Experimental Nondestructive Test for Estimation of Buckling Load on Unstiffened Cylindrical Shells Using Vibration Correlation Technique. *Shock and Vibration*, *2015*, 1–8. https://doi.org/10.1155/2015/729684

Kanyilmaz, A., & Castiglioni, C. A. (2017). Reducing the seismic vulnerability of existing elevated silos by means of base isolation devices. *Engineering Structures*, *143*, 477–497. https://doi.org/10.1016/j.engstruct.2017.04.032

Kenneth, S. . (2003). Progressive failure and imminent collapse of a steel storage silo. *Forensic Eng*, *29*, 508–517.

Khakimova, R., Castro, S. G. P., Wilckens, D., Rohwer, K., & Degenhardt, R. (2017). Buckling of axially compressed CFRP cylinders with and without additional lateral load: Experimental and numerical investigation. *Thin-Walled Structures*, *119*, 178–189. https://doi.org/10.1016/j.tws.2017.06.002

Khalili, F., & Showkati, H. (2012). T-ring stiffened cone cylinder intersection under internal pressure. *Thin-Walled Structures*, *54*, 54–64. https://doi.org/10.1016/j.tws.2012.01.015

Khouri, M. (2005). Comparison of various methods used in the analysis of silos without wall friction. *WIT Transactions on Modelling and Simulation, Vol 41,*.

Kildashti, K., Mirzadeh, N., & Samali, B. (2018). Seismic vulnerability assessment of a case study anchored liquid storage tank by considering fixed and flexible base restraints. *Thin-Walled Structures*, *123*, 382–394. https://doi.org/10.1016/j.tws.2017.11.041

Knoedel, P., Gkatzogiannis, S., Holtschoppen, B., & Ummenhofer, T. (2022). Seismic Design of Elevated Silos and Tanks – a Study on Behaviour Factors. *Ce/Papers*, *5*(4), 738–747. https://doi.org/10.1002/cepa.1814

Knoedel, P., & Ummenhofer, T. (2016). Practical Design of Aluminium Silos According to EC9-1-5. *Key Engineering Materials*, *710*, 97–102. https://doi.org/10.4028/www.scientific.net/KEM.710.97

Knoedel, P., Ummenhofer, T., & Rotter, J. M. (2017). 04.16: Rethinking imperfections in tanks and silos. *Ce/Papers*, *1*(2–3), 960–969. https://doi.org/10.1002/cepa.136

Knoedel, P., Ummenhofer, T., & Schulz, U. (1995). On the Modelling of Different Types of Imperfections in Silo Shells. *Thin-Walled Structures*, *23*, 283–293.

Kobyłka, R., Molenda, M., & Horabik, J. (2019). Loads on grain silo insert discs, cones, and cylinders: Experiment and DEM analysis. *Powder Technology*, *343*, 521–532. https://doi.org/10.1016/j.powtec.2018.11.032

Kobyłka, R., Molenda, M., & Horabik, J. (2020). DEM simulation of the pressure distribution and flow pattern in a model grain silo with an annular segment attached to the wall. *Biosystems Engineering*, *193*, 75–89. https://doi.org/10.1016/j.biosystemseng.2020.02.013

Kohrangi, M., Bazzurro, P., Vamvatsikos, D., & Spillatura, A. (2017). Conditional spectrum-based ground motion record selection using average spectral acceleration. *Earthquake Engineering & Structural Dynamics*, *46*(10), 1667–1685. https://doi.org/10.1002/eqe.2876

Krausmann, E., Girgin, S., & Necci, A. (2019). Natural hazard impacts on industry and critical infrastructure: Natech risk drivers and risk management performance indicators. *International Journal of Disaster Risk Reduction*, *40*, 101163. https://doi.org/10.1016/j.ijdrr.2019.101163

KRIEGESMANN, B., ROLFES, R., HÜHNE, C., TEßMER, J., & ARBOCZ, J. (2010). PROBABILISTIC DESIGN OF AXIALLY COMPRESSED COMPOSITE CYLINDERS WITH GEOMETRIC AND LOADING IMPERFECTIONS. *International Journal of Structural Stability and Dynamics*, *10*(04), 623–644. https://doi.org/10.1142/S0219455410003658

Kuczyńska, N., Wójcik, M., & Tejchman, J. (2015). Effect of bulk solid on strength of cylindrical corrugated silos during filling. *Journal of Constructional Steel Research*, *115*, 1–17. https://doi.org/10.1016/J.JCSR.2015.08.002

Lee, S. J. (1981). *Experimental study of cylindrical silos subject to seismic excitation*. The Ohio State University.

Li, Z., Pasternak, H., & Jäger-Cañás, A. (2021). Buckling of ring-stiffened cylindrical shell under axial compression: Experiment and numerical simulation. *Thin-Walled Structures*, *164*, 107888. https://doi.org/10.1016/j.tws.2021.107888

Liu, C., & Fang, D. (2020). Robustness analysis of vertical resistance to progressive collapse of diagrid structures in tall buildings. *The Structural Design of Tall and Special Buildings*, *29*(13). https://doi.org/10.1002/tal.1775

Liu, C., Fang, D., & Yan, Z. (2021). Seismic Fragility Analysis of Base Isolated Structure Subjected to Near-fault Ground Motions. *Periodica Polytechnica Civil Engineering*. https://doi.org/10.3311/PPci.15276

Liu, C., Fang, D., & Zhao, L. (2021). Reflection on earthquake damage of buildings in 2015 Nepal earthquake and seismic measures for post-earthquake reconstruction. *Structures*, *30*, 647–658. https://doi.org/10.1016/j.istruc.2020.12.089

Liu, Y., Gonzalez, M., & Wassgren, C. (2019). Modeling granular material segregation using a combined finite element method and advection–diffusion–segregation equation model. *Powder Technology*, *346*, 38–48.

https://doi.org/10.1016/j.powtec.2019.01.086

Luco, N., & Bazzurro, P. (2007). Does amplitude scaling of ground motion records result in biased nonlinear structural drift responses? *Earthquake Engineering & Structural Dynamics*, *36*(13), 1813–1835. https://doi.org/10.1002/eqe.695

Lurie, H. (1950). *Lateral Vibrations as Related to Structural Stability*. California Institute of Technology,.

Maj, M. (2017). Some Causes of Reinforced Concrete Silos Failure. *Procedia Engineering*, *172*, 685–691. https://doi.org/10.1016/j.proeng.2017.02.081

Maj, M., & Ubysz, A. (2020a). *Computational Models for Determining Silo Wall Displacements Caused by Dry Friction;* . Oficyna Wydawnicza Politechniki Wrocławskiej.

Maj, M., & Ubysz, A. (2020b). Estimation of loads' main statistics for hot materials silo. *In IOP Conference Series: Materials Science and Engineering;* .

Malhotra, P. K., Wenk, T., & Wieland, M. (2018). Simple Procedure for Seismic Analysis of Liquid-Storage Tanks. *Structural Engineering International*, *10*(3), 197–201. https://doi.org/10.2749/101686600780481509

Mansour, S., Pieraccini, L., Palermo, M., Foti, D., Gasparini, G., Trombetti, T., & Silvestri, S. (2022). Comprehensive Review on the Dynamic and Seismic Behavior of Flat-Bottom Cylindrical Silos Filled With Granular Material. *Frontiers in Built Environment*, *7*. https://doi.org/10.3389/fbuil.2021.805014

Mansour, S., Silvestri, S., & Sadowski, A. J. (2022). The 'miniature silo' test: A simple experimental setup to estimate the effective friction coefficient between the granular solid and a horizontally-corrugated cylindrical metal silo wall. *Powder Technology*, *399*, 117212. https://doi.org/10.1016/j.powtec.2022.117212

Maraveas, C. (2020). Concrete Silos: Failures, Design Issues and Repair/Strengthening Methods. *Applied Sciences*, *10*(11), 3938. https://doi.org/10.3390/app10113938

Mehretehran, A. M., & Maleki, S. (2018). 3D buckling assessment of cylindrical steel silos of uniform thickness under seismic action. *Thin-Walled Structures*, *131*, 654–667. https://doi.org/10.1016/J.TWS.2018.07.040

Mehretehran, A. M., & Maleki, S. (2021). Seismic response and failure modes of steel silos with isotropic stepped walls: The effect of vertical component of ground motion and comparison of buckling resistances under seismic actions with those under wind or discharge loads. *Engineering Failure Analysis*, *120*, 105100. https://doi.org/10.1016/j.engfailanal.2020.105100

Morelli, F., Laguardia, R., Faggella, M., Piscini, A., Gigliotti, R., & Salvatore, W. (2018). Ground motions and scaling techniques for 3D performance based seismic assessment of an industrial steel structure. *Bulletin of Earthquake Engineering*, *16*(3), 1179–1208. https://doi.org/10.1007/s10518-017-0244-1

Moya, M., Aguado, P. J., & Ayuga, F. (2013). Mechanical properties of some granular agricultural materials used in silo design. *International Agrophysics*, *27*(2), 181–193. https://doi.org/10.2478/v10247-012-0084-9

Muite, B. K., Quinn, S. F., Sundaresan, S., & Rao, K. K. (2004). Silo music and silo quake: granular flow-induced vibration. *Powder Technology*, *145*(3), 190–202. https://doi.org/10.1016/j.powtec.2004.07.003

Nateghi, F., & Yakhchalian, M. (2011). Seismic Behavior of Reinforced Concrete Silos Considering Granular Material-Structure Interaction. *Procedia Engineering*, *14*, 3050–3058. https://doi.org/10.1016/j.proeng.2011.07.384

Nateghi, F., & Yakhchalian, M. (2012). Seismic behavior of silos with different height to diameter ratios considering granular material-structure interaction. *International Journal of Engineering*, *25*(1 (B)), 25–35. https://doi.org/10.5829/idosi.ije.2012.25.01b.04

Niemunis, A., & Herle, I. (1997). Hypoplastic model for cohesionless soils with elastic strain range. *Mechanics of Cohesive-Frictional Materials*, *2*(4), 279–299. https://doi.org/10.1002/(SICI)1099-1484(199710)2:4<279::AID-CFM29>3.0.CO;2-8

Ning, X., & Pellegrino, S. (2015). Imperfection-insensitive axially loaded thin cylindrical shells. *International Journal of Solids and Structures*, *62*, 39–51. https://doi.org/10.1016/j.ijsolstr.2014.12.030

Niwa, A., & Clough, R. W. (1982). Buckling of cylindrical liquid-storage tanks under earthquake loading. *Earthquake Engineering & Structural Dynamics*, *10*(1), 107–122. https://doi.org/10.1002/EQE.4290100108

O'Rourke, M. J., & So, P. (2000). Seismic Fragility Curves for On-Grade Steel Tanks. *Earthquake Spectra*, *16*(4), 801–815. https://doi.org/10.1193/1.1586140

Paolacci, F., Giannini, R., & De Angelis, M. (2012). *Analysis of the Seismic Risk of Major-Hazard Industrial Plants and Applicability of Innovative Seismic Protection Systems*. www.intechopen.com

Peterson, P., Seide, P., & Weingarten, V. (1968). *Buckling ofThin-walled Circular Cylinders*.

Pieraccini, L., Palermo, M., Stefano, S., & Trombetti, T. (2017). On the Fundamental Periods of Vibration of Flat-Bottom Ground-Supported Circular Silos containing Gran-like Material. *Procedia Engineering*, *199*, 248–253. https://doi.org/10.1016/j.proeng.2017.09.015

Pieraccini, L., Silvestri, S., & Trombetti, T. (2015). Refinements to the Silvestri's theory for the evaluation of the seismic actions in flat-bottom silos containing grain-like material. *Bulletin of Earthquake Engineering*, *13*(11), 3493–3525. https://doi.org/10.1007/s10518-015-9786-2

Pineau, J. P., & Masson, F. (2001). Explosion in a grain silo Blaye (France). *Safe Handling of Combustible Dusts*.

Puzrin, A. M., Alonso, E. E., & Pinyol, N. M. (2010). Bearing Capacity Failure: Transcona Grain Elevator, Canada. In *Geomechanics of Failures* (pp. 67–84). Springer Netherlands. https://doi.org/10.1007/978-90-481-3531-8_4

Reimbert, M. L., & Reimbert, A. M. (1976). *Silos : theory and practice*.

Rejowski, K., Iwicki, P., Tejchman, J., & Wójcik, M. (2023). Buckling resistance of a metal column in a corrugated sheet silo-experiments and non-linear stability calculations. *Thin-Walled Structures*, *182*, 110206. https://doi.org/10.1016/j.tws.2022.110206

Rosen, A., & Singer, J. (1976). Vibrations and buckling of axially loaded stiffened cylindrical shells with elastic restraints. *International Journal of Solids and Structures*, *12*(8), 577–588. https://doi.org/10.1016/0020-7683(76)90004-4

Rotter, J. . (2001). *Guide for the Economic Design of Circular Metal Silos*. CRC Press.

Rotter, J. . (2006a). Cylindrical shells under axial compression. *Buckling of Thin Metal Shells*, 66–111.

Rotter, J. M. (1998a). Metal silos. *Progress in Structural Engineering and Materials*, *1*(4), 428–435. https://doi.org/10.1002/pse.2260010412

Rotter, J. M. (1998b). Development of Proposed European Design Rules for Buckling of Axially Compressed Cylinders. *Advances in Structural Engineering*, *1*(4), 273–286. https://doi.org/10.1177/136943329800100404

Rotter, J. M. (2006b). Elephant's foot buckling in pressurised cylindrical shells. *Stahlbau*, *75*(9), 742–747. https://doi.org/10.1002/STAB.200610079

Rotter, J. M. (2009). *Silos and Tanks in Research and Practice: State of the Art and Current Challenges*.

Rotter, J. M., & Hull, T. S. (1989). Wall loads in squat steel silos during earthquakes. *Engineering Structures*, *11*(3), 139–147. https://doi.org/10.1016/0141-0296(89)90002-3

Rotter, J. M., Jumikis, P. T., Fleming, S. P., & Porter, S. J. (1989). Experiments on the buckling of thin-walled model silo structures. *Journal of Constructional Steel Research*, *13*(4), 271–299. https://doi.org/10.1016/0143-974X(89)90032-1

Rotter, J. M., & Teng, J. (1989). Elastic Stability of Cylindrical Shells with Weld Depressions. *Journal of Structural Engineering*, *115*(5), 1244–1263. https://doi.org/10.1061/(ASCE)0733-9445(1989)115:5(1244)

Ruggieri, S., Porco, F., Uva, G., & Vamvatsikos, D. (2021). Two frugal options to assess class fragility and seismic safety for low-rise reinforced concrete school buildings in Southern Italy. *Bulletin of Earthquake Engineering*, *19*(3), 1415–1439. https://doi.org/10.1007/s10518-020-01033-5

Ruggieri, S., & Vukobratović, V. (2023). Acceleration demands in single-storey RC buildings with flexible diaphragms. *Engineering Structures*, *275*, 115276. https://doi.org/10.1016/j.engstruct.2022.115276

144

Sadowski, A. J., & Rotter, J. M. (2010). Study of Buckling in Steel Silos under Eccentric Discharge Flows of Stored Solids. *Journal of Engineering Mechanics*, *136*(6), 769–776. https://doi.org/10.1061/(ASCE)EM.1943-7889.0000112

Sadowski, A. J., & Rotter, J. M. (2011a). Buckling of very slender metal silos under eccentric discharge. *Engineering Structures*, *33*(4), 1187–1194. https://doi.org/10.1016/j.engstruct.2010.12.040

Sadowski, A. J., & Rotter, J. M. (2011b). Steel silos with different aspect ratios: II — behaviour under eccentric discharge. *Journal of Constructional Steel Research*, *67*(10), 1545–1553. https://doi.org/10.1016/j.jcsr.2011.03.027

Sadowski, A. J., & Rotter, J. M. (2011c). Steel silos with different aspect ratios: I — Behaviour under concentric discharge. *Journal of Constructional Steel Research*, *67*(10), 1537–1544. https://doi.org/10.1016/J.JCSR.2011.03.028

Sadowski, A. J., & Rotter, J. M. (2011d). Steel silos with different aspect ratios: II — behaviour under eccentric discharge. *Journal of Constructional Steel Research*, *67*(10), 1545–1553. https://doi.org/10.1016/J.JCSR.2011.03.027

Sadowski, A. J., & Rotter, J. M. (2012). Structural Behavior of Thin-Walled Metal Silos Subject to Different Flow Channel Sizes under Eccentric Discharge Pressures. *Journal of Structural Engineering*, *138*(7), 922–931. https://doi.org/10.1061/(ASCE)ST.1943-541X.0000530

Saleh, K., Golshan, S., & Zarghami, R. (2018). A review on gravity flow of free-flowing granular solids in silos – Basics and practical aspects. *Chemical Engineering Science*, *192*, 1011–1035. https://doi.org/10.1016/j.ces.2018.08.028

Salzano, E., Iervolino, I., & Fabbrocino, G. (2003). Seismic risk of atmospheric storage tanks in the framework of quantitative risk analysis. *Journal of Loss Prevention in the Process Industries*, *16*(5), 403–409. https://doi.org/10.1016/S0950-4230(03)00052-4

Sasaki, Y., & Yoshimura, J. (1988). Seismic Response of Concrete Stave Silos with Structural Discontinuity. . *Proceedings of the Ninth World Conference on Earthquake Engineering*.

Sassine, N., Donzé, F.-V., Harthong, B., & Bruch, A. (2018). Thermal stress numerical study in granular packed bed storage tank. *Granular Matter*, *20*(3), 44. https://doi.org/10.1007/s10035-018-0817-y

Schulze, D. (2021). *Powders and Bulk Solids  Behavior, Characterization, Storage and Flow*. Springer Cham.

Shimamoto, A., Kodama, M., & Yamamura, M. (1984). Vibration tests for scale model of cylindrical coal storing silo. *Proceedings of the 8th World Conference on Earthquake Engineering (Vol. 5*, 287–294.

Silvestri, S., Gasparini, G., Trombetti, T., & Foti, D. (2012). On the evaluation of the horizontal forces produced by grain-like material inside silos during earthquakes. *Bulletin of Earthquake Engineering*, *10*(5), 1535–1560.

https://doi.org/10.1007/s10518-012-9370-y

Silvestri, S., Ivorra, S., Chiacchio, L. Di, Trombetti, T., Foti, D., Gasparini, G., Pieraccini, L., Dietz, M., & Taylor, C. (2016). Shaking-table tests of flat-bottom circular silos containing grain-like material. *Earthquake Engineering & Structural Dynamics*, *45*(1), 69–89. https://doi.org/10.1002/eqe.2617

Silvestri, S., Mansour, S., Marra, M., Distl, J., Furinghetti, M., Lanese, I., Hernández-Montes, E., Neri, C., Palermo, M., Pavese, A., Rizzo Parisi, E., Sadowski, A. J., Selva, F., Taniguchi, T., Vadrucci, L., & Weber, F. (2022). Shaking table tests of a full-scale flat-bottom manufactured steel silo filled with wheat: Main results on the fixed-base configuration. *Earthquake Engineering & Structural Dynamics*, *51*(1), 169–190. https://doi.org/10.1002/eqe.3561

Simitses, G. J. (1986). Buckling and Postbuckling of Imperfect Cylindrical Shells: A Review. *Applied Mechanics Reviews*, *39*(10), 1517–1524. https://doi.org/10.1115/1.3149506

Simulia. (2012). *Dassault Systèmes Simulia, Abaqus CAE User's Manual*.

Skukis, E., Ozolins, O., Andersons, J., Kalnins, K., & Arbelo, M. A. (2017). Applicability of the Vibration Correlation Technique for Estimation of the Buckling Load in Axial Compression of Cylindrical Isotropic Shells with and without Circular Cutouts. *Shock and Vibration*, *2017*, 1–14. https://doi.org/10.1155/2017/2983747

Skukis, E., Ozolins, O., Kalnins, K., & Arbelo, M. A. (2017). Experimental Test for Estimation of Buckling Load on Unstiffened Cylindrical shells by Vibration Correlation Technique. *Procedia Engineering*, *172*, 1023–1030. https://doi.org/10.1016/j.proeng.2017.02.154

Sobhan, M. S., Rofooei, F. R., & Attari, N. K. A. (2017). Buckling behavior of the anchored steel tanks under horizontal and vertical ground motions using static pushover and incremental dynamic analyses. *Thin-Walled Structures*, *112*, 173–183. https://doi.org/10.1016/j.tws.2016.12.022

Song, C. Y. (2004). Effects of patch loads on structural behavior of circular flat-bottomed steel silos. *Thin-Walled Structures*, *42*(11), 1519–1542. https://doi.org/10.1016/J.TWS.2004.05.009

Song, C. Y., & Teng, J. G. (2003). Buckling of circular steel silos subject to code-specified eccentric discharge pressures. *Engineering Structures*, *25*(11), 1397–1417. https://doi.org/10.1016/S0141-0296(03)00105-6

Sun, X., Tao, X., Duan, S., & Liu, C. (2013). Kappa (k) derived from accelerograms recorded in the 2008 Wenchuan mainshock, Sichuan, China. *Journal of Asian Earth Sciences*, *73*, 306–316. https://doi.org/10.1016/j.jseaes.2013.05.008

Tascón, A. (2017). Design of silos for dust explosions: Determination of vent area sizes and explosion pressures. *Engineering Structures*, *134*, 1–10. https://doi.org/10.1016/j.engstruct.2016.12.016

Temsah, Y., Jahami, A., & Aouad, C. (2021). Silos structural response to blast

loading. *Engineering Structures*, *243*, 112671. https://doi.org/10.1016/j.engstruct.2021.112671

Teng, J. ., & Song, C. . (2001). Numerical models for nonlinear analysis of elastic shells with eigenmode-affine imperfections. *International Journal of Solids and Structures*, *38*(18), 3263–3280. https://doi.org/10.1016/S0020-7683(00)00222-5

Teng, J. G. (1996). Buckling of Thin Shells: Recent Advances and Trends. *Applied Mechanics Reviews*, *49*(4), 263–274. https://doi.org/10.1115/1.3101927

Teng, J. G., Lin, X., Michael Rotter, J., & Ding, X. L. (2005). Analysis of geometric imperfections in full-scale welded steel silos. *Engineering Structures*, *27*(6), 938–950. https://doi.org/10.1016/J.ENGSTRUCT.2005.01.013

Topkaya, C., & Rotter, J. M. (2011). Ring Beam Stiffness Criterion for Column-Supported Metal Silos. *Journal of Engineering Mechanics*, *137*(12), 846–853. https://doi.org/10.1061/(ASCE)EM.1943-7889.0000291

Topkaya, C., & Zeybek, Ö. (2018). Application of ring beam stiffness criterion for discretely supported shells under global shear and bending. *Advances in Structural Engineering*, *21*(16), 2404–2415. https://doi.org/10.1177/1369433218758476

Trahair, N. S., Abel, A., Ansourian, P., Irvine, H. M., & Rotter, J. M. (1983). *Structural Design of Steel Bins for Bulk Solids*. AustralianInstitute of Steel Construction.

Uckan, E., Akbas, B., Shen, J., Wen, R., Turandar, K., & Erdik, M. (2015). Seismic performance of elevated steel silos during Van earthquake, October 23, 2011. *Natural Hazards*, *75*(1), 265–287. https://doi.org/10.1007/s11069-014-1319-9

Vamvatsikos, D., & Allin Cornell, C. (2002). Incremental dynamic analysis. *Earthquake Engineering & Structural Dynamics*, *31*(3), 491–514. https://doi.org/10.1002/EQE.141

Vathi, M., & Karamanos, S. A. (2018). A simple and efficient model for seismic response and low-cycle fatigue assessment of uplifting liquid storage tanks. *Journal of Loss Prevention in the Process Industries*, *53*, 29–44. https://doi.org/10.1016/j.jlp.2017.08.003

Veletsos, A. S., & Younan, A. H. (1998). Dynamics of Solid-Containing Tanks. II: Flexible Tanks. *Journal of Structural Engineering*, *124*(1), 62–70. https://doi.org/10.1061/(ASCE)0733-9445(1998)124:1(62)

Vidal, P., Guaita, M., & Ayuga, F. (2005). Analysis of Dynamic Discharge Pressures in Cylindrical Slender Silos with a Flat Bottom or with a Hopper: Comparison with Eurocode 1. *Biosystems Engineering*, *91*(3), 335–348. https://doi.org/10.1016/j.biosystemseng.2005.03.012

Virella, J. C., Suárez, L. E., & Godoy, L. A. (2008). A Static Nonlinear Procedure for the Evaluation of the Elastic Buckling of Anchored Steel Tanks Due to Earthquakes. *Journal of Earthquake Engineering*, *12*(6), 999–1022. https://doi.org/10.1080/13632460701672714

Virella, J., Godoy, L., & Suárez, L. (2006). Dynamic buckling of anchored steel tanks subjected to horizontal earthquake excitation. *Journal of Constructional Steel Research*, *62*(6), 521–531. https://doi.org/10.1016/j.jcsr.2005.10.001

Vlasov, V. (1961). *Thin-walled elastic beams.* National Science Foundatio.

Volpato, S., Artoni, R., & Santomaso, A. C. (2014). Numerical study on the behavior of funnel flow silos with and without inserts through a continuum hydrodynamic approach. *Chemical Engineering Research and Design*, *92*(2), 256–263. https://doi.org/10.1016/j.cherd.2013.07.030

VON KARMAN, T., & TSIEN, H.-S. (1941). The Buckling of Thin Cylindrical Shells Under Axial Compression. *Journal of the Aeronautical Sciences*, *8*(8), 303–312. https://doi.org/10.2514/8.10722

von Wolffersdorff, P. A. (1996). Hypoplastic relation for granular materials with a predefined limit state surface. *Mechanics of Cohesive-Frictional Materials*, *1*(3), 251–271. https://doi.org/10.1002/(SICI)1099-1484(199607)1:3<251::AID-CFM13>3.0.CO;2-3

Vynne Southwell, R. (1914). V. On the general theory of elastic stability. *Philosophical Transactions of the Royal Society of London. Series A, Containing Papers of a Mathematical or Physical Character*, *213*(497–508), 187–244. https://doi.org/10.1098/rsta.1914.0005

Wagner, H. N. R., Hühne, C., & Janssen, M. (2020). Buckling of cylindrical shells under axial compression with loading imperfections: An experimental and numerical campaign on low knockdown factors. *Thin-Walled Structures*, *151*, 106764. https://doi.org/10.1016/j.tws.2020.106764

Wagner, H. N. R., Hühne, C., Niemann, S., & Khakimova, R. (2017). Robust design criterion for axially loaded cylindrical shells - Simulation and Validation. *Thin-Walled Structures*, *115*, 154–162. https://doi.org/10.1016/j.tws.2016.12.017

Walker, D. M. (1966). An approximate theory for pressures and arching in hoppers. *Chemical Engineering Science*, *21*(11), 975–997. https://doi.org/10.1016/0009-2509(66)85095-9

Winterstetter, T. A., & Schmidt, H. (2002). Stability of circular cylindrical steel shells under combined loading. *Thin-Walled Structures*, *40*(10), 893–910. https://doi.org/10.1016/S0263-8231(02)00006-X

Wójcik, M., Sondej, M., Rejowski, K., & Tejchman, J. (2017). Full-scale experiments on wheat flow in steel silo composed of corrugated walls and columns. *Powder Technology*, *311*, 537–555. https://doi.org/10.1016/j.powtec.2017.01.066

Wójcik, M., & Tejchman, J. (2015). Simulation of buckling process of cylindrical metal silos with flat sheets containing bulk solids. *Thin-Walled Structures*, *93*, 122–136. https://doi.org/10.1016/j.tws.2015.02.025

Yokota, H., Sugita, M., & Mita, I. (1983). Vibration tests and analyses of coal-silo model. *In Proc., 2nd Int. Conf. on the Design of Silos for Strength and Flow,* , 107–116.

Advanced seismic modeling and analysis of flat-bottom cylindrical steel silos interacting with stored granular-like materials.

Younan, A. H., & Veletsos, A. S. (1998). Dynamics of Solid-Containing Tanks. I: Rigid Tanks. *Journal of Structural Engineering*, *124*(1), 52–61. https://doi.org/10.1061/(ASCE)0733-9445(1998)124:1(52)

Zaccari, N., & Cudemo, M. (2016). Steel silo failure and reinforcement proposal. *Engineering Failure Analysis*, *63*, 1–11. https://doi.org/10.1016/j.engfailanal.2016.02.009

Zdravkov, L. (2018). Influencing factors on effective width of compressed zone in joint column - cylindrical shell of steel silo. *Challenge Journal of Structural Mechanics*, *4*(1), 1. https://doi.org/10.20528/cjsmec.2018.01.001

Zeybek, Ö., & Seçer, M. (2020). A design approach for the ring girder in elevated steel silos. *Thin-Walled Structures*, *157*, 107002. https://doi.org/10.1016/j.tws.2020.107002

Zeybek, Ö., Topkaya, C., & Michael Rotter, J. (2019). Analysis of silo supporting ring beams resting on discrete supports. *Thin-Walled Structures*, *135*, 285–296. https://doi.org/10.1016/j.tws.2018.11.001

żmuda-Trzebiatowski, Ł., & Iwicki, P. (2021). Impact of Geometrical Imperfections on Estimation of Buckling and Limit Loads in a Silo Segment Using the Vibration Correlation Technique. *Materials*, *14*(3), 567. https://doi.org/10.3390/ma14030567